HANDBOOK ON TECHNICAL BARGE CONCEPTS

for use under BSR specific navigation conditions

Work package: WP 2, Activity 2
Version: final
Date: 17th July 2018

Johan Lantz
AVATAR Logistics AB

Andrius Sutnikas
Klaipeda Science and Technology Park

Stefan Breitenbach
Port of Hamburg Marketing Reg. Assoc.

Boris Kluge
Federation of German Inland Ports

Content

1 BACKGROUND TO REPORT

Specific navigation conditions like shallow water, ice, narrow fairways hinder the development of inland waterway transport, as only small ships with relatively high unit cost can be serviced.

A possible solution can be to use barge types, which are adjusted to specific navigable conditions in the Baltic Sea Region to increase efficiency and or loading capacity compared to standard equipment.

This handbook includes existing barge concepts for specific navigation conditions like shallow water, low bridges, ice, etc. and targets mainly shipping lines thinking to setting up logistic services on inland waterways in the BSR.

It should motivate them to further investigate the issue and consider new Baltic Sea Region services in their portfolio.

Additionally, two concepts for the adaptation of existing European ship tonnage for specific navigational conditions are presented in this handbook in detail.

ICE CONDITIONS

The presence of ice on the water surface exerts huge issues on ships running through the water area in Swedish Inland Waterways. Therefore new ways have to find to use Inland Waterways more days in the year.

Analyses should then identify opportunities for improvement of vessels and better propulsion systems under these stronger conditions.

LNG HYBRID PROPULSION SYSTEM

To fulfil overall climate targets a hybrid propulsion system should substitute the existing fuel concept with a naturally based sustainable fuel concept.

For zero emission in special areas electric propulsion system should be analysed probably as a hybrid concept with the before mentioned sustainable fuel concept.

The Analyses should show the technical needs according to the conditions in the BSR here in Sweden and Lithuania as similar and the cost of such concept.

2 OVERVIEW ABOUT AVAILABLE EUROPEAN SHIP TONNAGE

The European fleet is characterized by its great array of vessel types. The two main types of vessels which are used in varieties of sizes and specifications on the European waterways are the self-propelled motor freight vessel (MV) and the pushing unit ([PU] consisting of a push tug and non-motorized barge).

As such you could distinguish by propulsion technology on the one hand and vessel type (container, dry cargo, liquid cargo etc) on the other hand.

2.1 Propulsion technology

Modern inland waterway shipping disposes of three different types of propulsion technologies, adjusted to the requirements of the motor vessel, pushing unit and the compound formation. All of these systems are able to fulfill a large bandwidth of transport tasks in terms of types and forms of goods transported with a multi-purpose basis vessel, as well as a few specialized vessel types. A closer look at the advantages and disadvantages of the different propulsion technologies will follow hereunder.

2.1.1 Motor vessel

The "large motor cargo vessel" acts as the so called "lead ship" for the dimensioning of the extension and construction of canals. Its dimensions are: length – 110 m, width – 11.40 m, and maximum loaded draft is 2.80 m, tonnage capacity ca. 2,500 t.

The advantages of a self-propelled inland water vessel can be summarized as follows:

- o Flexibility, efficiency: impulsion and thus movement possibility available at any given time
- o Usage in vessel types with commodity-specific auxiliary equipment (i.e. pump system)
- o In connection to the relevant vessel type the depiction of the right speed and maneuverability necessary:
    - o When used on free-flowing rivers with higher stream velocities
    - o On all waters an increased average velocity of ca. 1-2 km/h can be reached (compared to pushing units)
    - o Favorable fuel consumption accordingly
- o Use with minimal crew concept , for example with only a 2-man team

An overview of the basic types of motor cargo vessels is given in the following table.

Table 1: Standard sizes of self-propelled river ships in Europe[1]

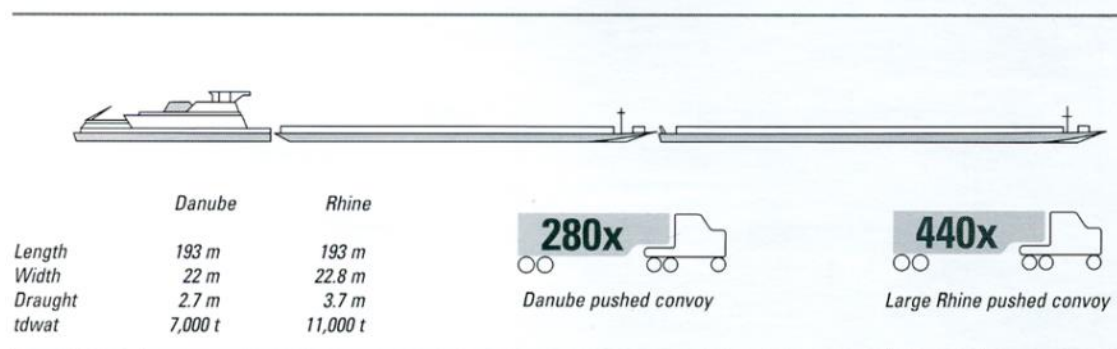| Vessel type	Dimensions (L x B)	Tonnage capacity at a draught of				
		1,50m	2,00m	2,50m	2,80m	3,50m
Large river motor ship	110,00 m x 11,40 m	600 t	1200 t	1800 t	2100 t	3000 t
Europe ship	85,00 m x 9,50 m	570 t	930 t	1350 t	-	-
'Johann Welker'	80,00 m x 9,50 m	600 t	940 t	1280 t	-	-
'Gustav Koenigs' (extended)	80,00 m x 8,20 m	500 t	800 t	1100 t	-	-
'Gustav Koenigs'	67,00 m x 8,20 m	420 t	670 t	1000 t	-	-
'Kempenaar'	50,00 m x 6,60 m	400 t	600 t	650 t	-	-
Peniche	38,50 m x 5,00 m	250 t	300 t	400 t*	-	-
BM-500	56,50 m x 7,60 m	415 t	475 t	-	-	-

2.1.2 Pushing unit (barges and push boats)

Based on the towage technique[2], the pushing unit is formed by a variable number of non-motorized barges interlinked with a tug. Depending on the waterway prospects, different formations are possible. On the Lower Rhine, on the ARA port relations (Amsterdam, Rotterdam, and Antwerp) and the Ruhr area, up to 6 European barges can be connected. On the Middle and Lower Danube, a pushing unit with up to 9 interlinked barges can be used. As the "lead ship" for the extension of the international cargo traffic relevant canal system (waterway class Vb), the single-lane, two-part pushing unit with the following dimensions was determined: length 185 m, width 11.40 m, maximum loaded draft 2.80 m, tonnage capacity ca. 3,600 t.

---

[1] Cf: PINE, p. 15

[2] The towage, that is, the pulling of non-propelled barges (naval units for the carriage of goods with helmstand) through tug boats, is no longer a common practice today.

Figure 1: Pushing unit with four barges[3]

	Danube	Rhine
Length	193 m	193 m
Width	22 m	22.8 m
Draught	2.7 m	3.7 m
tdwat	7,000 t	11,000 t

280x — Danube pushed convoy

440x — Large Rhine pushed convoy

Pushing units are particularly suitable for ore, coal, grain, animal feedstuff, fertilizer, construction- and recycling material (bulk cargo). The most frequently used barge is the "Europe-barge-class type IIa". There are other longer and shorter barges available that have been adjusted in their dimensions, according to their designated navigation area and waterway requirements. An overview is provided in the following table:

Table 2: Standard sizes of pushed barges in Europe[4]

| Barge type	Dimensions (L x B)	Tonnage capacity at a draught of				Area of use
		2,00m	2,50m	2,80m	4,00m	River or corridor
Europe Type I	70,00 m x 9,50 m	940 t	1240 t	-	-	Rhine, MLK
Europe Type II	76,50 m x 11,40 m	1250 t	1660 t	1850 t	-	Rhine, MLK, Danube
Europe Type IIa	76,50 m x 11,40 m	1140 t	1530 t	1800 t	2800 t	Rhine
Europe Type IIb	76,50 m x 11,00 m	1100 t	1500 t			Danube
GSP-54	54,00 m x 11,00 m	900 t				Elbe, Oder
SP-65	65,00 m x 8,20 m	900 t				Elbe, Oder
SP-35	32,50 m x 8,20 m	415 t				Elbe, Oder
LASH	18,70 m x 9,50 m	250 t	335 t	385 t		Weser, Rhine
See-Bee	29,75 m x 10,70 m	490 t	640 t	730 t		Weser, Rhine
Interlichter	38,25 m x 11,40 m	585 t	775 t	900 t		Danube
OBP-500	45,50 m x 9,60 m	480 t	-	-	-	Oder

Boats that are not transporting cargo themselves and are pushing one or more barges are referred to as push boats.

---

[3]   Cf: MDN, p. 59 (A4 – 45)

[4]   Cf: PINE, p. 16

Push boats on the river Rhine are built with a size of up to 40 x 15 meters. The draft is 1.90 m. The big push boats, which can carry up to six barges, are mostly equipped with diesel engines with a total power of 6,000 PS. A voyage from Rotterdam to Duisburg and loaded with 10,000 tons of ore, takes 26 hours. The empty downstream 12 hours. These push boats are operating 24/7.

Figure 2: Possible formations and unit combinations with push boats[5]
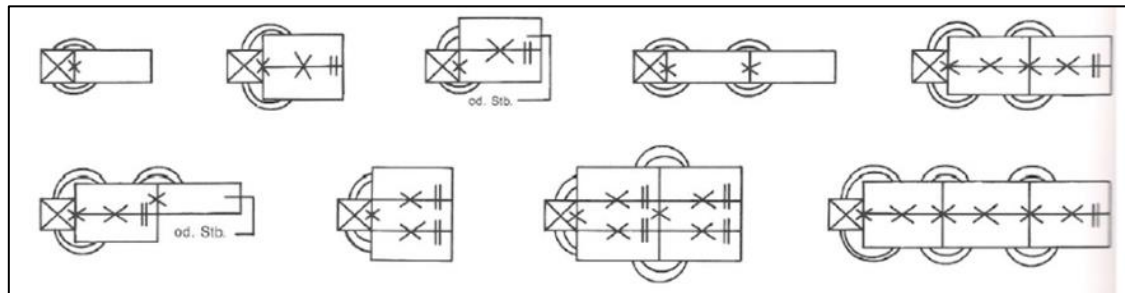
| Key | | push boat | | barge |

The advantages of a structural separation of loading equipment and driving component in pushed tow systems are the following:

o   Variability of pushed tow systems depending on the current demand or the adaption to waterway requirements, representation of very large tow systems on demand and on major waterways
o   Favorable part load characteristics of pushed tow systems (barges)
o   Larger amount of interlinked barges possible compared to self-propelled vessels, also due to the possibility of decoupling the barges in locks (however, this is associated with loss of time and higher personnel expenses)
o   Flexible operation on relations with several ports of call and the possibility to leave behind or picking up of individual barges
o   Individual compilation of barges for specific purposes or robust operational conditions

This is offset by system-specific disadvantages that have to be considered when deciding which system to use:

o   Higher traction resistance, with an average speed of about 1-2 km/h less than when using self-propelled motor vessels (mainly in use on short- to medium haul, not so much on long haul relations)
o   Maneuverability of long pushed tow systems may be problematic under certain circumstances (weather conditions, bottlenecks)
o   More personnel required (one additional person needed for the coupling and decoupling of the barges)
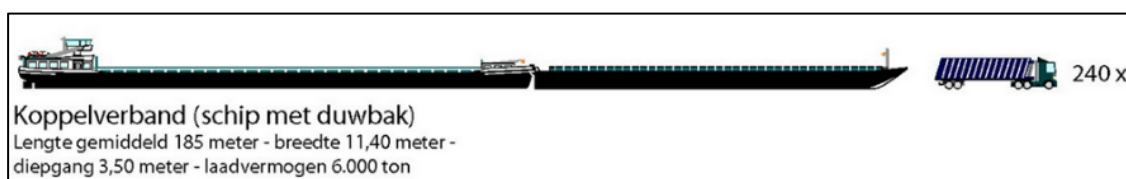
---

5   own diagram, HHM 2015

2.1.3   Pushed tow systems

The possibility to transport big capacities by interlinking barges is also used in combination with self-propelled motor vessels of same or similar size. In this case the merits of the self-propelled motor vessel are combined with those of the pushed tow system.

The engine power of modern motor vessels (up to 1.99 kW (2,600 PS)) and their navigational and technical equipment allows for up to three additional "Europe" barges, which increases the loading capacity to as far as 10,000 t.

Figure 3: Compound foundation (motor vessel + a barge)[6]

Koppelverband (schip met duwbak)
Lengte gemiddeld 185 meter - breedte 11,40 meter -
diepgang 3,50 meter - laadvermogen 6.000 ton

240 x

Here too the advantage lies in the possibility to individually control the capacity, depending on demand and relation, which would not be possible in that manner with single, self-propelled motor vessels.

o   Mostly vessel and barge types for waterways of class IV and V are used in pushed tow systems
o   Self-propelled motor vessels used in pushed two systems usually have higher engine power and a specific bow form for the coupling of the barges.
o   An interlinked coupling in a linea manner is just as possible, as parallel coupling (interconnected through simple rope connections). It is only subject to fairway conditions
o   It was mentioned repeatedly as a disadvantage of the pushed tow system that it is not possible to handle cargo of the self-propelled unit and the barge parallel, although desired due to the lack of time.
o   Maintenance work can only be organized acceptably efficient
o   Cargo specific auxiliary systems, such as pump systems, tank heating for liquefied cargo and the respective power consumption, are necessary for pushed tow units and can be provided when necessary.7 In the past years more and more pushed boat systems consisting of self-propelled boat and specific barges are being build and are mainly in use on the Rhine basin.

---

[6]   Cf: schiffundtechnik
[7]   Cf: Linde 2008, p. 129 et seq.

2.2 Vessel type

The inland water vessels differ in size and tonnage capacity, depending and adjusted to the conditions of its relation (shipping route and waterway classification), as well as in its engine power and navigation-technical equipment. Today's composition of inland water vessel types, as far as it relates to types and shapes of cargo, can be represented as follows:

- Multi-purpose dry cargo vessel
- Tanker (petroleum products, chemicals)
- Tanker (LPG)
- Container vessel
- Roll-on/Roll-off-vessel (RoRo-vessel)

The European inland water transport sector is currently carried out with 19,000 motor vessels, barges, pushing boats and tug boats. 49 % of these are motor vessels, 35 % are barges and tugboats. The majority of the fleet with 84 % is allotted to the multipurpose dry cargo vessel fleet.

Table 3: Active European cargo fleet in 2013[8,9]

Active European cargo fleet in 2013	Rhine countries	Danube countries[x]	Elbe countries[x]	Total	Other European countries
Dry cargo vessels	6,340	383	115	6,838	660
Tank vessels	1,846	45	0	1,891	
Pushboats/slow boats	1,895	691	298	2,884	dna[x]
Dry cargo barges	2,843	2,371	645	5,859	461
Tank barges	197	309	0	506	
Total	**13,121**	**3,799**	**1,058**	**17,978**	**1,121**
Total without pushboats and slow boats	11,226	3,108	760	15,094	
Active European fleet + other European countries					19,099

---

[8] Cf: Danube Statistics (2013)

[9] Cf: Eurostat

[10] x) Without German fleet, dna - data not available

**Table: Tonnage of the active European cargo fleet in 2013**

Tonnage EU-Fleet	Dry cargo fleet		Tank fleet		total		Fleet
	Vessels	**Barges**	**Vessels**	**Barges**	**dry**	**liquid**	**total**
Rhine countries	7,215,091	4,190,634	3,377,628	251,276	11,405,725	3,628,904	**15,034,629**
Danube countries[x]	429,911	3,145,917	49,948	277,092	3,575,828	327,040	**3,902,868**
Elbe/Oder countries[x]	97,453	300,787	0	0	398,240	0	**398,240**
total[xx]	**7,742,455**	**7,637,338**	**3,427,576**	**528,368**	**15,379,793**	**3,955,944**	**19,335,737**

x) without German fleet, xx) without other European countries

As can be seen in the above tables, the main part of the European inland water vessel fleet with more than 13,100 vessel units, or around 73 %, is based in the Rhine basin. This is on one side related to the higher nautical standards on this river basin and on the other hand due to the strong economic centers located along these river basins and subsequently with the generally higher transport demand.[11]

In general the average age of the European inland water vessel fleet is high. Thus, more than 52 % of the dry cargo and tanker vessels in Western Europe and 64 of the total fleet are older than 37 years, as illustrated in below figure. For the fleet in the Danube area, an even higher average age can be assumed. The current development, as well as the slow reduction of existing capacities have resulted in a renewal of the inland water vessel fleet.

Figure 4: Years of construction Western European Fleet - Tank & Dry Cargo[12]

---
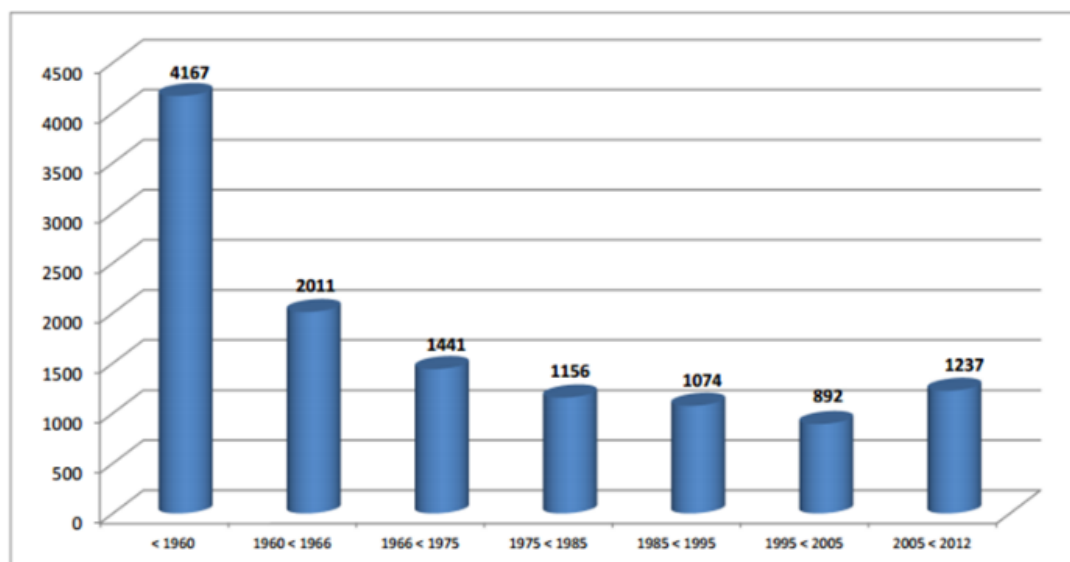
[11]   Cf: PINE, p.17

[12]   Cf: IVR Construction (2013)

It is estimated that the investment in new-buildings of the Western Europe inland water vessel fleet during the past ten years has notably followed the economic activity, although to different degrees in the three sub-sections of the fleet (dry cargo vessels, tanker vessels and passenger vessels).

As cause for this development, especially the continuing overcapacity in the dry cargo shipping, the marginal increases in demand for transportation and the stagnation of rates are identified.[13]

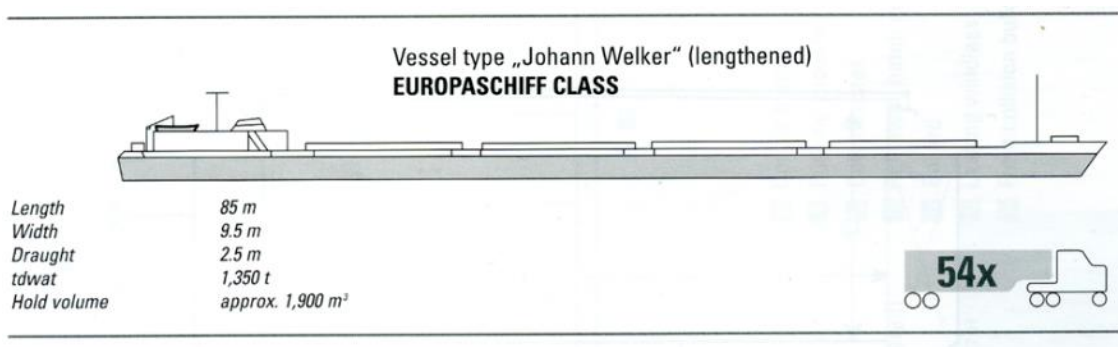### 2.2.1 Multi-purpose dry cargo vessel

The majority of self-propelled European inland water vessels are dry cargo vessels. Their current payload is around 7.7 million tdw, of which 48 % are on the Rhine axis and 11 % in the Danube area. Depending on the waterway classification, the following vessel types are mainly in use: the "Gustav Koenig-", the "Europe-" and the "large motor cargo vessel" class vessel.

Figure 5: Multipurpose dry cargo vessel of the "Gustav Koenigs Class"[14]
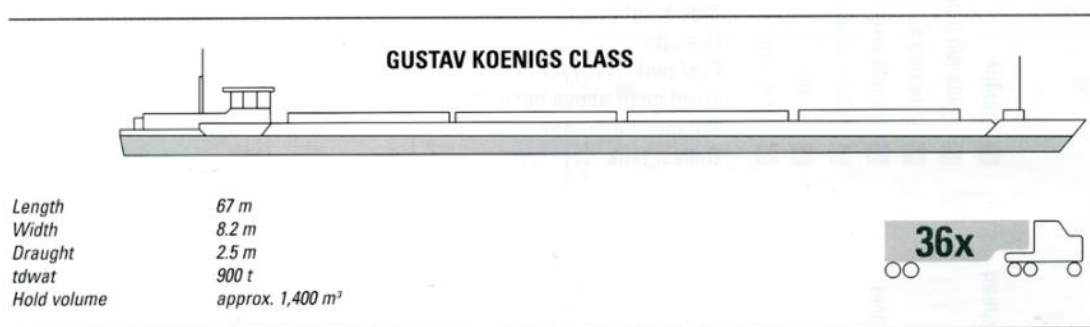
The vessels of the "Gustav Koenig" class are canal-going. Their engines have been upgraded frequently over the past years and the hull often also extended to a length of about 80 meters. Through this, its tonnage capacity increases up to 1,200 tonnes.

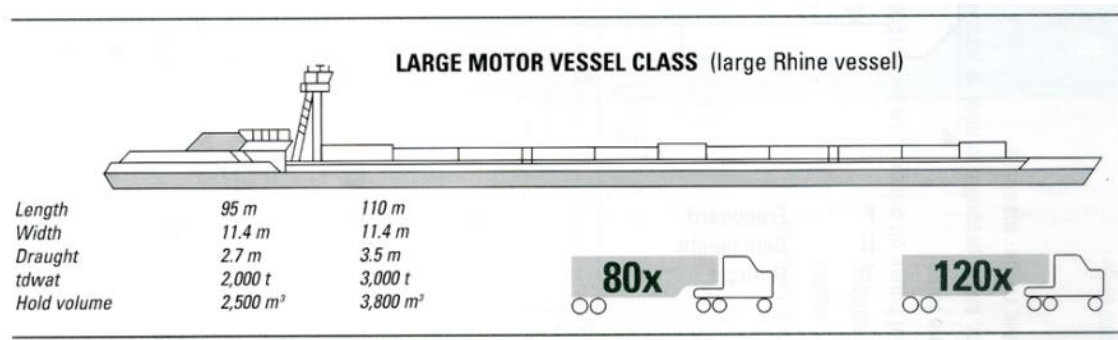**Figure 6: Multipurpose dry cargo vessel "Johan Welker" of the "Europe Class"[15]**

---

[13] Cf: ZKR (2014), p. 66 et seq.

[14] Cf: MDN, p. 51 (A4 – 37)

[15] Cf: ibidem

Figure 7: Multipurpose dry cargo vessel of the "Large Rhine vessel class"[16]

Dry cargo vessels are universally utilizable. Due to its multifunctional use, empty trips can be reduced immensely. Among the most important criteria of a multi-purpose dry cargo vessels are:

Double hull construction, meaning - double bottom and double shell plating.

The cargo hold is predominantly unseparated – one cargo hold, mobile division and separation is possible.

Vertically accessible, open, "box-shaped" cargo hold, even inner floor, even inner- and side walls, minimal or little loss of cargo hold (minimal or little loss due to not readily accessible stowage areas).

Hatch cover system, with the usual longitudinal and transverse coaming height with outer walking passage, hatch covers are weatherproof, roll hatch- or pontoon hatch cover, manually handled or with mechanical support, robust and weatherproof cargo no need for hatch and thus increased cargo loading height and cargo hold usage (light bulk cargo, container, heavy cargo).

Ballast water capacity within the double hull structure, i.e. for draft and trim improvement on empty trips or with light cargo, for example empty container.[17]

2.2.2   Tanker

Tankers are used for the transport of liquid cargo, such as mineral oil, derivatives, liquid chemical products, as well as edibles. The payload of the European Tanker fleet was around 3.4 million tons in 2013, of which 98.5 % are on the Rhine axis and just 1.5 % in the Danube area. Again, there are vessels of different size which are adapted to the various waterway classifications in the relevant relation.

---

[16]   Cf: ibidem

[17]   Cf: Linde 2008, p. 109 et seq.

Figure 8: Rhine tanker[18]

Length	110 m
Width	11.4 m
Draught	3.5 m
tdwat	3,000 t
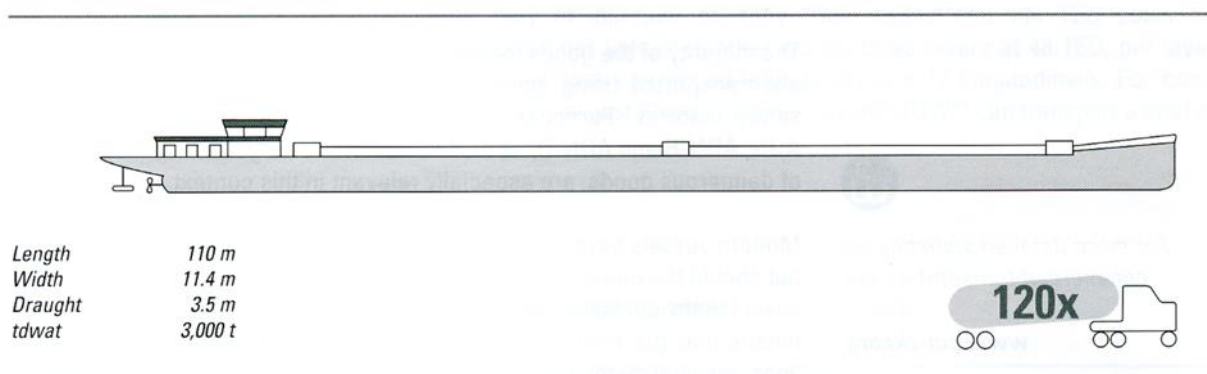
The majority of the cargos transported are dangerous goods, for which special tankers with the required security equipment need to be used. When doing so, it is especially important to bear in mind the requirements and recommendations such as the national dangerous goods laws and the ADN-2013.[19] Among the most important criteria of a tanker are:

o Cargo tank area built from the hull so that the cargo hold limitations are created by the vessels' tank floor, deck, side walls, as well as transverse and longitudinal bulkhead.

o Divided tank, the amount and size of the separate tanks depends primarily on the diversification and specification of the cargo itself, that is – count and quantities simultaneously and independently transported goods.

o High transport technical flexibility, that is – number of cargo tanks, partially same-, partially of different size.

o Double hull construction, double floor, double shell plating, due to international and national regulations for the transport of dangerous goods of certain hazard degree (i.e. dangerous goods regulations for inland waterway transports, ADN-2013).[20]

o Gradual retirement of single hull tankers that still exist, ultimately by 2018, relevant intermediate steps in 2009, 2012, 2015, as well as modification of single hull tankers to double hull tankers generally possible.

o Segregated-Ballast-Capacity (within the double hull) to control the floating position during empty state.[21]

2.2.3   Tanker (LPG)

Within the tanker vessel section, there is the specific form of transport for liquefied petroleum gas. As per directive 2008/106/EG, "'liquefied-gas tanker' means a ship constructed or adapted and used for the

---

[18]   Cf: MDN, p. 56 (A4 – 42)

[19]   Cf: ADN-2015

[20]   Cf: ADN-2015

[21]   Cf. Linde 2008, p. 113 et seq.

carriage in bulk of any liquefied gas or other product as listed in Chapter 19[22] of the International Gas Carrier Code[23], in its up-to-date version*".

Among the most important criteria for liquefied gas tankers are:

o   Transportation of gaseous petrochemical and other chemical products, liquefaction of the product by increasing the pressure, carried out on landside facilities.
o   Arrangement of cylindrical pressure cargo tanks below deck area separate from the hull structure
o   High transport technical flexibility
o   Relative high under deck volume i.e. through "trunk" construction. That is – by exceeding the deck area height over the side height.
o   Double hull alignment, waterproof division according to ADN-regulation.
o   Tank materials and tank protection systems for aggressive cargo as per individual case.24

2.2.4   Container Vessel

Container vessels are built explicitly for the transport of containers, which ensure an optimized utilization over the dry cargo vessels also used for the transportation of containers. Their main area of use is currently the Rhine river stream.

Figure 9: Container vessel of the JOWI-Class[25]
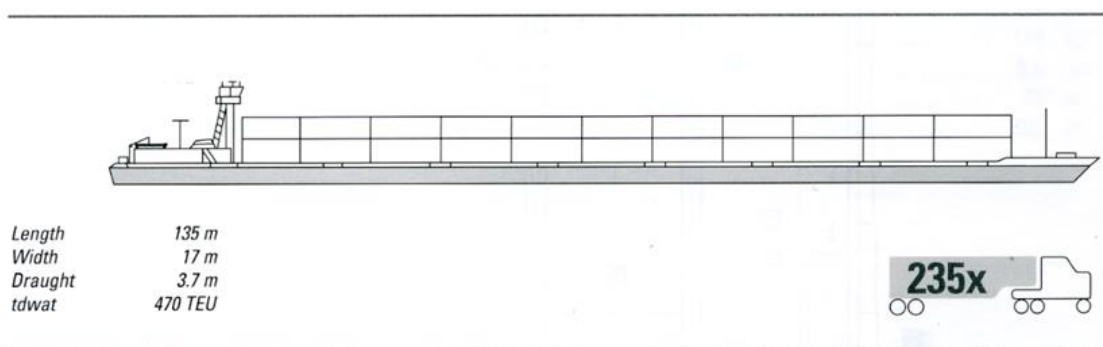
The big container vessel class was the newly introduced generation of inland waterway vessels in 1998. These vessels are up to 135 meters long and up to 17.50 meters wide and are mainly designed for the container transport. The first vessel was the MV Jowi.

The container vessel is similar to the multi-purpose dry cargo vessel in its essential features (5.3.1.1). It differs mainly in its size to enable frequent transports of large amounts of containers. Another specificity is the permanently installed "cell guide", allowing for easier loading and unloading of containers.

---

[22]   Chapter 19 includes a list of materials as well as the minimum requirements for the transportation of these goods
[23]   Cf: International Code for the Construction and Equipment of Ships Carrying Liquefied Gases in Bulk (IGC-Code)
[24]   Cf: Linde 2008, p. 113 et seq.
[25]   Cf: MDN, p. 54 (A4 – 40)

2.2.5 Roro vessel

Ro/Ro vessels (Roll on Roll off) enable the self-driven transportable objects to be loaded or unloaded via harbor ramps or the ship's ramp. This reduces the cargo handling time, enables a smooth transshipment of cargo and offers greater flexibility in cargo composition. The higher manufacturing costs are a disadvantage, since Ro/Ro vessels are special vessels and thus the limited market influences the costs for building such vessels.

Figure 10: Ro/Ro-Vessel[26]

Length	105 m
Width	9.5 m
Draught	1.4 m

270x
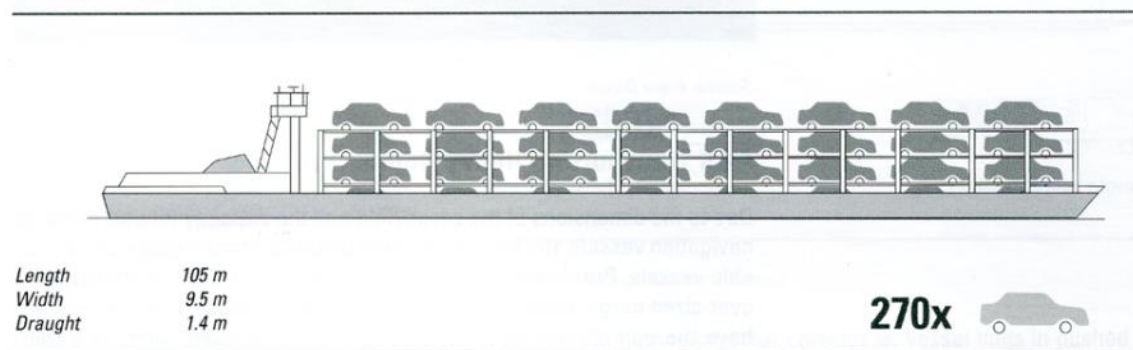
The substantial criteria of a Ro/Ro vessel are as follows:

o   Principle of horizontal self-driven-, or "wheeled" cargo handling.
o   Characteristic subordinate types of vessels:
    o   Allround-type (all kinds and forms of new cars, mobile machinery, etc.)
    o   Trailer-Type
    o   Car-Type
    o   Heavy Lift-Type
o   The number of loading decks is a distinctive characteristic, highest possible amount of decks is important for the best usage of the available cargo hold in vertical direction. Otherwise relevant for fixed points, that is the vertical clearance to bridges.27

---

[26]   Cf: MDN, p. 57 (A4 – 43)
[27]   Cf: Linde 2008, p. 117 et seq.

2.3   Baltic Sea Region specifics

Analyses showed a variety of different ship types in operation with in Europe. There is a ship for nearly every possible cargo and waterway characteristic.

The EMMA project website provides an overview of available European vessel types which can be found on www.project-emma.eu. The actual table is shown below, however the database will be update on the website.

Further analyses showed that some BSR specifics like ice conditions in the Scandinavian countries or the energy transition in general requires adapted inland ships. Chapter three will provide an overview on how adaptation measures on existing vessels could help to meet the Baltic Sea Region waterways specifics as well as could support energy transition in shipping.

IW Class	Vessel type	Class / Name	Length	Breadth	Draught	Capacity Container	Capacity dry cargo	Capacity liquid cargo	Number of cars	Own Engine
I or >		Cargo lighter "Finow"	31.30 m	5.00 m	1.70 m		210 tons			no
I or >	Dry cargo	Peniche/Spitz	38.50 m	5.00 m	2.50 m		400 tons			yes
II or >		Kempenaar/New Kempenaar	55.00 m	6.60 m	2.50 m		650 tons			
III or >		SP-35	32.50 m	8.20 m	2.00 m		415 tons			no
III or >	Liquid cargo	Liquid bulk lighter	32.50 m	8.20 m	2.20 m			500 tons		no
III or >		SL-65 (lighter)	65.00 m	8.20 m	2.30 m		975 tons			no
III or >		BM-500 (Motorschiff)	56.60 m	7.60 m	2.00 m		475 tons			yes
III or >		Cargo lighter	32.50 m	8.20 m	2.10 m		430 tons			no
III or >	Dry cargo	Gustav König (extended version)	80.00 m	8.20 m	2.50 m		1100 tons			yes
III or >	Dry cargo	SL 36/37 (Bulk Cargo lighter)	32.50 m	8.20 m	2.10 m		470 tons			no
III or >	Dry cargo	Gustav König	67.00 m	8.20 m	2.50 m		1000 tons			yes

IW Class	Vessel type	Class / Name	Length	Breadth	Draught	Capacity Container	Capacity dry cargo	Capacity liquid cargo	Number of cars	Own Engine
III or >		Dortmund-Ems-Canal ship	67.00 m	8.20 m	2.50 m		1000 tons			yes
IV or >	Dry cargo	OBP-500	41.30 m	9.00 m	1.70 m	24 TEU	475 tons			no
IV or >		Lighter aboard ship (LASH)	18.70 m	9.50 m	4.00 m		380 tons			yes
IV or >	RoRo	GSL URSUS	64.50 m	9.50 m	4.70 m					no
IV or >	RoRo	Ro-Ro lighter GSP 65	65.00 m	9.50 m	2.30 m		1066 tons			no
IV or >	Dry cargo	Johann Welker ship	80.00 m	9.50 m	2.50 m		1280 tons			yes
IV or >	Container	SL-36/37 - 9,50 (Container lighter)	32.50 m	9.50 m	2.20 m	24 TEU	530 tons			no
IV or >		Europe Ship (Rhein-Herne-Kanalschiff)	85.00 m	9.50 m	2.50 m		1350 tons			yes
IV or >	Container	SL-65 - 9,50 (Container lighter)	65.00 m	9.50 m	2.40 m	54 TEU				no
Va or >		Large river motor ship	135.00 m	11.40 m	3.50 m		3000 tons			yes
Va or >	Container	TC 1000 (Container lighter)	71.00 m	10.50 m	2.50 m	54 TEU	1450 tons			no
Va or >		GSP-54	54.00 m	9.50 m	4.70 m		900 tons			no

IW Class	Vessel type	Class / Name	Length	Breadth	Draught	Capacity Container	Capacity dry cargo	Capacity liquid cargo	Number of cars	Own Engine
Va or >		GMS (Large Motor Vessel)	110.00 m	11.40 m	2.80 m		2100 tons			yes
Va or >	Container	Standard container barge	110.00 m	11.40 m	3.00 m	200 TEU				yes
Va or >		RoRo vessel	110.00 m	11.40 m	2.50 m				530cars	yes
Va or >	RoRo	Ro-Ro lighter GSP 54	54.00 m	11.00 m	2.10 m		960 tons			no
Va or >	Liquid cargo	Tanker (LPG)	110.00 m	11.40 m	3.50 m			3000 tons		yes
Va or >	Liquid cargo	Standard Inland tank barge	110.00 m	11.40 m	3.50 m			3000 tons		yes
Vb or >		Pushing unit with two barges	172.00 m	11.40 m	4.00 m		5500 tons			yes
Vb or >		Pushed tow system	185.00 m	11.40 m	3.50 m		6000 tons			yes
VIa or >		Pushing unit with four or six barges	193.00 m	34.20 m	4.00 m		16500 tons			yes
VIa or >	Container	Large container barge	135.00 m	17.00 m	3.50 m	500 TEU				yes
VIb or >	Liquid cargo	Large Inland tank barge	135.00 m	21.80 m	4.40 m			9500 tons		yes

3 ADAPTATION OF EUROPEAN TONNAGE TO BSR SPECIFIC NAVIGATIONAL CONDITIONS

The cases will analyse the general possibilities of re-fitting available ship tonnage, pre- and post-effects of the new ship design linked to navigability, cargo intake and emissions

3.1 Case I: Design study on re-fit an inland barge to resist ice impacts in Nordic countries

3.1.1 Case overview and involved parties

The general objective of this case was to investigate how an inland motor barge based on average European standards, IWW class Zone 3, can be modified for navigation in the Swedish Lake Mälaren during ice conditions.
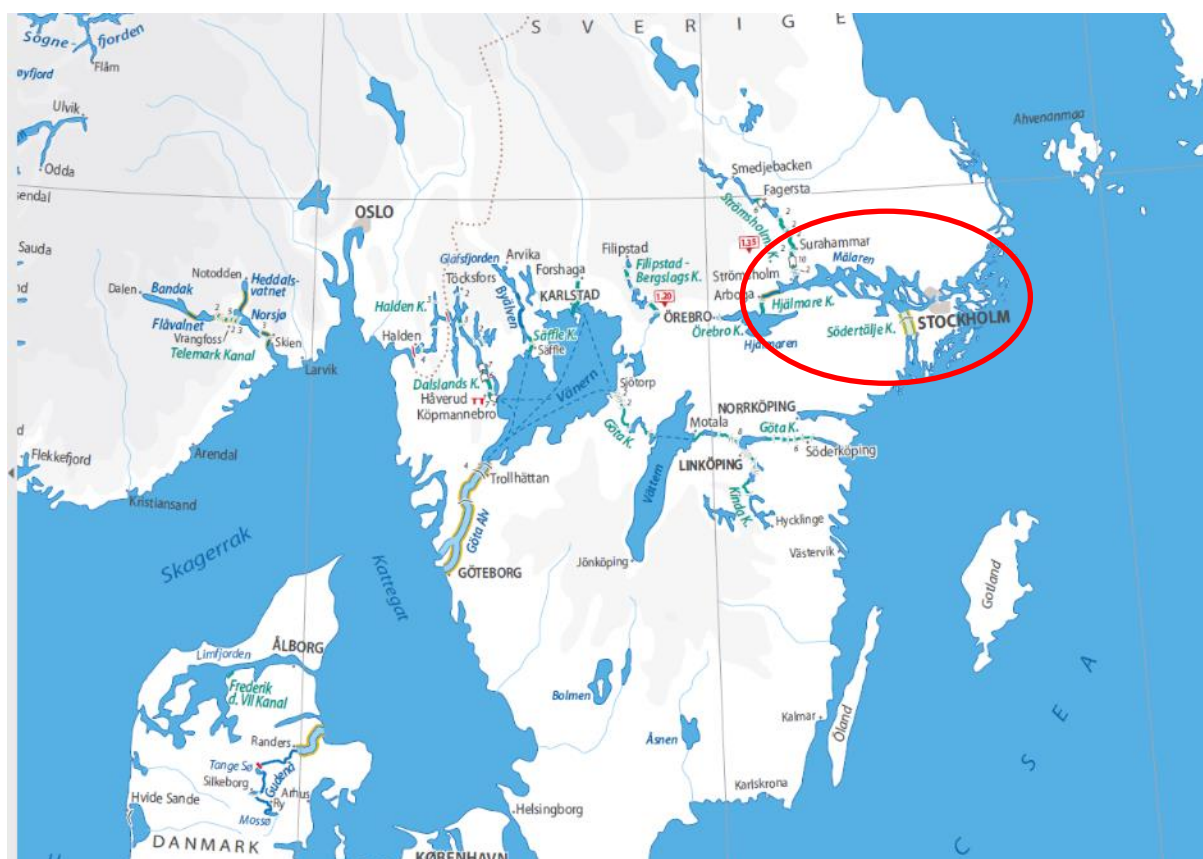

Figure 11 - Lake Mälaren in Sweden

The assignments geographic area is within the borders of Lake Mälaren in Sweden. Lake Mälaren, with access to the Baltic Sea, is a fresh water lake classified as IWW Zone 3 (wave height up to 0,6m). According to the Swedish Transport Agency technical regulations, a river Rhine standard barge can be accepted for navigation undertaken some modifications.

The lake Mälaren has vessels restrictions due to the lock in Södertälje (L=124,0m, B=18,0m Draught=6,80m) and the lock in Hammarby (L=110,0m, B=15,0m Draught=5,50m).

During the winter period Lake Mälaren normally has an ice period of 8-12 weeks and ice restrictions for vessels are common during these periods. Annual statistics regarding type of ice and its thickness is kept in officially records by the Swedish Maritime Administration www.sjofartsverket.se

The analyses undertaken is verified manly through hull modelling and to some extent through experimental work executed by the Swedish Royal Institute of Technology (KTH) in cooperation with the German Technical University Hamburg (TUHH) and AVATAR Logistics AB. The analyses was separated in different work packages which content is briefly explained in the following:

WP1. Background and ice loads (KTH)

In order to establish an answer that question we first need to address and determine the loads acting on the hull structure under winter conditions. This will depend e.g.

- o Ice conditions
- o Wave height and frequency
- o Vessel speed and speed limitations (for other vessels)
- o Depth
- o Classification rules / National rules
- o Vessel specifics

This first part will investigate and determine the above specifics and interval. Additional parameters may be added if needed.

WP2. Hull loading from operation in ice (TUHH)

Based on the results from WP1 relevant ice models (for Lake Mälaren) and ice load models will be used to estimate the loads acting on the hull structure as function of the variables set in WP1, i.e. vessel speed, ice conditions etc.

WP3. Structural analysis and redesign (TUHH)

This work package will perform a structural analysis on the selected barge using input load data from WP2 investigating the global response, panel and supporting structure stresses and deformation. Based on the results hull modifications are proposed such that the response meet set allowable from rules/authorities (WP1).

WP4. Operational effects (KTH)

Based on the outcome from WP5 this WP will investigate how the suggested modifications will affect the

- o Increased vessel total weight
- o Reduced cargo intake
- o Increased fuel consumption
- o Limitations on manoeuvrability of the vessel

WP5. Experimental verification (TUHH/KTH)

Maximum stresses and on selected panels of the Vessel will be monitored and measured under Lake Mälaren ice conditions. This is performed by instrumenting the vessel with strain gauge equipment alternative optical fibres (pending on accessibility. The result from this WP is thus dependent on vessel availability and "good" climate and winter conditions during the period of this project. The plan is to leave mounted gauges for continued (outside this project) monitoring.

WP6. Reporting and admin (KTH)

This work package is responsible for the project detailing, time plan, communication with project owner and report compilation. In line with the request from the project owner and as specified in the tender the test results will be published in an official handbook, with recommendations for navigation with inland barges during ice conditions in Lake Mälaren.

3.1.2   Results

The attached study and development of ice navigation for inland barges is an important step to establish inland navigation in Sweden and the BSR Region. It figures out how an inland motor barge based on European standards, Inland waterway (IWW) class Zone 3, can be modified for navigation in Lake Mälaren in ice conditions.

The main research aspects focus on the following four aspects with regards to the ice-induced problems:

- Ice Load: including finding out the ice properties and predicting the load impact load based on ice condition in Lake Mälaren;
- Structural Strength Performance: evaluating structural strength problems both from global and local aspects;
- Potential Propulsion Problems: find out relationship between ship speed and ice thickness (h-v curve).
- Vessel Operating Scenarios: decide how many days the barge can operate under certain ice conditions

As a case study the Amice barge is chosen. This already existing barge is designed based on DNV GL IWW notation where ice loads are not considered, i.e., the ship is not designed to operate under ice conditions. Thus, to study the influence of ice is important in order to bring the barge into Lake Mälaren. Based on the done calculation, the shwon bow structural reinforcements are necessary in order to make sure that the barge can operate in Lake Malaren under winter conditions. In order to ensure the structural safety, it is recommended to increase plate thickness, and increase the dimensions and number of frames.

Generally, the proposed design curve for Amice is applicable for all ships operating on Lake Mälaren. Since in the process of achieving the expression, only the ice situation is considered. The same approach can be used to attain design curve for other inland waterway ice conditions.

It is recommended to use Riska method to predict resistance when the ship is operating on level ice and to use Brash ice method when ship runs at brash ice channel. In addition, the engine power factor

(engine power/ship displacement) has a significant influence on the ship performance in terms of resistance.

In general, the faster the ship goes, the lighter ice condition it can go through, and more navigable days will be. However, the structural problem should be bear in mind for making decisions.

3.2 Case II: Design study on re-fit an inland barge with LNG/LBG hybrid propulsion systems

3.2.1 Case overview and involved parties

Klaipeda Science and Technology Park, AVATAR Logistics AB in cooperation with the Western Baltic Engineering Group investigate the possibility to retrofit a ships propulsion system from diesel to LNG/LBG hybrid engine. This is according to possible needs inland navigation is faced with regarding environmental protection and emission control in Scandinavia.

Additionally inland navigation fleet needs to reach better environmental standards concerning emissions in future in general. A design and feasibility study for inland ships operating in BSR waters is of importance, as such tonnage is often not the same as regular European tonnage. This study supports the inland navigation sector in the BSR to prepare for future needs.

A three strep approach will be followed in the analyses and shall be included in the description of tasks within the tender documents:

○ Analyses of existing vessel(s) suggested by AVATAR Logistics and possibility of retrofit the propulsion system from diesel to LNG/LBG/HYBRIDE engine and documentation

○ Identification of possible modifications needed including documentation

○ Evaluation and documentation of how the suggested modifications impacts of, total weight, cargo intake, fuel consumption and the manoeuvrability of the vessel

○ Evaluation and documentation of vessels emission comparing before and after the retrofit.

3.2.2 Results

The attached explanatory note describes the concept of re-equipping an existing inland waterway vessel with a diesel power plant into a vessel with zero harmful emissions in the exhaust. As an initial vessel for the conversion, a hypothetical chemical tanker for inland waterways, similar to "Veendam", was chosen.

To reduce sulfur, nitrogen and carbon oxides, as well as solid particles in the ship's emissions, as required by Annex VI of MARPOL MC, it is proposed to use liquefied biological gas (LBG) as a fuel. When using LBG as fuel, the reduction in emissions will be reduced to 90%.

To optimize the operation of the power plant in fractional modes at a speed of 7 knots or less, or in case of a failure of the main engine (ME), it is proposed to use an electric drive. In this case the main engine is disconnected from the reduction gear by a coupling.

4 REFERENCES

ADN-2015. (2015) European Agreement concerning the International Carriage of Dangerous Goods by Inland Waterways. [Online] Available from: http://www.unece.org/fileadmin/DAM/trans/danger/publi/adn/adn2015/English/ECE-TRANS-243-corr2-e.pdf . [Accessed: 8th July 2015]

Danube Statistics (2013). Danube Commission. Danube navigation statistics for 2012-2013. [Online] Available from: http://www.danubecommission.org/uploads/doc/STATISTIC/Statistics%202012-2013%20Rev%201%20DE.pdf. [Accessed: 17th November 2015]

Eurostat (2015). Goods transport by inland waterways. [Online] Available from: http://ec.europa.eu/eurostat/tgm/table.do?tab=table&plugin=1&language=en&pcode=ttr00007. [Accessed: 8th of July 2015]

Eurostat (2015a). Navigable inland waterways by carrying capacity of vessels. [Online] Available from: http://appsso.eurostat.ec.europa.eu/nui/show.do?dataset=iww_if_infrastr&lang=en. [Accessed: 1st October 2015]

Linde, Horst, 2008, "Begleittext zur Lehrveranstaltung Binnenschifffahrt", Accompanying notes, TU Berlin.

PINE. Prospects of Inland navigation within the enlarged Europe. [Online] Available from: http://ec.europa.eu/transport/modes/inland/studies/doc/2004_pine_report_report_concise.pdf. [Accessed: 8th July 2015]

MDN. Via Donau. (2007) Manual on Danube Navigation. [Online] Available from: http://www.prodanube.eu/images/stories/downloads/Manual_Danube_Navigation_2007.pdf. [Accessed: 19th November 2015]

schiffundtechnik. Binnenschiffstypen. [Online] Available from: http://www.schiffundtechnik.com/lexikon/b/binnenschiffstypen.html. [Accessed: 8th of July 2015]

IVR Construction (2013). (2013) Years of construction Western European Fleet - Tank & Dry Cargo. [Online] Available from: http://www.ivr.nl/fileupload/statistieken/2013/Years_of_construction_tank_and_dry_cargo_-_2012.pdf. [Accessed: 19th November 2015]

ZKR (2014). The market of the inland water transportation in 2013 and a forecast on 2014/2015. In: market observation European inland water transport, publisher: Central Commission for the Navigation of the Rhine, September 2014, ISSN 2070-6723. [Online] Available from: http://www.ccr-zkr.org/files/documents/om/om14_en.pdf. [Accessed: 8th of July 2015]

5 ATTACHEMENTS

Handbook on technical barge concepts

for use under BSR specific navigation conditions

by Meng Zhang Royal Institute of Technology in cooperation with Technical University Hamburg

Chemical tanker concept project of re-equipment

by Klaipeda Science and Technology Park in cooperation with Western Baltic Engineering BLRT Grupp

HANDBOOK ON TECHNICAL BARGE CONCEPTS

for use under BSR specific navigation conditions

Meng Zhang
mengzh@kth.se
2018/2/18

Table of Contents

1. Aim of the Project

The general objective of this project, as specified by the project owner, is to investigate how an inland motor barge based on European standards, Inland waterway (IWW) class Zone 3, can be modified for navigation in Lake Mälaren in ice conditions. The study and development of ice navigation for inland barges is an important step to establish inland navigation in Sweden and the BSR Region.

Within the scope of the target, one specific barge is studied to demonstrate both the potential and problem if it must be adapted to the Swedish IWW environment.

2. Problems and Aspects of Interests

In this chapter, the Inland Waterway transportation associated with winter navigation is presented; the state of the art, pros and cons and the utilization potential for Sweden. The ice-induced problems are identified and issues like the ice load, the ship structural strength performance, potential propulsion problems and vessel operating scenarios are discussed. These are the main topics addressed in this work. In addition, the general information of the barge Amice, which will serve as a benchmark, is given herein.

2.1 Inland Waterway Transportation (IWT)

IWT is, on many European transport corridors, a competitive alternative to road and rail transport, offering a sustainable and environment-friendly mode of transport [1]. IWT is still under-utilized (Figure 12) and faces a number of traditional and new challenges from infrastructure, institutional, legal and technical barriers, which call for pro-active policies by Governments and international bodies [2].

For Sweden, a country characterized by its long coastline and its geographical situation, the Short-Sea Shipping constitutes a significant part of the infrastructure, connecting land based transportation modes to neighbouring countries, as shown in Figure 13. Due to its potential towards reducing road traffic congestion, air pollution, noise emissions and accidents, there is an increasing demand for development of IWW. Following some debates over the last years, the Swedish Authorities have implemented the EU Directives (TSFS 2014:96) into the Swedish legislation in year 2014, thus providing new conditions for an increased utilization of Swedish inland waterways.
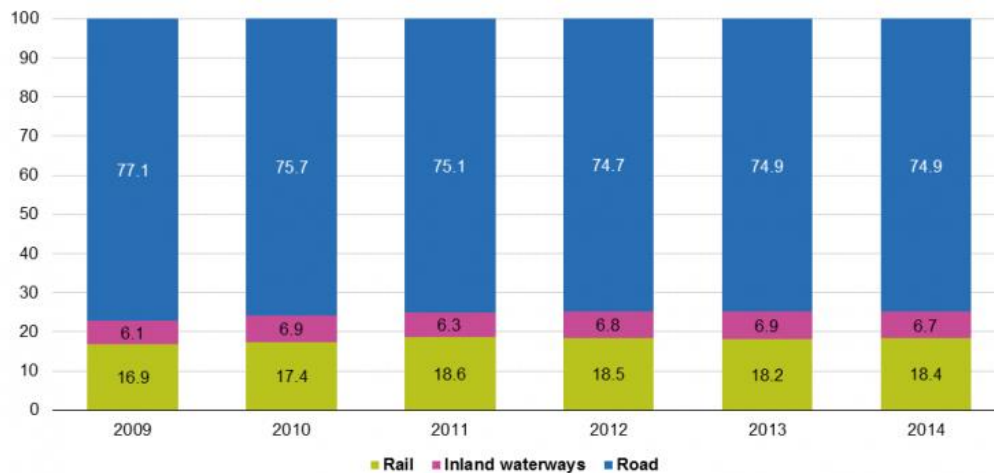
Figure 12 Three modes of transportation and their shares estimations (source: Eurostat)
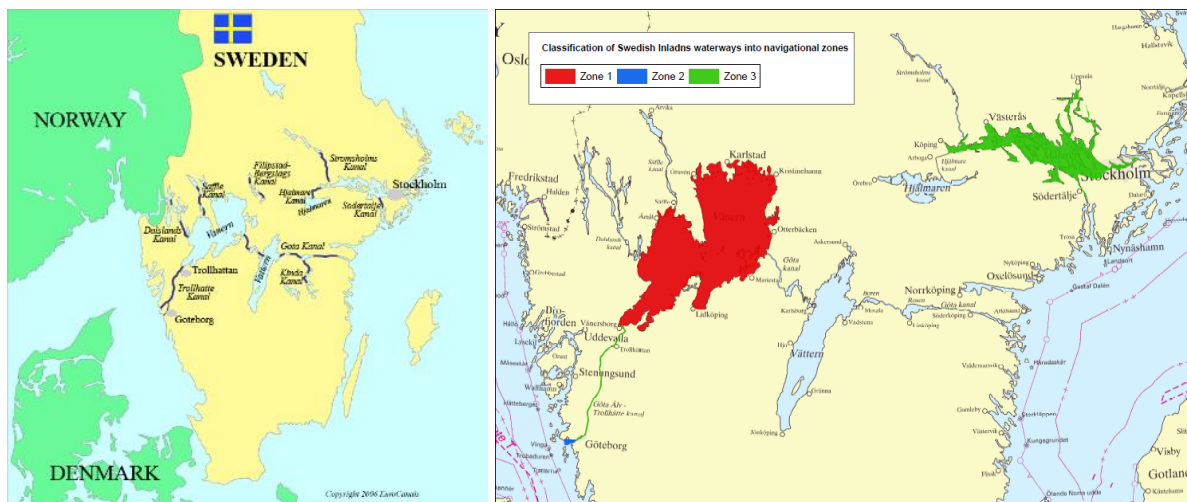
Figure 13 Swedish IWW and class zones

Ice bound shipping poses more safety issues compared to shipping under non-ice conditions. Over 45% of the Baltic sea can be covered in ice during winter time [3]. For Nordic countries like Sweden, lakes and rivers are covered with ice during winter time which can last for four or five months depending on the latitude. For ships operating in inland waterways, winter conditions impose a great potential hazard as ship structures designed for IWW are relatively weaker than for sea going vessels based on the classification societies as the wave and wake are insignificant compared to sea conditions. Since ice loads are not accounted for by classification design rules for IWW vessels, the transit in IWW is put on hold during periods with ice covered waters for countries like Germany, Sweden etc. One of the key issues associated with winter condition is ice (e.g. level ice, brash ice) generated on the water surface. The impact load from floating ice blocks can be dangerous to ship structures and can induce additional cost due to extra reinforcement and maintenance, which makes the ship non-profitable for long term operation. In order to make sure the structural strength is sufficient enough to withstand impacts from collisions, potential impacts between ice and ship structure should be resolved in the early design stage.

However, due to the lack of research and experience on effect of ice on ships in IWWs, it is not an easy task to determine the ice load acting on the ship structure. In addition, the known existing studies are more related to hull-ice interaction behaviour in sea ice that cannot be applied directly since the ice type and thickness vary broadly.

2.2 Problems Caused by Ice

The presence of ice on the water surface exerts huge issues on ships running through the water area. Demonstration of the ice-covered waterway can be seen in *Figure 14*.

Figure 14 Ice -covered inland waterways

The main research aspects focus on the following four aspects with regards to the ice-induced problems:

- Ice Load: including finding out the ice properties and predicting the load impact load based on ice condition in Lake Mälaren;
- Structural Strength Performance: evaluating structural strength problems both from global and local aspects;
- Potential Propulsion Problems: find out relationship between ship speed and ice thickness (h-v curve).
- Vessel Operating Scenarios: decide how many days the barge can operate under certain ice conditions.

2.3 The Barge Under Study: Amice Barge

As a case study the Amice barge is chosen. This already existing barge is designed based on DNV GL IWW notation where ice loads are not considered, i.e., the ship is not designed to operate under ice conditions. Thus, to study the influence of ice is important in order to bring the barge into Lake Mälaren. The figure and main particulars of the barge can be seen in Figure 15.

Amice	
L	135,00
B	11,45
D	4,25
Vmax	13,70
draft	3,40
W(kW)	1588,00
Tonnage(tons)	3938,00

Figure 15 The Amice barge and main particulars

3. Lake Mälaren - Ice Information

The first thing is to identify the specific ice conditions for Lake Mälaren, including ice thickness, salinity, type etc. Those factors will influence the ice mechanical properties. This chapter summaries the available ice information on Lake Mälaren and associated ice properties. Four datasets of ice thickness are collected from SHMI. The statistical analysis is used to achieve the significant ice thickness using these four datasets. Estimated ice properties are calculated on basis of an empirical formulae together with reference data.

3.1 Ice Data From SMHI

Ice data (include form and thickness) for Lake Mälaren is extracted and summarized from Swedish Meteorological and Hydrological Institute (SMHI,2018) website [4], as shown in *Figure 16 - Figure 19*.

Daily data are only available since year 2007. A detailed ice research study is performed for one mild winter in 2017, one normal winter in 2013 and one severe winter in 2011. All the days with ice on the lake are analysed, as shown in *Figure 16 - Figure 18*. The yearly maximum ice thicknesses from 1980 are summarized; as shown in Figure 19. It can be observed clearly that

fast ice, new ice and level ice are the dominant ice types and the thickest ice occurs in early Spring. In Lake Mälaren, ice usually appears in December and vanishes in April. During harsh winter, the thickness can be up to $0.45\,m$ which is twice during the mild winter. In general, the ice thickness recorded by the SMHI shows a maximum value of $0.5\,m$. According to Tõns [5] and based on measurement on Northern Sea Route (NSR), first-year ice can be divided into three sub-groups: thin first-year ice $(0.3 - 0.7\,m)$, medium first-year ice $(0.7 - 1.2\,m)$ and thick first-year ice $(1.20 - 2.0\,m)$. By using analogous classification, the recorded data indicates that thin first-year ice is the concern for this study.
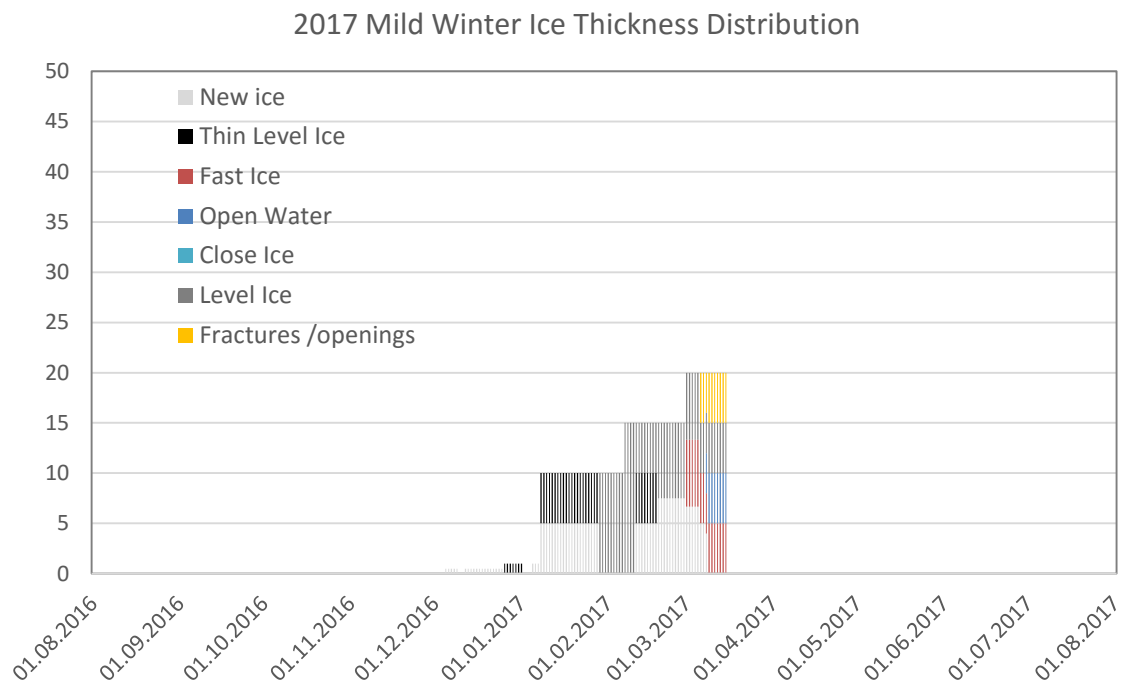
Figure 16 2017 Mild Winter Ice Thickness Distribution (unit: cm)
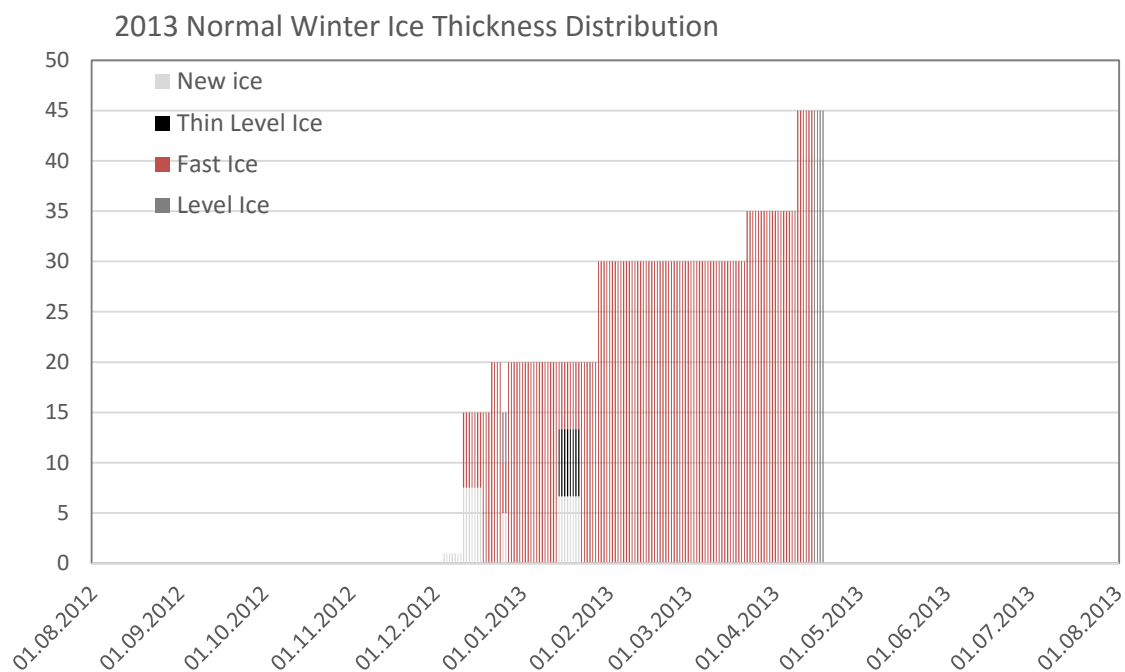
Figure 17 2013 Normal Winter Ice Thickness Distribution (unit:cm)
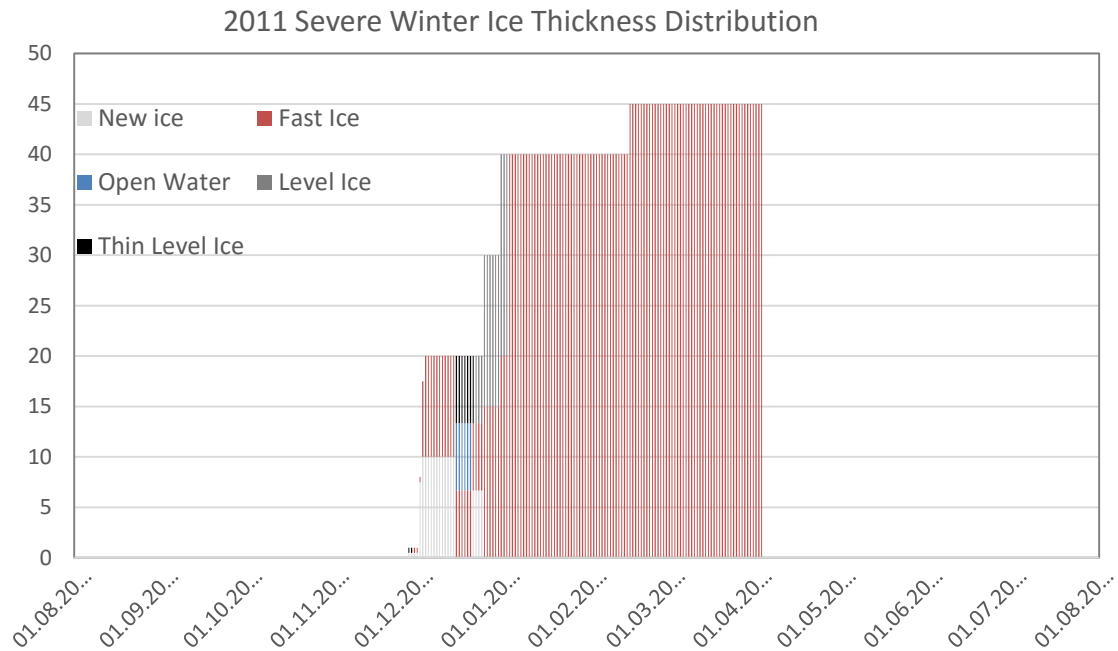
Figure 18 2017 Mild Winter Ice Thickness Distribution (unit:cm)
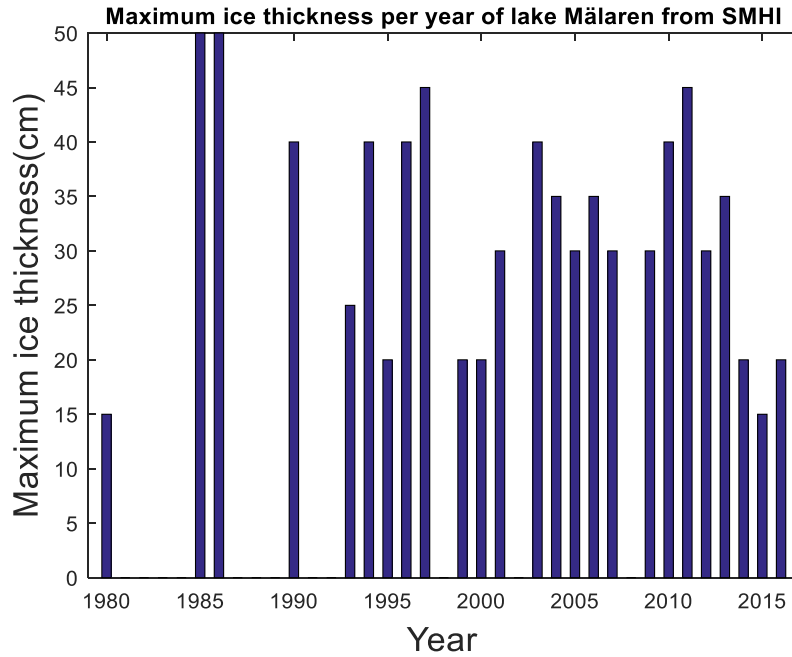
Figure 19 Maximum ice thickness per year recorded from SMHI for Lake Mälaren

3.2 Ice Thickness (h)

Ice thickness is the most important factor for estimating ice impact loads on a ship hull. Even though the maximum thickness can be depicted from the histogram, as shown in *Figure 19*. An average\mean value per year or over the past decades is needed to describe the significant characteristic of ice thickness. Due to the stochastic nature of ice thickness, a statistical study can be applied. Several methods are available and could be used to fit the ice thickness data.

Here we choose four sets of data to be analysed, single year data from 2011, 2013, 2017, and 20-years data. The Weibull distribution fits well for all datasets, results are given in Figure 20 and Figure 21. The Probability Distribution Function f(x) PDF, Cumulative Distribution Function F(x) CDF and mean value E(x) can be expressed as follows,

$$f(x) = \begin{cases} \dfrac{k}{\lambda}(\dfrac{x}{\lambda})^{k-1}e^{-(x/\lambda)^k} & x \geq 0 \\ 0 & x < 0 \end{cases} \tag{1}$$

$$F(x) = \begin{cases} 1 - e^{-(x/\lambda)^k} & x \geq 0 \\ 0 & x < 0 \end{cases} \tag{2}$$

$$E(x) = \lambda\Gamma(1 + 1/k) \tag{3}$$

where k is the shape parameter and λ is the scale parameter. The estimated parameters for four datasets of Weibull distribution using Maximum Likelihood Estimation method are given as in Table 4.

Table 4 Estimated parameters for Weibull distribution fit

dataset	k	λ
20 years	35.7	3.5
year 2010-11	38.4	3.3
year 2012-13	30.6	3.8
year 2016-2017	15.4	3.9
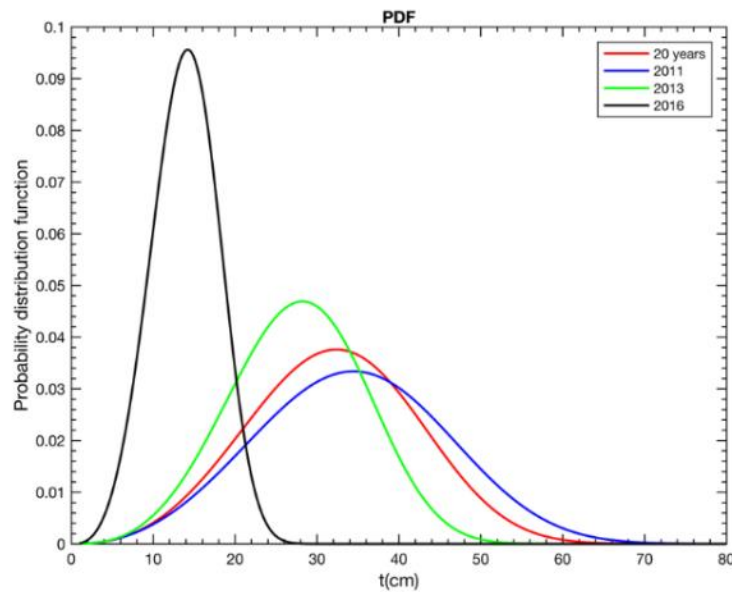
Figure 20 Weibull distribution PDF of ice thickness

Figure 20 shows the Cumulative Distribution Function for four datasets. It shows the thickness distributions vary for different years. In reality, ice thickness data is continuous, while the recorded ice thickness is a discrete random variable. However, *Figure 20* is useful to read the possibilities of different ice thicknesses.

Figure 21 gives the Cumulative Distribution Function plots for four datasets with regards to ice thicknesses. Three statistical distributions are selected to fit the datasets: Weibull distribution, Gumball distribution and Exponential distribution. Wafo toolbox is installed in Matlab. The ice thickness data is imported and Maximum likelihood estimation method is used to derive the parameters for the three distributions. The CDF plots are generated based on estimated parameters. Those plots are shown in *Figure 21* and compared with the empirical CDF from recorded data. It can be seen that Weibull distribution fits well for all datasets.

Figure 21 CDF plot using different statistical methods (a) Data for 20 years ice thicknesses. (b) Data for year 2011 ice thicknesses. (C) Data for year 2013 ice thicknesses. (d) Data for year 2017 ice thicknesses

Figure 22 illustrates the empirical CDF, Weibull CDF, histogram of ice thickness for 20-year dataset. In addition, the 4th subplot is the Weibull line plot which is used to verify whether Weibull distribution is ideal for predicting the ice thickness distribution. The processes can be seen below.

1. Assume ice thickness is of Weibull distribution

$$F(x) = 1 - e^{-(x/\lambda)^k} \tag{4}$$

2. Assume $F_n(x)$ is the empirical distribution,

$$F_n(x) = 1 - e^{-(x/\lambda)^k} \tag{5}$$

3. Take the logarithm of both sides,

$$\ln\big(-\ln\big(1 - F_n(x)\big)\big) \approx k\ln(x) + a \tag{6}$$

4. Plot $X = \ln\big(-\ln\big(1 - F_n(x)\big)\big)$ in x-axis, $Y = ln(x)$ in y-axis.

If the data points are approximately lying along a straight line (see Fig.11, the 4th subplot), it means that the data is Weibull distributed. From Figure 23, it shows that all data can be regarded as Weibull distributed.
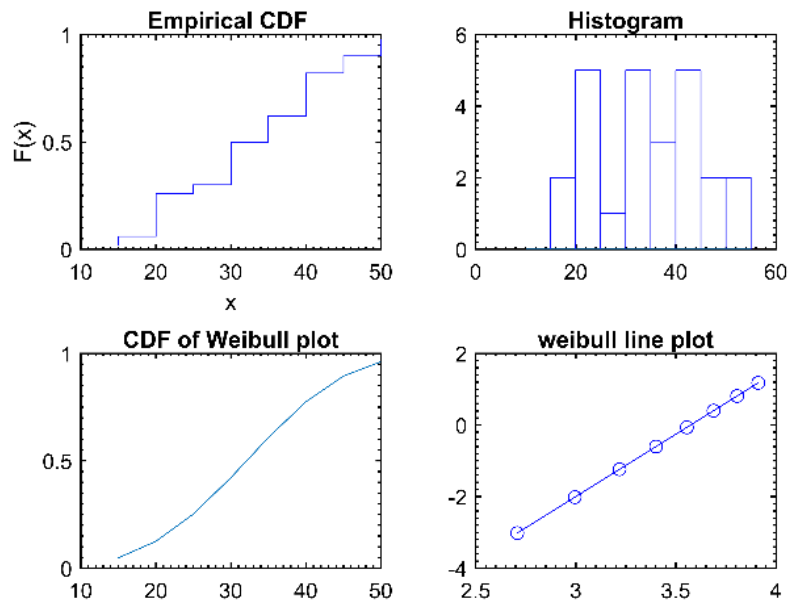
Figure 22 Plots for 20-years data

Base on SMHI records, the statistical analysis and FSICR, the ice thicknesses are summarized in *Table 5*. These data have different meanings and can be used for different estimation purposes. In this report, $H = 0.32m$ from statistical analysis is used to determine the ice floe size for probabilistic approach, while $H = 0.22m$ according to requirement from FSICR IC is used when deciding the design load height using rules.

Table 5 Ice thickness summary (unit: cm)

Source	Type	20 years	2011	2013	2017
Statistics	Mean	**32.10**	34.46	23.53	13.91
SMHI	Maximum	**50**			
FSICR	Ice class IC	**22**			[Section 4.1]

(b)

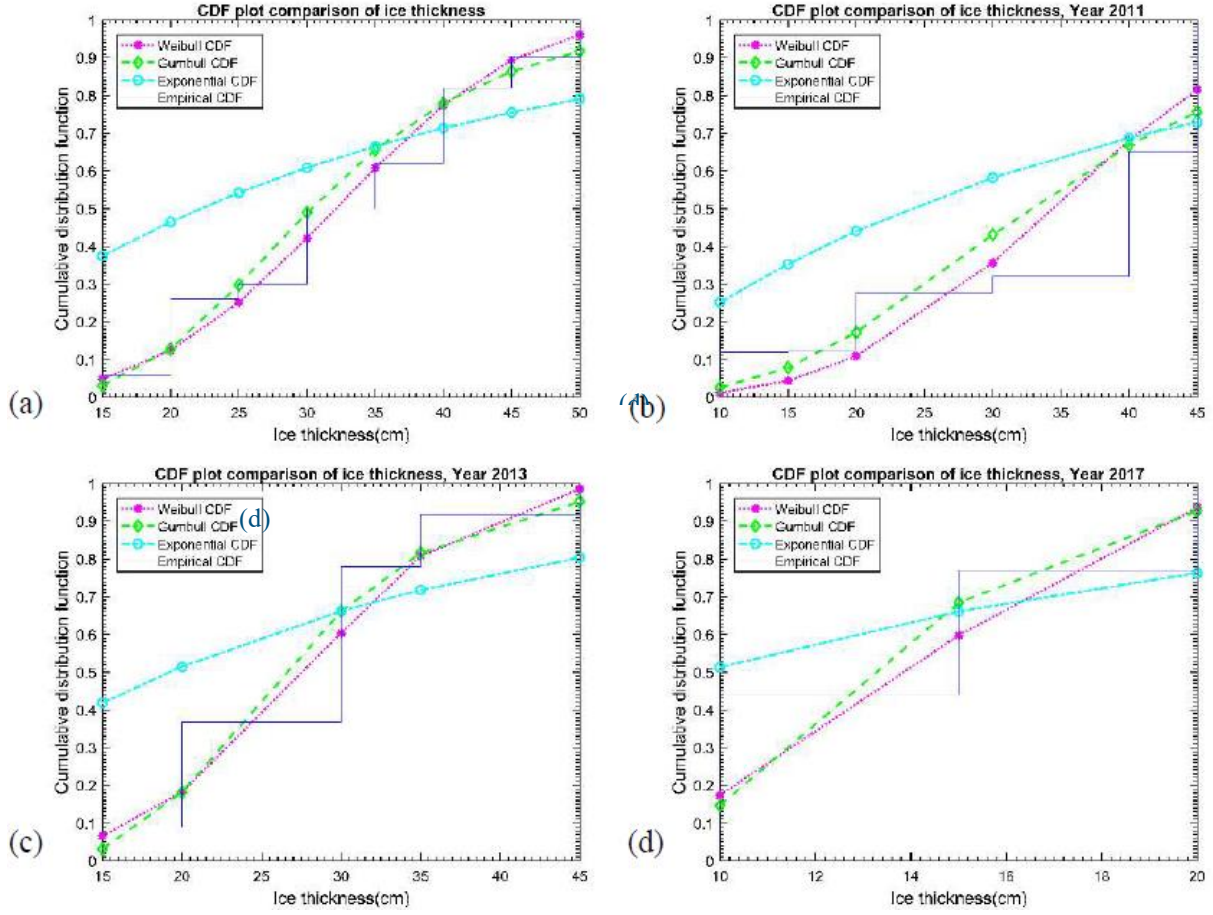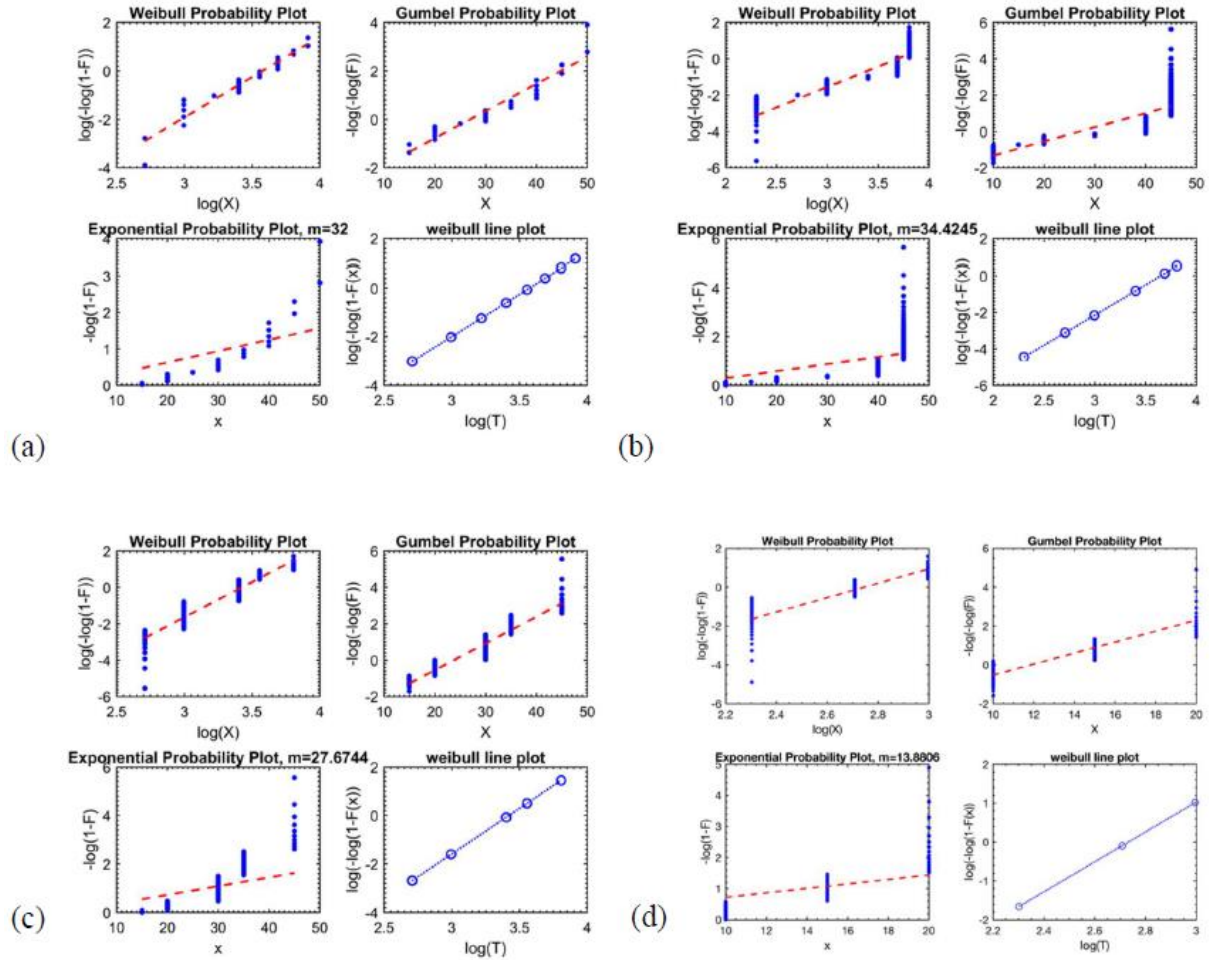*Figure 23 Statistical fit for (a)Data for 20 years ice thicknesses. (b) Data for year 2011 ice thicknesses. (C) Data for year 2013 ice thicknesses. (b) Data for year 2017 ice thicknesses*

3.3 General Ice Properties

Ice is a geophysical material. It is

- non-homogeneous (varying grain size and distribution of impurities);
- non-isotropic (since the temperature gradient affects mechanical properties);
- orthotropic (because its strength depends on crystal structure orientation) [6].

Ice properties will affect the hull-ice interaction and the ice load acting on the structure. Ice is in nature a complex material and it is difficult to determine its mechanical properties, which makes the flexural strength difficult to measure.

Researchers have performed a lot of research investigating and formulating the ice properties. As Lake Mälaren has fresh water, brine volume is zero, the corresponding properties can be summarized using the formulae below [7][8],

$$\rho = 920\ [\frac{kg}{m^3}] \tag{7}$$

$$E = 10^9\ [Pa] \tag{8}$$

$$v = 0.3 \tag{9}$$

$$\sigma_t = 4.278 v^{T^{-0.6455}} \tag{10}$$

$$\sigma_f = 1.76 e^{-5.88\sqrt{v_b}} \tag{11}$$

$$\sigma_c = 37(\dot{\varepsilon})^{0.22} \left[1 - \sqrt{\frac{v_T}{270}} \right] \tag{12}$$

$$\sigma_{pc} = \frac{0.065}{\sqrt{A}} \text{[MPa]} \tag{13}$$

where ρ is density, E is Young's modulus, v is Poisson ratio, σ_t is tensile strength, σ_f is flexural strength, σ_c is compressive strength, σ_{pc} is crushing strength, V_b is brine volume, V_t is the total porosity.

The flexural strength of ice on Lake Mälaren is 1.76 MPa according to the Eq.11 for fresh water as brine volume $V_b = 0$.

$$\sigma_f = 1.76 \text{ MPa} \tag{14}$$

However, from *Figure 24*, it can be seen clearly that flexural strength for water with root brine volume under 0.1 doesn't have sufficient data and research. $\sigma_f = 1.76\ MPa$ is not reliable. When calculating the ice-induced resistance from Riska method, the fresh water-ice flexural strength is usually taken as 500kPa [9].
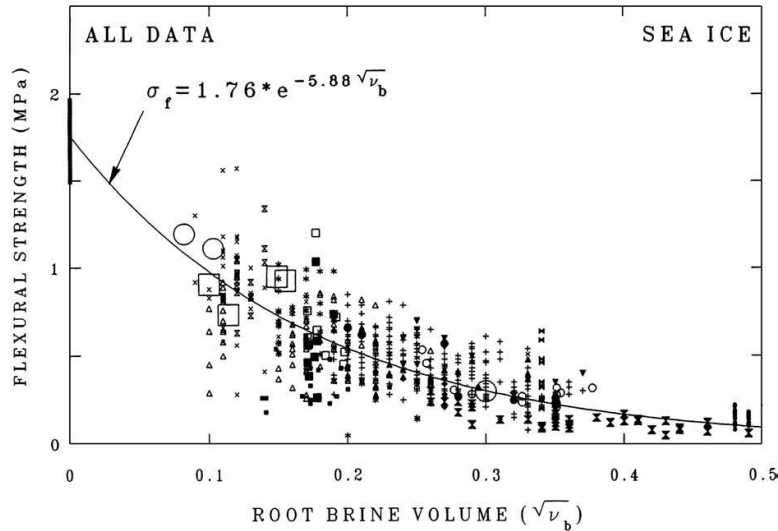
Figure 24 Flexural strength versus the square root of the brine volume for first-year sea ice [7]

The ice flexural strength, σ_f, is important when trying to calculate the ice impact load. Based on the past research, some data is gathered and summarized in terms of σ_f, ice thickness, and ice types, as shown in *Table 6*, *Figure 25* and *Figure 26*.
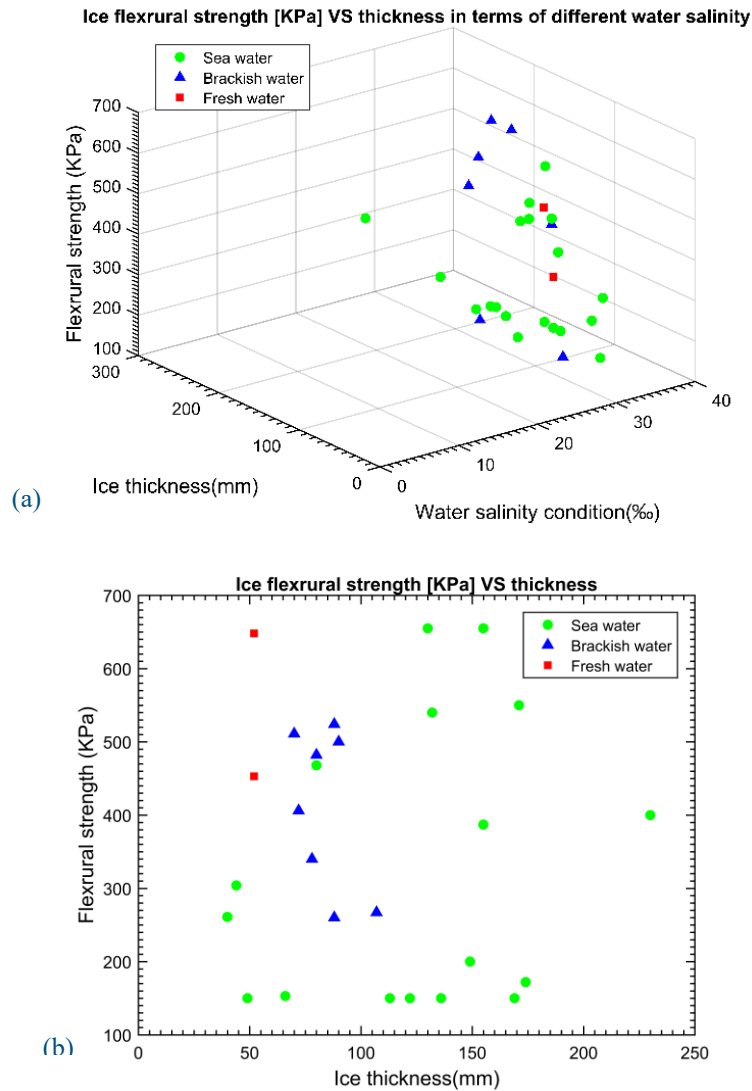
Figure 25 Ice data plots include info on thickness, flexural strength, salinity, (a) 3D plot consists of info on ice thickness, flexural strength, and salinity, (b) 2D plot.

Table 6 Reference data in terms of σ_f, h, salinity [5][17].

Ship	Date (Yeat/month)	Location and water	Ice	Flexural Index σ_f (KPa)	Ice Thk. (m)	T (°C)
FRANKIN	80-01	Lake Melville(B)	L,C,M	511	0.62-0.70	-5
	80-03	Lake Melville(B)	L,M	260	0.74-0.88	0
Pierre Radisson	78-07,08	Baffin Bay(S)	L,M	<150	0.80-1.22	0
	79-02	ST. Lawrence (S/B)	L,M	407-524	0.16-0.88	-12
Arctic	86-05,06	Baffin Bay(S)	L,C	<150	0.85-1.13	-4
	86-06	Strathcona Sound(S)	L,C	<387	1.02-I.55	-4

	80-10	LANCASTER SOUND(S)	L, M	304	0.33-0.44	-12
	81-02,03	Lake Melville(B)	L, M	267	0.58-I.07	0
PolarStern	84-05,06	Hebron Fjord(S)	L,C,M	<150	0.90-1.22	-5
PolarSea	84-01	McMurdo Sound(S)	L	172	0.94-I .74	-10
/Star	82-04	BERING SEA SOUTH(S)	L	<150	0.18-0.49	1
		BERING SEA NORTH(S)	L	261	0.30-0.40	-16
	85-04	McMurdo Sound(S)	M	200	1.12-I .49	
L S ST. Laurent	79-07	Strathcona Sound(S)	M	<150	0.74-I .36	
OTSO	86-03	Baltic Sea(B)	L, C	330-482	0.6S-0.8	
Katmai Bay	79-01,02	Great Lakes(F)	L,C,M	648	0.32-0.52	-20
Oden	89-03	Baltic Sea(B)	L,C,M	406	0.50-0.70	1
Mudyug	87-04	SPITSBERGEN (S)	L M	370-54	0.49-1.32	
Mobile Bay	86-02	Lake Michigan (F)	L	453	0.27-0.52	-7
ANN Harvey	89-03	North Coast(S)	L,C,M	153	0.40-0.66	-7
Kigoriak	79-10,80-03	BEAUFORT SEA(S)	L,C,R,M,T,P	436-550	0.65-1.71	-30
	80-06	BEAUFORT SEA(S)	L,M	150	1.39-1.69	0
	81-05	BEAUFORT SEA(S)	L R M	NA	1.27-1.37	0
	82-11,12	BEAUFORT SEA(S)	L	444-468	0.66-0.80	-24
Rgbert Lemeur	82-11,12	BEAUFORT SEA(S)	L,C,R,M,	444-469	0.66-0.81	-24
Terry Fox	84-01	BEAUFORT SEA(S)	L,C,M,T	487"655	0.14-1.55	-28
Kalvik	86-08.09	Viscount Melville Sound(S)	L,C,R,M	1.50-400	1.00-2.30	-4
Ikaluk	84-01	BEAUFORT SEA	L,C,M	487-655	0.44-1.30	-22
Max Waldeck	81-03	Baltic Sea	L,C,R,M	450-500	0.30-0.90	
	82-03	Baltic Sea	L,C,R,M	300-340	0.59-'0.78	

Notes: S - ICE FORGED FROM SALINE WATER;   B - ICE FORMED FROM BRACISH WATER;

F - ICE FORMED FROM FRESH WATER;   S/B - DEPENDS ON THE LOCATION IN THE ST. LAWRENCE

L - LEVEL ICE

          M – MANOEUVERING

C – CHANNEL

          T – TRANSIT

R - RIDGES

          P – PROPULSION/ICE INTERACTION
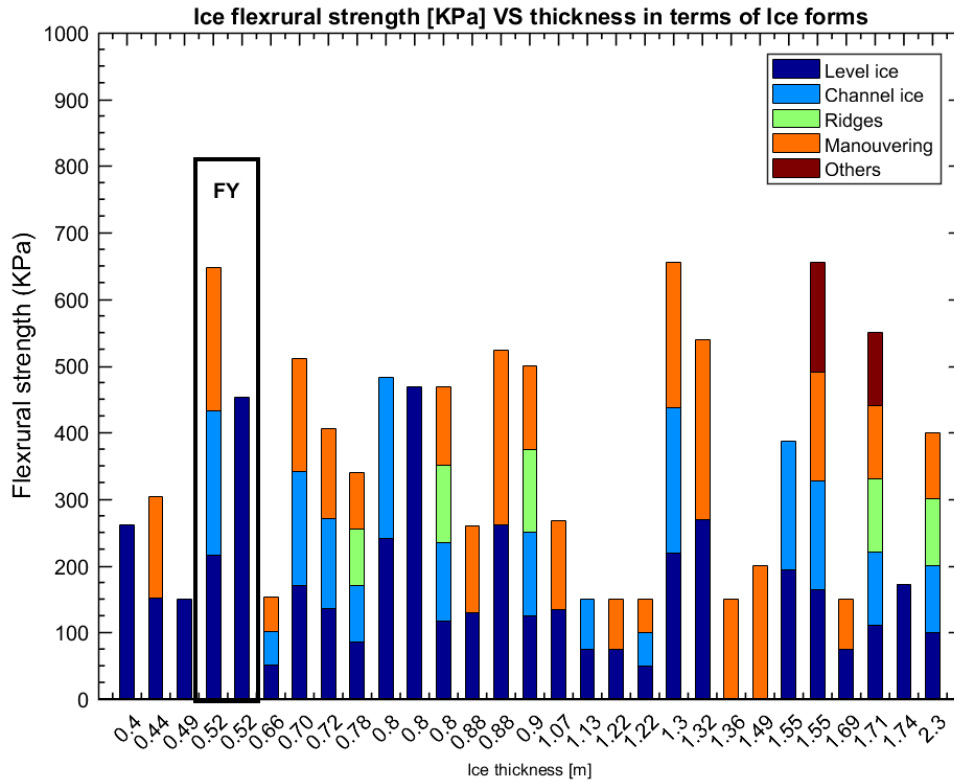
Figure 26 Ice data plot includes info on thickness, flexural strength, salinity, and forms (FS: First Year ice)

The first thing that can be observed is that σ_f for sea water has a large scatter in *Figure 25* as ice types and thicknesses have large scatter. The dataset consists of a narrow range of brackish water ice where σ_f changes from $280KPa$ up to $540KPa$. Only two datasets with respect to fresh water ice are available from literature. Both datasets have a thickness of $50cm$, which is same as the maximum ice thickness in Lake Mälaren. However, σ_f values have large variations. One possible reason can be revealed from *Figure 26*, which shows the ice type plays an important role in influencing the σ_f value. In *Figure 26*, the colour contour only indicates the existing ice types under the measurement. The height of the bar gives ice flexural strength in terms of ice thickness. The study in section 3.1 shows fast ice, new ice and level ice are the dominant ice types in Lake Mälaren. By only investigating level ice instead of all forms will provide a conservative result. Nevertheless, the data from Great Lakes can be utilized for Lake Mälaren since similar ice conditions can be found in literature, both with level ice and 50cm of thickness.

To conclude from Table 3: for ice thickness of 0.5m, the flexural strength of pure level ice can be taken as: $\sigma_f = 453KPa$. For a conservative assessment, $\sigma_f = 648KPa$ can be used as equivalent strength which considers a complicated composition of ice forms.

Table 7 Ice Properties

Factor	value
H	$0.32m$
σ_t	$167KPa$

σ_f	$1.76 Pa$
σ_c	$738 KPa$
σ_{pc}	$196 KPa$

4. Issue I: Ice Load

Two approaches are used to predict the impact load: the deterministic approach and the probabilistic approach. The deterministic approach is suitable when all variables are known and it refers to traditional rule-based design. As for first year thin ice condition, FSICR (Finnish Swedish Ice Class Rules) is the most practicable one identified. The probabilistic approach may be used when some crucial variables are unknown, e.g. ship geometry and ice-ship interaction process. In this approach, these parameters can be interpreted as random variables.

This part focus on the probabilistic design method. Firstly, the design contact area and high-pressure area are calculated. Then, a direct calculation is preformed based on inputs from previous research and references. A more thorough calculation is made where two reference methods are used, Taylor [10] and Rahman [11]. The two methods differ in the way they account for different exposure conditions. In addition, these two different operation scenarios are considered, one single trip and one full year operation. And finally, the design curve presenting the relationship between design pressure and design contact area valid for Lake Mälaren is proposed. This can be expressed as $\alpha = 0.265a^{-0.57}$ where α is the design pressure and a is the design ice-ship contact area.

4.1 Deterministic Design - Classification Rules

4.1.1 Requirements based on FSICR

The current version of Finnish Swedish Ice Class Rules(FSICR) [12] includes requirements for hull, machinery and minimum propulsion power. The strength level of four available ice classes (IA Super, IA, IB, IC) corresponds roughly to loading from a certain level of ice thickness. The design scenario is a collision on ice channel edge having a minimum speed of 5 knots, with yield design state.

For Lake Mälaren, the ice class IC is used and the design requirement for this ice class correspond to operation in brash ice channels with a thickness of $0.6m$ ($H_M = 0.6m$). The ship is assumed to operate in open sea conditions corresponding to a level ice thickness not exceeding $0.4\ m$ (h_0). The design ice load height (h) of the area actually under of ice pressure is assumed to be $0.22\ m$.

The definition of ice pressure and ice load is an integral part of the hull factors. The design pressure is defined by,

$$p = c_d \cdot c_p \cdot c_a \cdot p_0 \tag{15}$$

where p_0 is nominal ice pressure $5.6\ MPa$. It is constant for all ice classes, as the ice properties throughout the Baltic Sea do not change significantly during an average winter; c_d is a factor that takes into account the influence of displacement, Δ, and engine power of the ship, P. It is given as,

$$c_d = \frac{a \cdot k + b}{1000} \tag{16}$$

$$k = \sqrt{\frac{\Delta \cdot p}{1000}} \tag{17}$$

19

The value of a and b are defined according to value of k and the designed hull. Factor c_p adjusts the design pressure in accordance to hull region where it occurs. Ship is divided into bow, mid-body and stern regions and c_p values range from 1.0 (bow region for all ice classes) to 0.25 (stern region for IC ice class). The last factor c_a is dependent on the load length that influences response in each structural member. It is calculated as,

$$c_a = \sqrt{\frac{l_0}{l_a}} \tag{18}$$

with maximum 1.0, minimum 0.35, $l_0 = 0.6 \, m$.

The elastic response of the plating can be express as,

$$P_{PL} = \frac{9}{4} \left(\frac{t}{s}\right)^2 \frac{\sigma}{1.3 - \frac{4.2}{(h/s + 1.8)^2}} \tag{19}$$

while the plastic response is calculated as,

$$P_P = \frac{16 \cdot t^2 \cdot \sigma_y}{s^2 (\sqrt{3 + (s/L)^2} - s/L)^2} \cdot \frac{1}{0.6701 \cdot (h/s \cdot (s/t)^2) - 0.133 \cdot (h/s \cdot (s/t)^2)} \tag{20}$$

The thickness of the plate can be calculated based on,

$$t = 667 \cdot s \cdot \sqrt{\frac{f_1 \cdot P_{PL}}{\sigma_y}} + t_c \, [mm] \tag{21}$$

where P_{PL} is equivalent plate pressure at $0.75P$.

The frame scantlings can be determined as,

$$Z = \frac{q \cdot s \cdot l_a}{m \cdot \sigma_y} \qquad A = \frac{1}{2} \cdot \frac{1.2 \cdot q \cdot l_a}{\tau_y} \tag{22}$$

The rule-based design pressure can be seen in Table 5.

Table 8 Rule-based design ice pressure for different parts of the barge

Design ice pressure (MPa)	Forward	Midship	Aft
Transverse shell member	1.708	0.655	0.327
Longitudinal shell member	1.611	0.617	0.308

4.2 Probabilistic Design Method

The interaction between the ship and ice is a complex process and depends on the ice properties, the hull geometry and the relative velocity [13]. The local ice pressure is more significant

compared to global forces [14]. In other words, emphasis should be on the local pressure during the design of the ship structure. From Figure 27, the nominal contact area is developed during the whole interaction process, while the area with a higher pressure is smaller than the nominal area [14]. This local area with extremely high pressure has been termed as critical area or High-Pressure Zone (HPZ) [15].
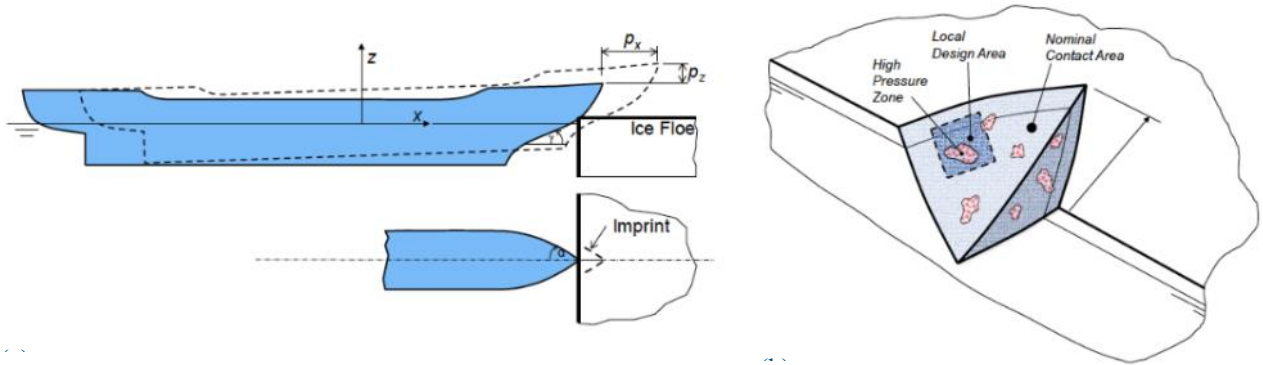
Figure 27 Illustrations of ice interacting with a structure (a) the global and (b) local areas [15]

The ice load affecting area governs the local design of steel plate thickness and spacing as well as the size of bracing[16]. The most important thing to consider when designing the ship structure for ice conditions is the ice load pressure, which allows the assessment of stiffness and strength of the structure under given circumstance.

4.2.1   Description of the Probabilistic Approach

Ice loads acting on the ship structure can be analyzed statistically and extensive research on this topic exists. A detailed survey and analysis on local ice pressures has been conducted and proposed by Masterson and Frederking [16] and developed by Jordaan [14], Taylor [10], Rahman [11] later, which is known as the probabilistic method. By using the data from real ship impacts, field tests and large-scale platforms, the design criteria covering the contact area from 1 m^2 up to 100 m^2 can be developed for large displacement ships and impacts with large ice masses. The pressure data were compiled and ranked, and curves were fitted through the tail of the plots using event-maximum concept.

When analyzing data, extra attention should be paid to the exposure conditions,

    (i)   the number of panels or areas;
    (ii)   the length of interaction for individual events;
    (iii)   the location on the ship or structure;
    (iv)   the number of events (hits or misses), N.

For longer durations (short duration is not covered herein), the distribution may be expressed as a double-exponential (Gumbel) form, i.e.,

$$F_x(x) = \exp\{-\exp[-(x - x_0)/\alpha_1]\} \tag{23}$$

where α_1 and x_0 are constants.

The maximum pressure **Z** per unit time based on one-year measurement can be expressed as,

$$Z = \max(X_1, X_2, \ldots, X_N) \tag{24}$$

where there are N events X_i in the time interval.

The effective event, **m** (hits), is considered by the proportion factor, **r**,

$$m = rn \tag{25}$$

If M and N are random,

$$\mu = rv \tag{26}$$

where n and v are the expected number of events with hits (M) and events (N), respectively, per unit time. Thus, the distribution of maximum **Z** is given by a close approximation (which follows from the distribution of extreme values based on the cumulative distribution with n events) if,

(1) N=n, a fixed number,

$$F_z(z) = \exp\{-\exp[-(z - x_0 - x_1)/\alpha]\} \tag{27}$$

where $x_1 = \alpha(\ln n + \ln r)$.

(2) N is binomial or Poisson-distributed

$$F_z(z) = \{1 - p[1 - F_X(z)]\}^m \tag{28}$$

where p is the probability of an event per trail.

Based on the analysis, the relationship between the local design (nominal contact) area, a in m^2 and pressure α in MPa, can be formulated as,

$$\alpha = 1.25a^{-0.7} \tag{29}$$

The equation is applied to a range of local contact areas $0.6 - 6\ m^2$. It serves as an appropriate upper bound for the local design and is applicable widely during the primary design stage when ice loads are required.

Given the exceedance probability P_e, the design load value Z_e can be estimated as,

$$P_e = 1 - F_Z(Z_e) \tag{30}$$

$$Z_e = x_0 + \alpha\{-\ln[-\ln F_Z(Z_e)] + \ln v + \ln r\} \tag{31}$$

The general form of equation (29) can be rewritten as,

$$\alpha = Ca^D \tag{32}$$

Equation (31) and (32) together establish the foundation of the probabilistic method. The parameters in the formula should be decided according to the real target situation. A series of best-fit curves of equation (32) can be seen in *Figure 28*. It can also be concluded that the pressure is dependent on the physical characteristic of the interaction, such as ice type, thickness, or temperature. Higher C values tend to give rise to data under heavier ice conditions while lower values indicate lighter ice conditions [10].
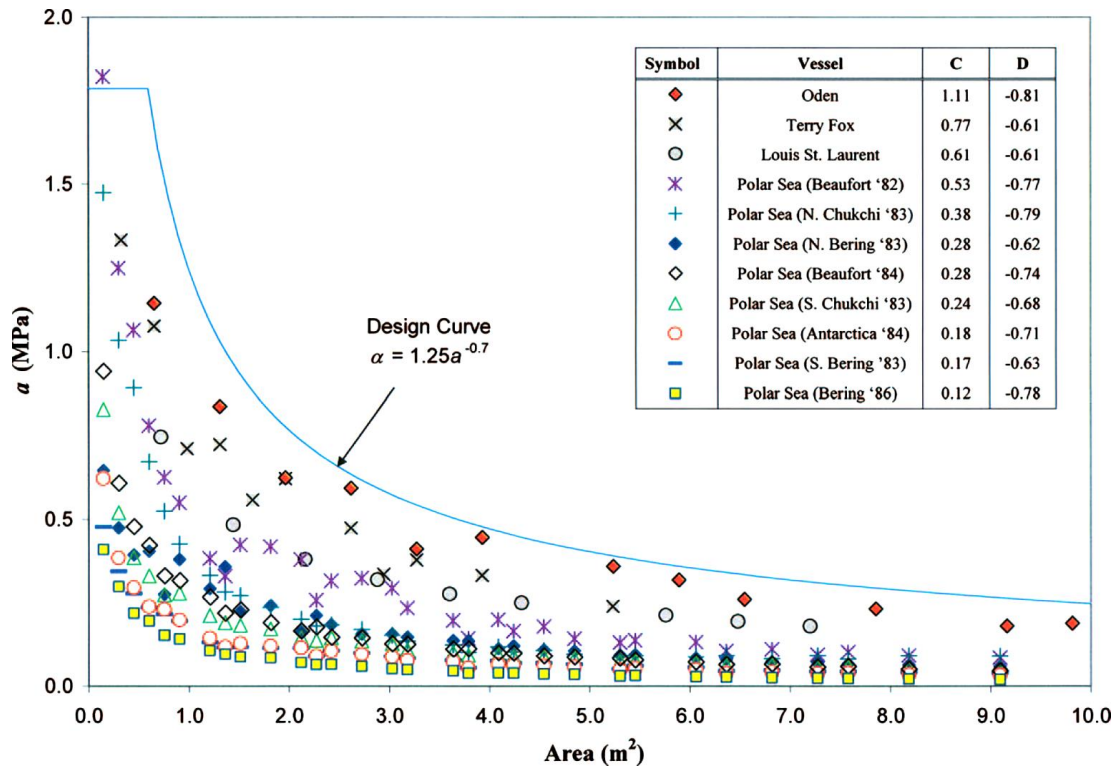
Figure 28 Plots of ice pressure versus area for ship-ice interaction based on different sets of data [10]

As ice conditions vary dramatically between sea and lake with regards to ice type, thickness, salinity etc, the Design Curve cannot be utilized directly to derive the ice loading for light inland waterway ice conditions and will result in an extremely conservative prediction. Thus, the target ice conditions and properties must be studied in order to use probabilistic method. The general approach is given in *Figure 29*. This study is only concerned with first-year thin level ice.
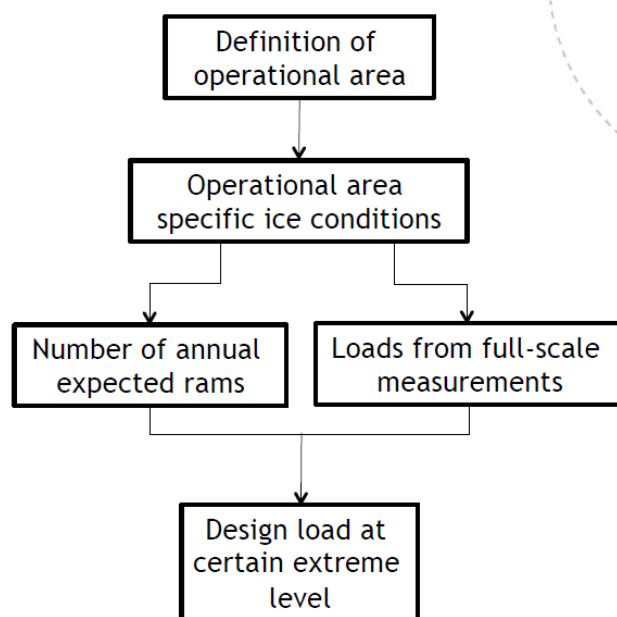
Figure 29 A general review for prediction of extreme loads using parent dataset

As written in Section 3.2, different ice thicknesses can be used, which gives us the corresponding design area A, as shown in *Table 9*.

$$A = s \cdot h \tag{33}$$

where s is the frame spacing, equals to 1.8 m.

Table 9 Design contact areas on the panel

	FSICR	Statistics	SMHI
h (m)	0.22	0.32	0.5
A (m²)	0.396	0.576	0.9

4.2.2 Determination of local High-Pressure Zone (HPZ)

The extreme loads can be found on a small local area, which has to be distinguished from the nominal area, see Figure 27. As the probabilistic method predicts the extreme load pressure, the HPZ needed to be identified in order to get the extreme loading force.

The analysis of ice edge failure is idealized by using a 2D model (Figure 30) to define the contact height, h_c and contact length l_c [8]. Then, High Pressure Zone A_c, under consideration, can be formulated as,

$$A_c = h_c \cdot l_c. \tag{34}$$
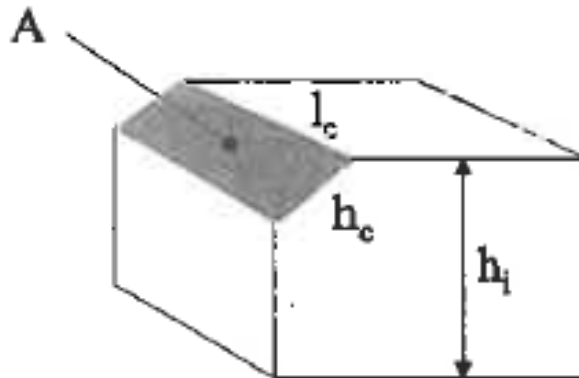
Figure 30 Definition of high-pressure contact area

Noting the maximum open water speed as v_{ow} and the maximum level ice breaking capability as h_{max}, the ship speed, v_i in level ice, with ice thickness, h_i, can be described as,

$$
\begin{aligned}
v_i &= v_{ow}\left(1 - \frac{h_i}{h_{max}}\right), & h_i \leq h_{max} \\
v_i &= 0, & h_i \geq h_{max}
\end{aligned}
\tag{35}
$$

where $v_{ow} = 11.3\ knots$ for loaded condition, h_{max} is assumed to be the ice thickness h_i under consideration, here taken as 0.32m based on FSICR (Table 6).

According to Kujala et al. [13], the contact height required to produce a bending failure is related to the variables: ice thickness h_i, ice flexural strength σ_f, and compressive crushing strength σ_{pc},

$$h_c = \frac{a_1(1 + 1.5(v_i sin\alpha_w)^{0.4})hi^{1.7}\sigma_f}{(\beta_n - 8.7^o)\sigma_{pc}}, \beta_n > 8.7^o \tag{36}$$

where $a_1 = 7.02$ when SI-unites are used for the variables; β_n is the normal frame angle, such that $\beta_n = 55°$; α_w is waterline angle, $\alpha_w = 45°$; h_i is ice thickness, here takes as 0.32m.

By using the global contact area (frame spacing× mean ice thickness), nominal contact area and HPZ are obtained as,
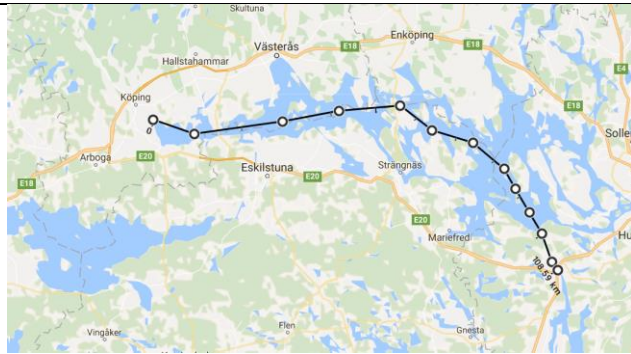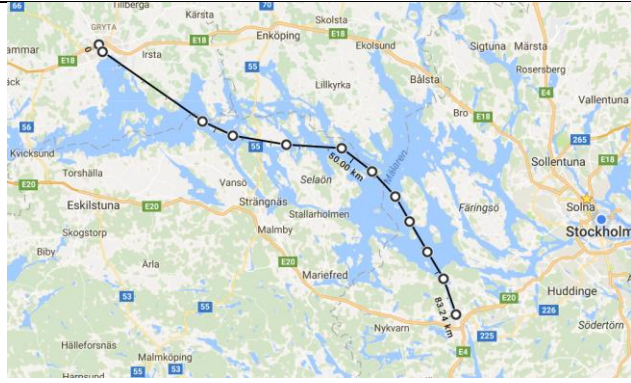
$$\begin{aligned} Base\ on\ statistics, h_i = 0.32m\,, h_c = 0.192m,\ A_c \\ = 0.096m^2, \\ Based\ on\ FSICR, h_i = 0.22m\,, h_c = 0.119m,\ A_c = 0.060m^2. \end{aligned} \tag{37}$$
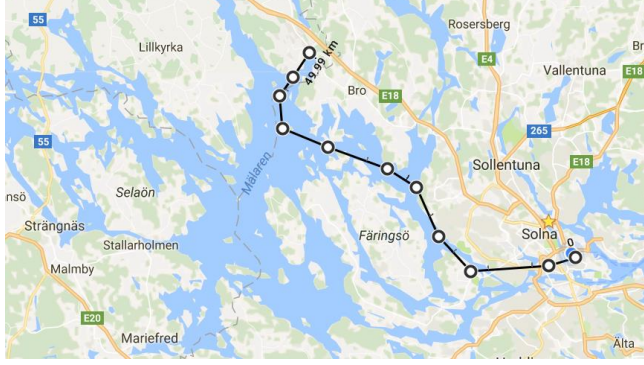
As mentioned in the beginning of this chapter, the design pressure curve is related to nominal contact area. Then extreme pressure can be gained by utilizing the parent curve. To obtain the extreme load, the predicted high pressure and local High Pressure Zone should be combined together.

4.2.3 Direct calculation without modification for ram number

A scenario based on the example routes are provided to show implementation of the method. Regarding the routes, three alternatives are given in Table 10.

Table 10 Planned Routes for Amice barge

Route	map	Approx. distance(km)
1. Södertälje to Köping		110
2. Södertälje to Västerås		85

3. Stockholm city to Bålsta.		50

The longest route chosen is from Södertälje to Köping, i.e. the western end of Mälaren to the eastern. Thus, the ice condition taken into consideration is from the western part as it suffers the worst winter condition. The speed of Amice when empty is 13.7 knots and when loaded with 3500 tons of cargo and a draft of 3.40 is 11.3 knots. It has a duration of 5.2 hours per trip in loaded condition.

Let's assume that the ship operates daily doing a return trip during one year. The ice-covered period for the lake is 4 months. Assumptions of stationary ice conditions and ice concertation of 0.5 are made. The mean frequency of loading events is assumed to be $1.07 \ s^{-1}$ [19]. Using the event duration of $0.934s$, calculated from Kujala (2009) with a poisson process, the expected number of events is 1.11 million.

Design load patch height for FSICR is determined based on the loading height (class factor) and structural arrangement. For IC, the loading height is 0.22 m. Along with, for example, webframe spacing of 1.8 m, it gives the design pressure patch area of $0.396 \ m^2$. The ship is designed for an exceedance level (P_e) of 10^{-2}, which corresponds to the design recommendation in FSICR, i.e., reaching the yield limit once every winter. The proportion of true hits is taken as $r = 0.5$. Exposure constant, x_0, dependent on the design area is calculated according to Taylor et al. (2009) for N. Bering 1983 dataset. With 1.11 million events along the route and using Equation 38, the number of ram is,

$$\mu = v \cdot r \cdot \frac{t}{t_k} = 1.11 \times 10^6 \times 0.5 \times \frac{0.9037}{0.7} = 7.378 \times 10^5 \tag{38}$$

The corresponding design pressure for a 10^{-2} target exceedance probability, α, μ and x_0, is given as,

$$
\begin{aligned}
Z_e &= x_0 + \alpha\{-\ln[-\ln F_Z(Z_e)] + \ln v + \ln r\} \\
&= 0.27 + \alpha(4.6 + \ln(7.378 \cdot 10^5)) \\
&= 0.27 + 5.07 \cdot A^{-0.62}
\end{aligned}
\tag{39}
$$

Using(a) $\alpha = 0.28A^{-0.62}$ for North Bering Sea 1983 dataset and (b) $\alpha = 0.12A^{-0.75}$ for Bering Sea 1986 dataset, with corresponding values of x_0 and design area A, the design curve is obtained, and the design pressures can be calculated.

For design area of 0.396 m^2(*Table 9*, the smallest one gives the highest pressure), x_0 is equal to 0.27 and the design pressure ranges from 9.27 MPa to 4.62 MPa for the bow area, see *Figure 31*.

Local pressure design curve for the chosen route
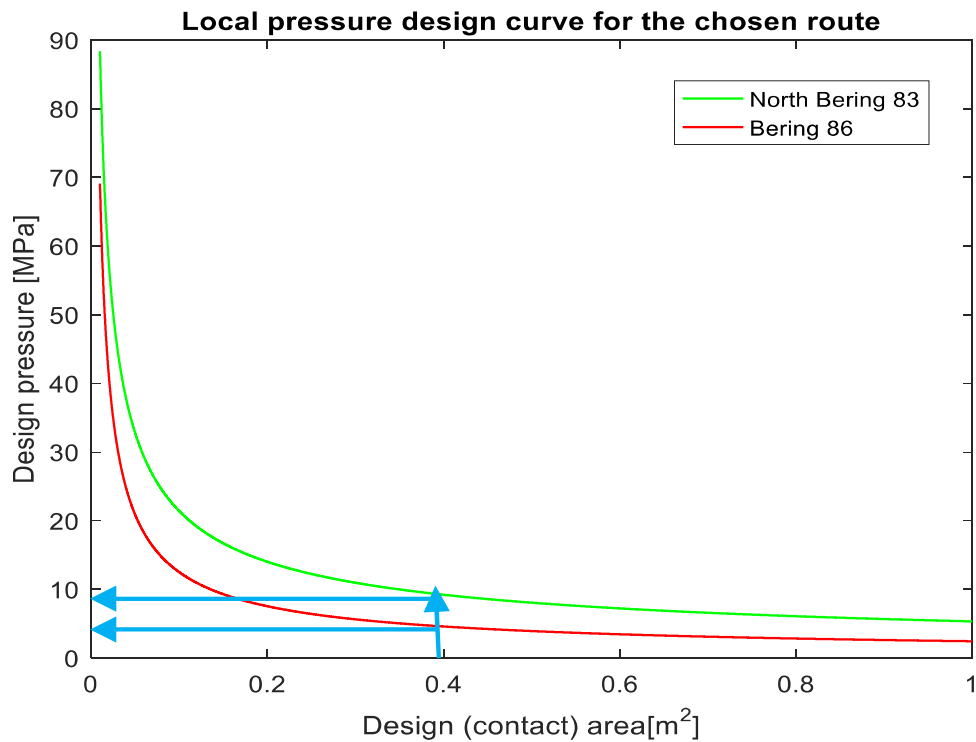
Figure 31 Local design pressure estimation for Amice barge based on two reference datasets

4.2.4 Calculation with modification for rams

One single trip (Section 4.2.3.1 and 4.2.3.2) and one-year (Section 4.2.3.3) design scenarios are used in this part utilizing two design methods (Taylor, 2010 and Rahman, 2005). Different design strategies are considered as well, which are useful to identify the effects from different parameters.

- *Taylor et al., 2010*

In consideration of the physical weather and ice conditions, North Bering Sea 1983 dataset is selected to predict the extreme ice load [10]. The information with regards to the test is given in Table 11.

Table 11 Information of reference dataset [10]

factors	value	ice concentration	Range	value
X_0	0,27	C_L	0,4-0,5	0,5
C	0,28	C_M	0,6-0,7	0,65
D	-0,62	C_H	0,8-0,9	0,85

Exposure conditions (includes rams per time, ice concentration) are essential to estimate the number of rams when using probabilistic method for ice loads as local circumstances are considered and adjusted. Number of ram events on the panel are represent by,

$$\mu = v \cdot r \cdot \frac{t}{t_k} \tag{40}$$

where v is the expected number of events for a time period, r is the hit proportion (the actual event), t is the event duration, t_k is the reference event duration in terms of design curve from Jordaan et al. (1993). The average impact duration based on average penetration, is $t \sim 3s$ [18]. For North Bering 83 dataset, average impact frequency [events/hour] =8.2, while for 1st year ice average impact duration is, t, is assumed to be 2s [5].

For simplification, the proportion for the number of hits on a specific plate section is taken as,

$$r = \frac{1}{B} \cdot C_i \tag{41}$$

where B is vessel width, C_i is ice concentration.
The estimated number of events per trip is,

$$v = r \cdot S \tag{42}$$

where S is the distance travelled per trip, is equal to 110km (59,4 nm).
The design pressure can be computed when probability of exceedance is given,

$$Z_e = x_0 + \alpha\{-\ln[-\ln F_Z(Z_e)] + \ln v + \ln r\} \tag{43}$$

Two design strategies are chosen and compared in order to give a reasonable prediction. Firstly, the emphasis is to generate the ice loads most likely to happen. Thus, the Probability of exceedance, P_e is taken as the mean value, 50%,

$$P_e = 1 - F_Z(Z_e) = 0.5 \tag{44}$$

Table 12 Results summary when $P_e = 0.5$ based on Taylor et al., 2010

C_i	$P(MPa)$	Load ($F = P \cdot A_c$ [KN]) with different h	
		$0.32\ m$	$0.22m$
C_L	2.522	242.1	150.0
C_M	2.134	204.9	127.0
C_H	3.638	349.3	216.5

Secondly, the extreme design ice load is predicted with a probability of exceedance of,

$$P_e = 1 - F_Z(Z_e) = 10^{-2} \tag{45}$$

Table 13 Results summary when $P_e = 10^{-2}$ based on Taylor et al., 2010

C_i	$P(MPa)$	Load ($F = P \cdot A_c$ [KN]) with different h	
		$0.32\ m$	$0.22m$
C_L	4.191	402.3	249.3
C_M	3.400	326.4	202.3
C_H	5.744	551.4	341.7

The results of extreme design pressure and force can be seen in Table 12, Table 13 and Figure 32.

Figure 32 Local load prediction for one trip in terms of different design strategies and probabilities of exceedance (a) $P_e = 0.5$; (b) $P_e = 0.01$

- *Rahman et al., 2015*

Another reference dataset is selected for comparison using method by Rahman [11]. The corresponding factors are given in Table 14. The field test in 2014 is used as a reference to investigate the influence of ice concentration factor C_i. However, the average ice floe mass for the field test was approximately 1.25 times the mass of the ship.

The estimated events per trip with regard to the 2014 field test is given as,

$$\nu = \nu_0 \cdot S \qquad (46)$$

$$r = \frac{1}{B} \cdot C_i \qquad (47)$$

Table 14 Parameter summary for 2014 field test [11]

Ice concentration C_i	Factor	α (MPa)	$x_0(MPa)$	No. of event per km ν_0
C_H	8-9	0.095	0.020	1550
C_M	6-7	0.087	-0.014	1150
C_L	5	0.076	-0.008	750

The design pressure can be calculated using the parameters in *Table 14*, when the probability of exceedance is given,

$$Z_e = x_0 + \alpha\{-\ln[-\ln F_Z(Z_e)] + \ln \nu + \ln r\} \tag{43}$$

The two design scenarios used are the same as given in section 4.2.3.1: $P_e = 0.5$ and $P_e = 10^{-2}$. The results are given in *Table 15* and *Table 16*. Compared to Taylor [10], the results of Rahman (2015) are lower but close to rule-based results, which seem to be non-conservative. One important reason is that when considering α in Equation (43), Rahman [11] method uses the recorded data from field test directly (As shown in Table 10). The α values don't take account the effect of loading area. No matter what contact area will be, it keeps constant. However, Taylor [10] uses $\alpha = Ca^D$ which considers the small loading area effect.

Table 15 Results summary when $P_e = 0.5$ based on Rahman et al., 2015

C_i	$P(MPa)$	Load ($F = P \cdot A_c$ [KN]) with different h	
		$0.32\ m$	$0.22m$
C_L	0.642	61.6	38.2
C_M	0.790	75.8	47.0
C_H	0.952	91.4	56.6

Table 16 Results summary when $P_e = 10^{-2}$ based on Rahman et al., 2015

C_i	$P(MPa)$	Load ($F = P \cdot A_c$ [KN]) with different h	
		$0.32\ m$	$0.22m$
C_L	0.964	92.5	57.4
C_M	1.159	111.2	68.9
C_H	1.354	130.0	80.6

- *One-year design scenario*

When evaluating the design pressure, the design period is usually taken as one year. The previous calculations are based on one trip. In 4.2.3, the ice-covered period for the lake is 4 months with a duration of 5.2 hours per trip. The total journeys per year can thus be regarded as,

$$2 \times 30 \times 4 = 240 \tag{48}$$

The total number of events should be multiplied by this factor, which affects the number of ram for calculation. The predicted pressure curves based on one-year period are plotted in Figure 33.
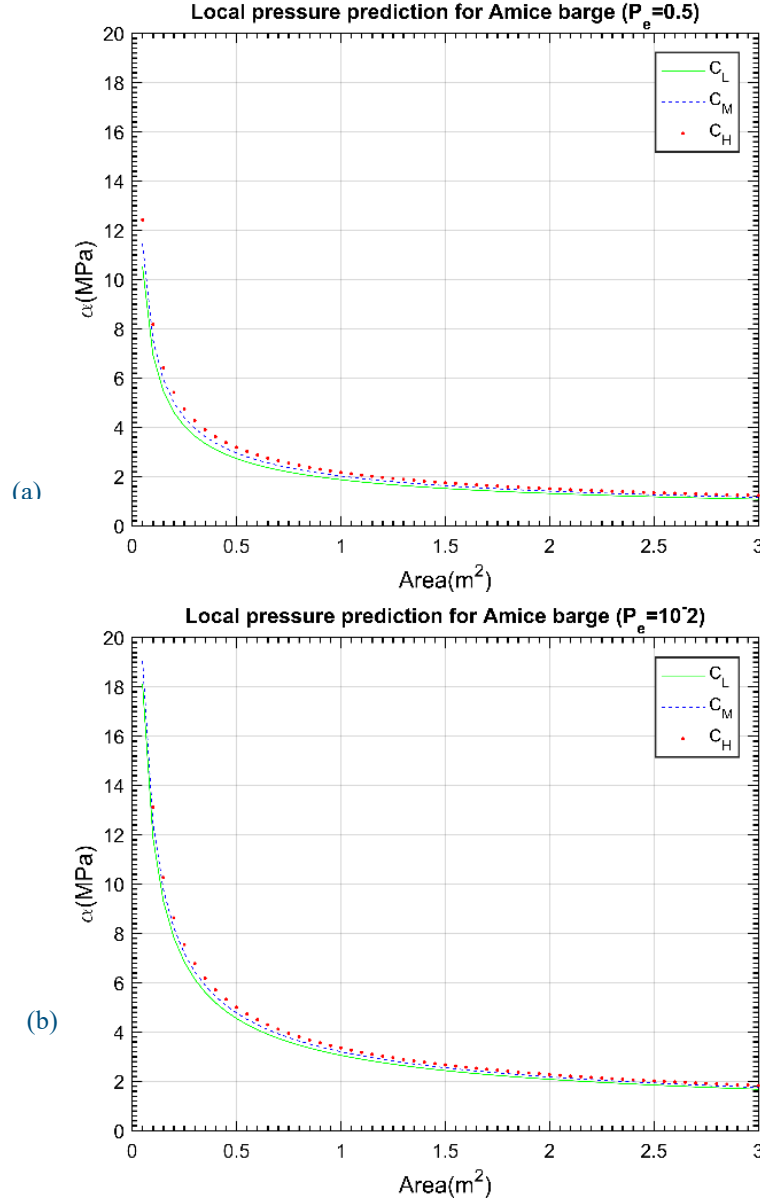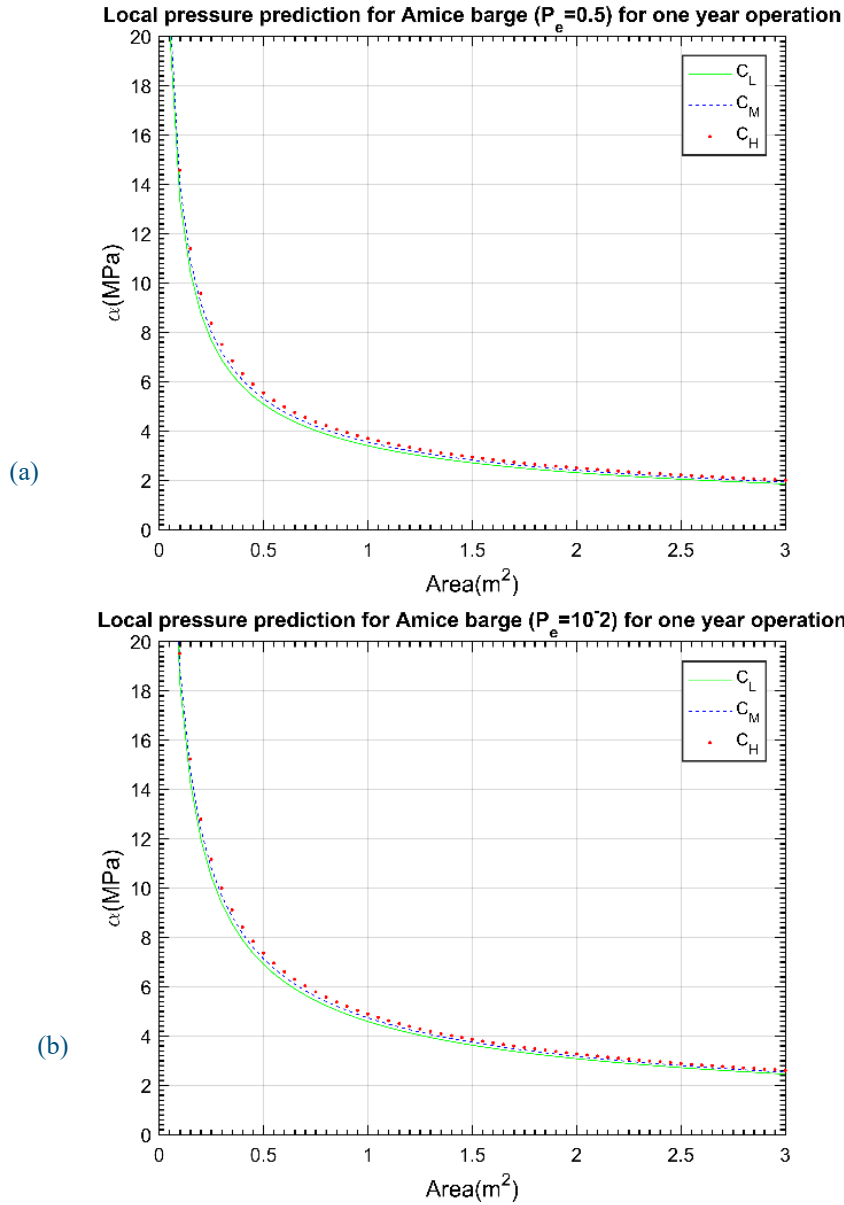
Figure 33 Local load prediction for one-year operation in terms of different design strategies and probabilities of exceedance (a) $P_e = 0.5$ (b) $P_e = 0.01$

4.2.5 Discussion

The emphasis will be put on these aspects: ice concentration and design area, as the highest ice concentration gives the highest design pressure, the smallest area gives highest values. Plots with regards to different simulation cases are summarized in Figure 34. The case defination can be read in the legend in *Figure 34*. It shows that larger event number results in higher pressure and lower P_e gives higher pressure.
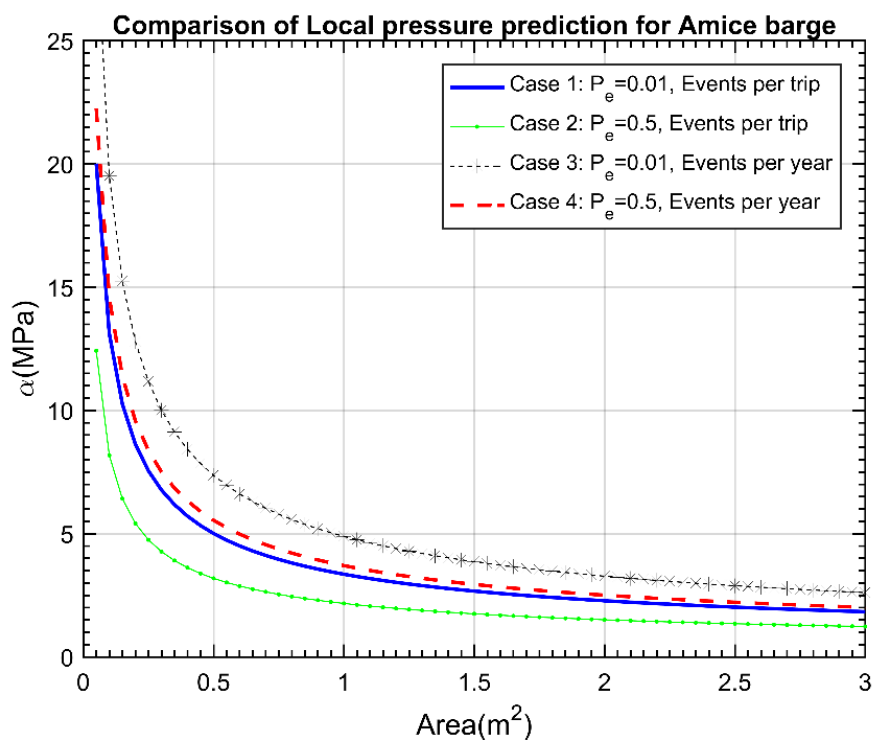
Figure 34 Comparison of four design strategies
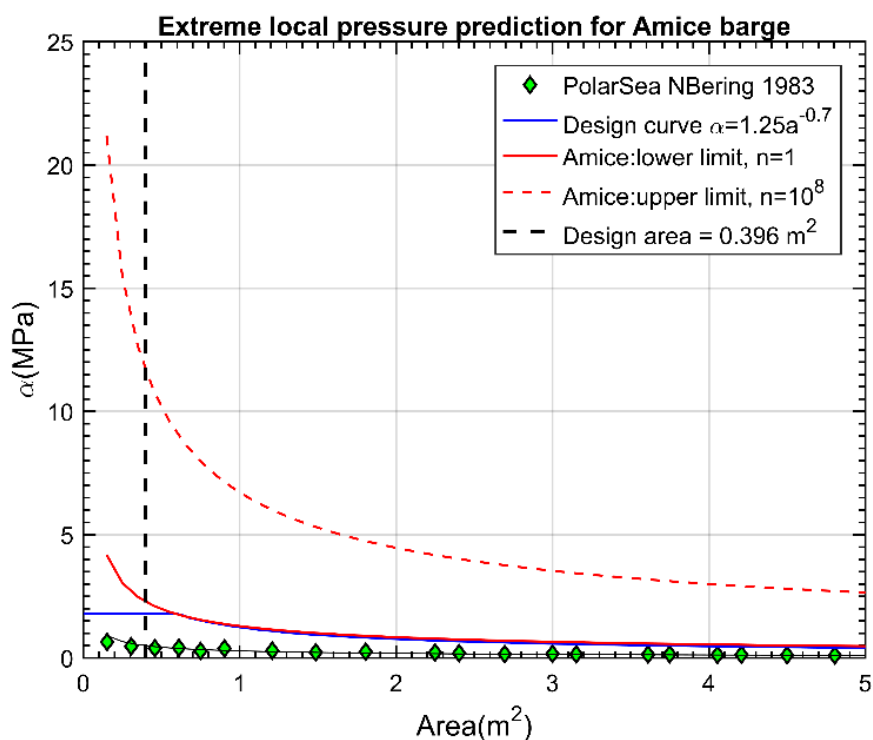
Figure 35 Extreme local pressure prediction

Based on the calculations, different factors will influence the extreme pressures. Furthermore all these factors are related to the ram number. An extreme calculation is performed based on

two extreme ram conditions: (1) $n = 1$ (lower bound); (2) $n = 10^8$ (upper bound). From Figure 35, it can be seen that the extreme design pressure varies from 2.5 to 12 MPa for Amice barge.

The effects from key influencing factors are summarized in Table 17. '+' indicates the positive relationship between the factor and extreme design pressure, while '-' stands for negative relationship.

Table 17 Effects of different factors

Factor	Effect
Ice concentration Ci	+
Design area a	-
Probability of exceedance p_e	-
No of rams	+

4.3 Design Curve for Amice barge

The predicted extreme pressure curve of case 3 (the most critical one) in *Figure 34* from Section 4.2.4 are taken as the extreme predicated pressure for Amice barge. Now it would be interesting to derive the design curve for Amice based on the this predicted pressure. The Eq. 31 and 32 can be reformulated as,

$$\alpha = Ca^D = \frac{Z_e - x_0}{4.6 + \ln \mu} \tag{49}$$

Different values of ram number and x_0 are introduced to investigate their effects on influencing the C and D parameters. Two most relevant results are given in *Table 18*. One distinct trend is that the design pressure will go higher with the increase of ram numbers. Moreover, x_0 has a significant influence. When computing the pressure in previous section 4.2.3.3, the ram number is of magnitude of 10^6. Keep consistency with the ram number, two design curves (1 and 2) are shown in *Figure 36*.
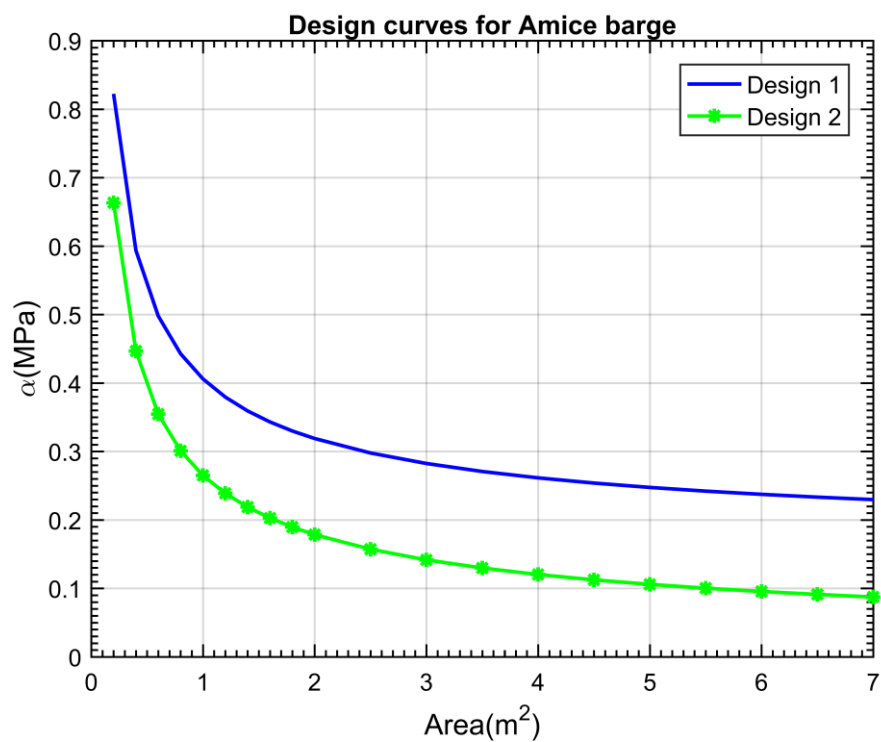
Figure 36 Design curves for Amice
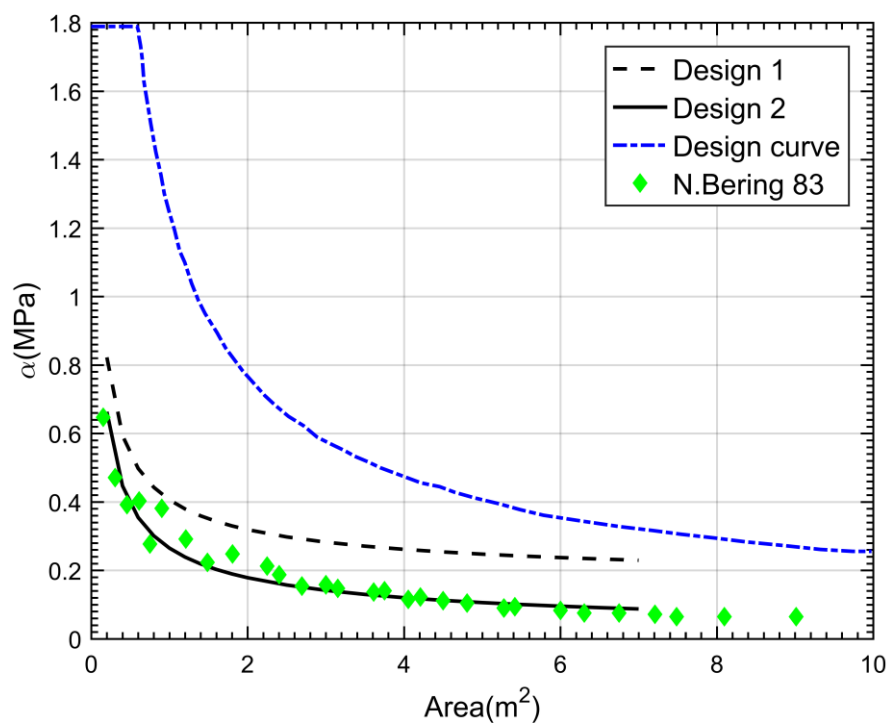
Figure 37 Comparison the design curve with reference datasets

Table 18 Parameters for design cases

Case	μ	x_0	C	D
Design 1	10^6	0.15	0.256	-0.6
Design 2	10^6	0	0.265	-0.57
N. Bering83	-	0.27	0.28	-0.62

The two design curves are plotted together with the selected dataset and the Design Curve in *Figure 36*. Design 2 is closer to the reference one, N. Bering 83. However, literature [10] shows x_0 for some cases are larger than 0, as shown in *Figure 38*. Even for the N. Bering 83 expression, x_0 is 0.27. Generally, $x_0 = 0$ is conservative for smaller design area and the current study, as shown in *Figure 37* and *Figure 38*. Thus, the design equation for Lake Mälaren of Amice barge can be formulated as below which refers to the Design curve 2 in the study.

$$\alpha = 0.265a^{-0.57} \tag{50}$$
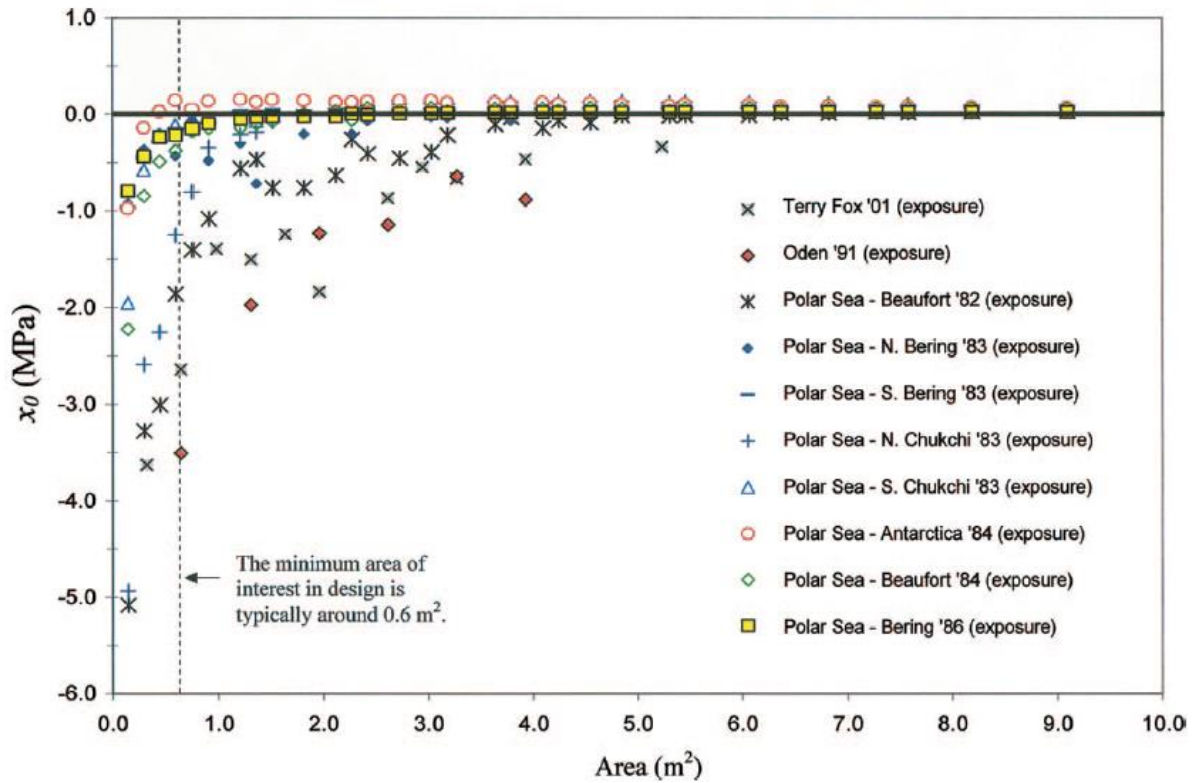
Figure 38 Plot of x_0 versus [10]

For the further application on Lake Mälaren, an exposure factor q_r can be introduced to account for the probability of impacts of a targeted ship compared with a ram event number of 10^6.

$$\mu = v \cdot r \cdot q_r \tag{51}$$

4.4 Concluding Remarks

4.4.1 Result summary

The results come from the two methods (rule-based method and probabilistic method) can be seen in Table 8 and *Table 12 - Table 16*. For the second method, by comparing section 4.2.4.2 and 4.2.4.3, it can be concluded that the two approaches (Taylor 2010 [10], Rahman, 2005 [11]) produce similar results. However, the pressure and force differ a lot. But Rahman gives similar results compare to FSICR. This is most likely due to the difference in the data used. Data in Taylor are based on large vessels in heavy ice conditions, while data in Rahman is based on smaller vessel ($m = 3665kg$,) in lighter ice conditions. Based on the literature with the consideration of the load magnitude, the Table 13 and Table 16 can be used for structural strength evaluation with an extreme load contact area of $0.096m^2$. Two load cases will be considered in next Chapter for structural analysis.

Table 19 Load case definition

Load case 1	$P_1 = 1.354MPa, F_1 = 130KN;$
Load case 2	$P_2 = 5.744MPa, F_2 = 550KN$

4.4.2 Comparison of two methods

In Table 20, the pros and cons of two approaches are summarized. And the design ice load patch can be read in Figure 39. From (b), it can be seen the design pressure is assumed to be constant. While (c)(d) show the spatial variations for real ice loading cases.

Table 20 Comparison of two approaches

Ice class rules	Probabilistic approach
- Ice class rules do not directly account for spatial and temporal variations found in ice load measurements; - General safety margins for different structural elements; - No exposure to ice loads & no route-specific ice conditions; - Rule-based load can yield non-conservative designs.	- Probabilistic approach derives the design load in a straightforward and physical way; - Selection of the target ice loads can consider seasonal and regional variability and the number of loading events; - Probabilistic design load causes local plastic deformations on plates, frames and web frames, requiring an increase in scantlings to remain within the design limit; - Probabilistic approach allows us to establish link between actual operational area and design loads.
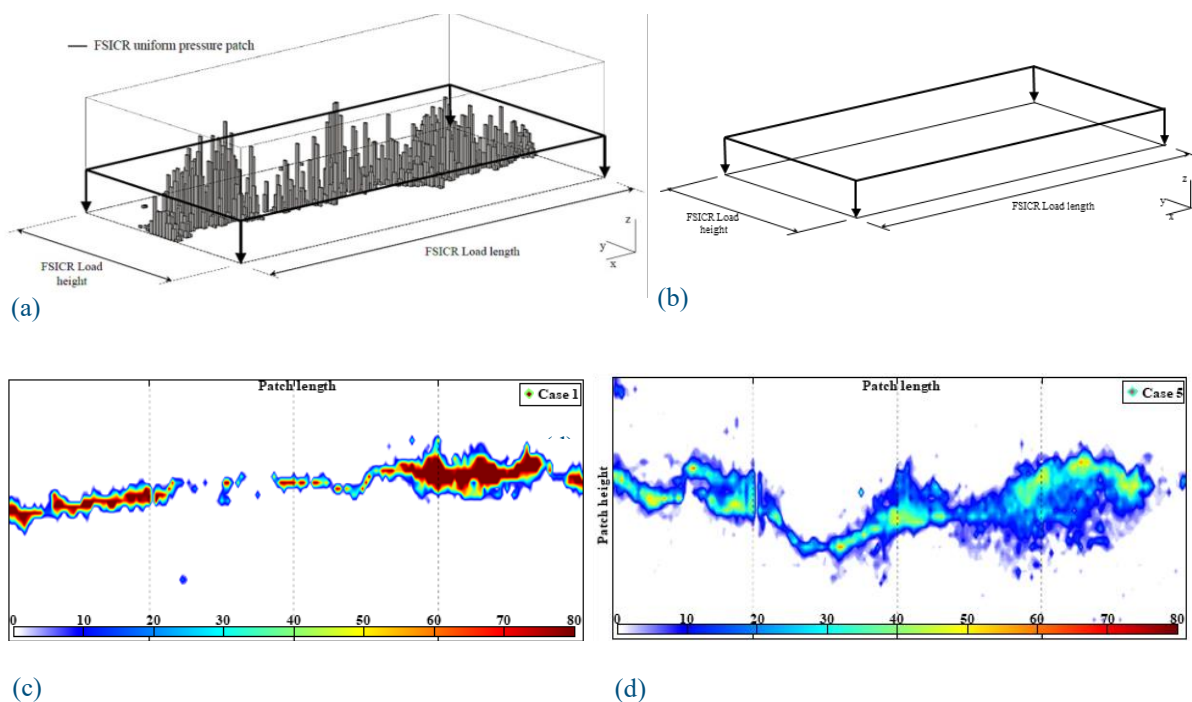
Figure 39 Plots of (a)Design pressure patch for FSICR and real pressure distribution(histogram); (b) Design pressure patch for FSICR; (c) ice pressure distribution; (d) ice pressure distribution [20]

One important thing to bear in mind is the speed limitation. FSICR by default is applicable for speed below 5 knots, where probabilistic methods are generated from field tests where low speed were settled. The influence of the speed is not investigated in the report.

5. Issue II: Structural Strength Performance

The bow part of Amice barge is considered for a local strength evaluation necessary for winter navigation. Both the ice impact pressure/load from the FSICR and the Probabilistic method are used as input.

For FSICR, the calculations are made based on equations from the rules. Our findings are that the bow structure of Amice barge does not meet the scantling requirements. Recommendations for new structure dimensions are proposed based on the requirements. FE simulation is performed using the predicted pressure/load from the Probabilistic method. It is found that the bow structure will not meet the requirement. Even when the suggested structures based on FSICR are used, the bow will still fail.

Based on the calculation in this part, the bow structural reinforcements are necessary in order to make sure that the barge can operate in Lake Malaren under winter conditions.

For the global structural problem, the possible issue is the buckling since the ice impact load comes from the bow part will transferred to the mid-body. Amice barge has big openings for cargo tank and no transverse bulkheads existed. In the beginning of the study, buckling is evaluated under ice load of F=1000KN and no significant buckling problem will happen. The two load cases are smaller than 1000KN thus no extra buckling problem will be occured. Therefore, this work won't be covered in the report.

5.1 Structural Strength Calculation Based on FSICR

Based on the FSICR, the required plate thickness in the ice belt area should be evaluated and the computing results are given in *Table 21*.

Table 21 Required plate thickness

Plate thickness in the ice belt(mm)	Forward	Midship	Aft
Shell member	20.0745	13.1943	9.9156

While the shell plate of the Amice barge is 10mm, it cannot meet the requirement according to the IC rules. The typical stiffened panel in the bow area is given in Figure 40 and the scantlings can be found in *Table 22*. The computing results show neither web frames nor stringers can meet the criterion, and the recommended scantlings are given as well, as shown in *Table 23*.

(a)

(b)
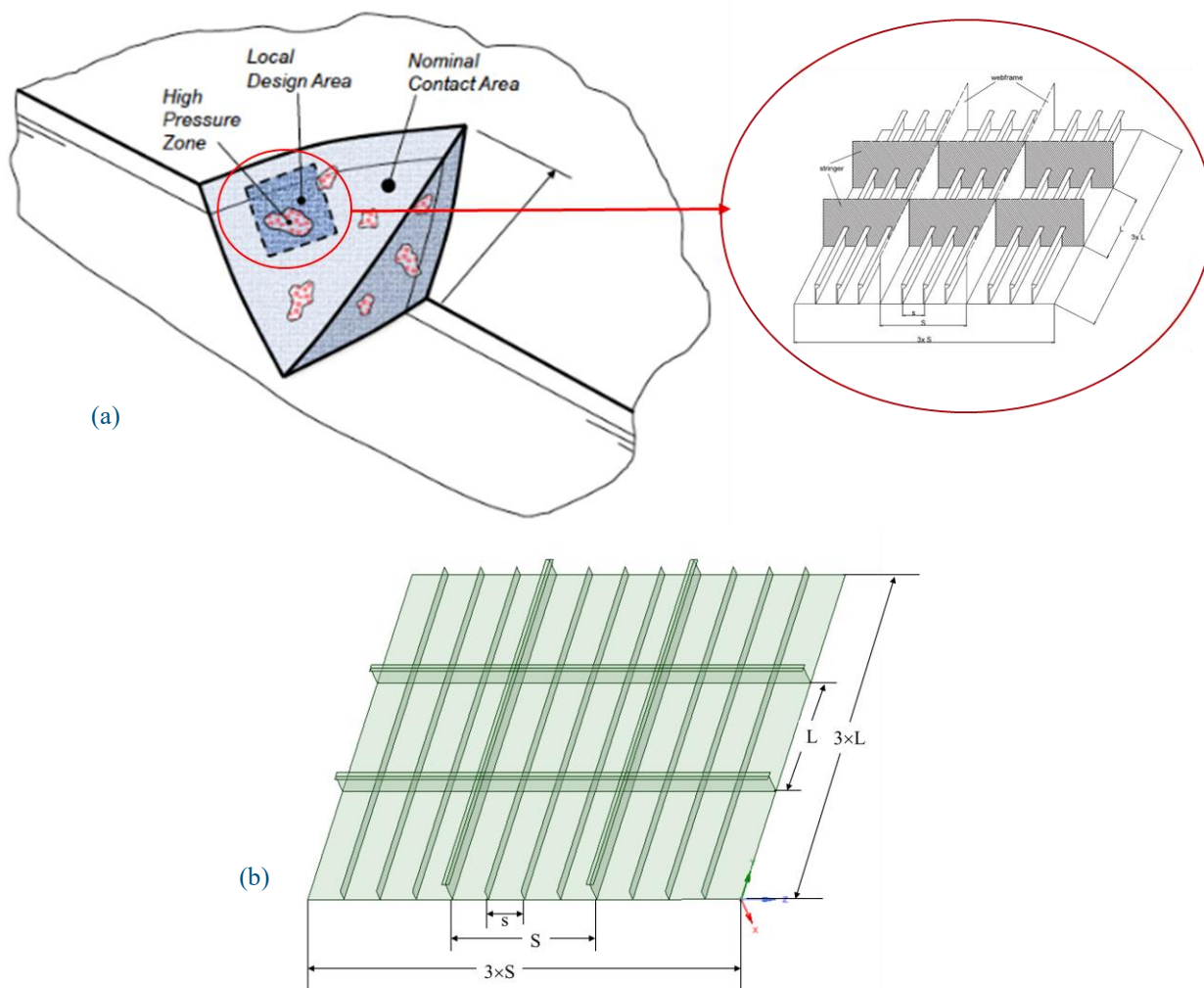
Figure 40 Example of stiffened panel of the bow area: (a) illustration scantling, (b) Amice barge.

Table 22 Bow structural Dimensions for Amice barge

Structural member	Dimensions	
Plate thickness	10(mm)	
Stiffener	HP160x8(mm)	W=34 (cm^3) A=13 (cm^2)
Web frames/ (Ice)stringer	T 300x8/100x10(mm)	W=179 (cm^3) A=34 (cm^2)

Table 23 Required Structure dimension for IC

Structural member	Requirement	Recommendation: one example

Transverse frame	W=315 (cm^3)	Same as ice stringer	
Longitudinal frame	W=202 (cm^3) A=22 (cm^2)	T300 x 10/100 x 10	W=215 (cm^3) A=40 (cm^2)
Ice stringer	W=327 (cm^3) A=21 (cm^2)	T350 x 12/120 x 10	W=340 (cm^3) A=54 (cm^2)
Note: the transverse frame is considered as ice stringer.			

5.2 FE Static Analysis

The simulation is performed to check if the bow structure will survive under ice load. Two load cases are considered from *Table 19*. The stiffened panel is made of steel. The material properties of all structural parts in the model are given in *Table 24*. The material model is simplified to an elastic model and the yield stress determines whether we are in the elastic regime or not. Furthermore, residual stresses in the welded structures are not considered in the simulation models.

Table 24 Material properties

Poisson's ratio	Young's modulus (GPa)	Density (kg/m^3)	Yield strength (MPa)
0.3	200	7850	235

5.2.1 Load case 1

The simulation is performed for ice loading $F = 130KN$. The geometry and mesh are given in Figure 41. The four edges are considered as simply supported. Load is applied on the High Pressure Zone along the ship longitudinal direction, as shown in Figure 42. The Von Mises stress results are given in
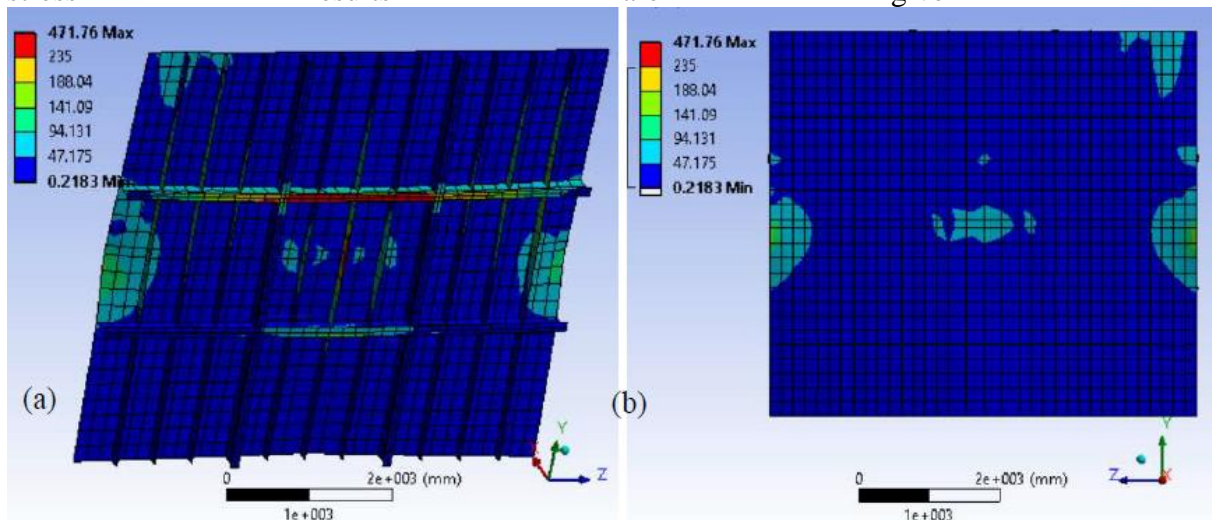
Figure *43*. It can be clearly seen that the plate can withstand the design pressure in this case.
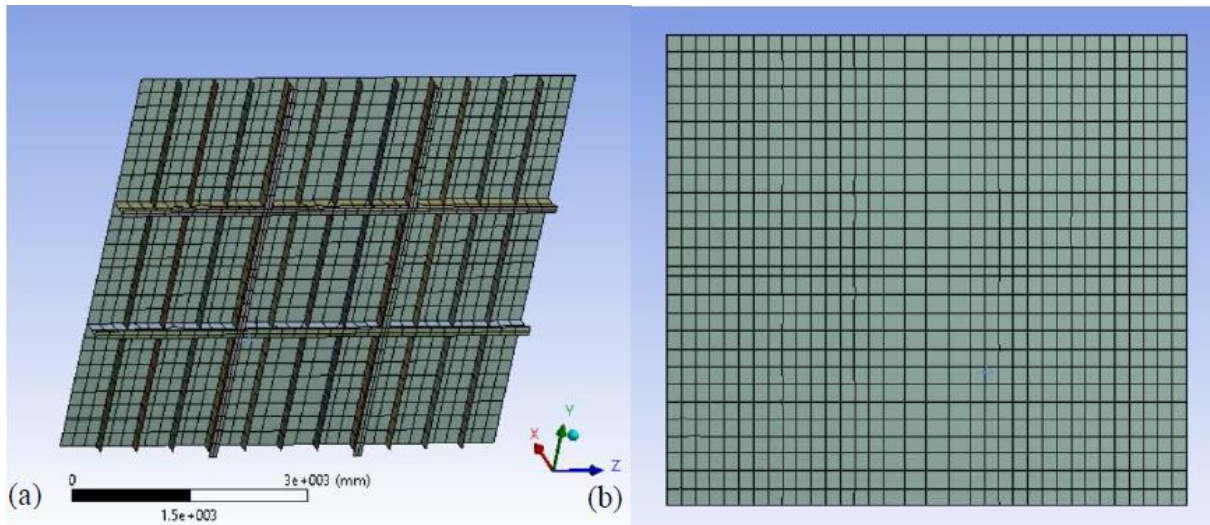
Figure 41 Geometry and mesh of stiffened bow panel
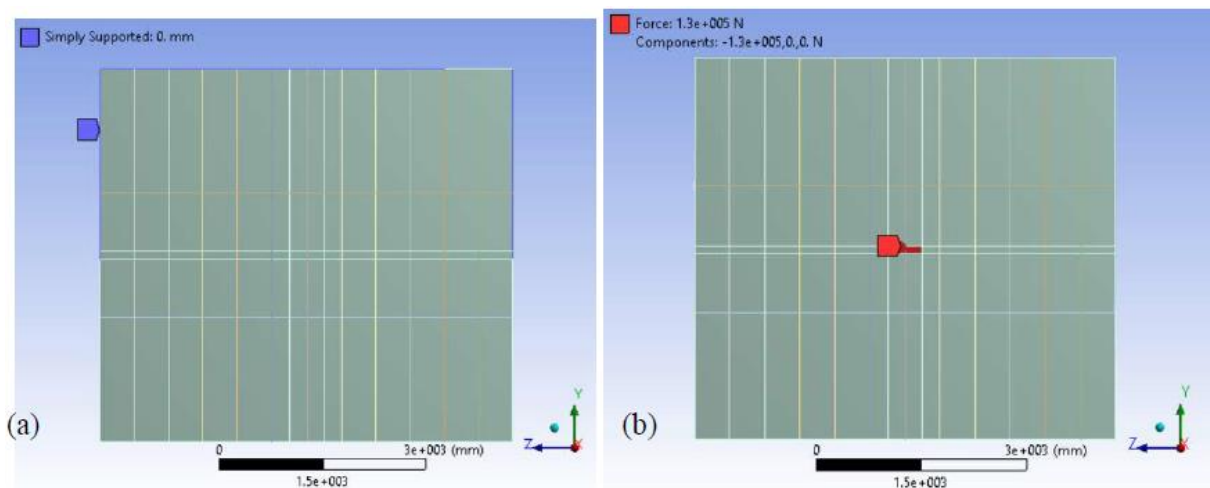
Figure 42 Boundary conditions and applied pressure
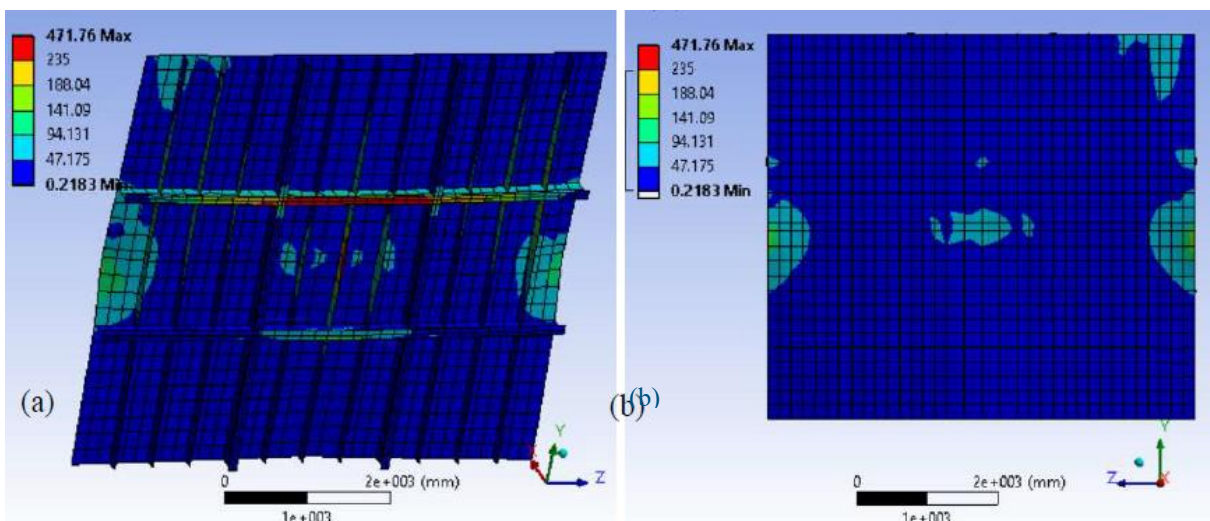
Figure 43 Von Mises stress distribution of the panel

5.2.2 Load case 2

For load case 2 where $F = 550KN$, the von Mises stress distribution of the panel is given in Figure 44. It shows the panel will fail under this loading condition.
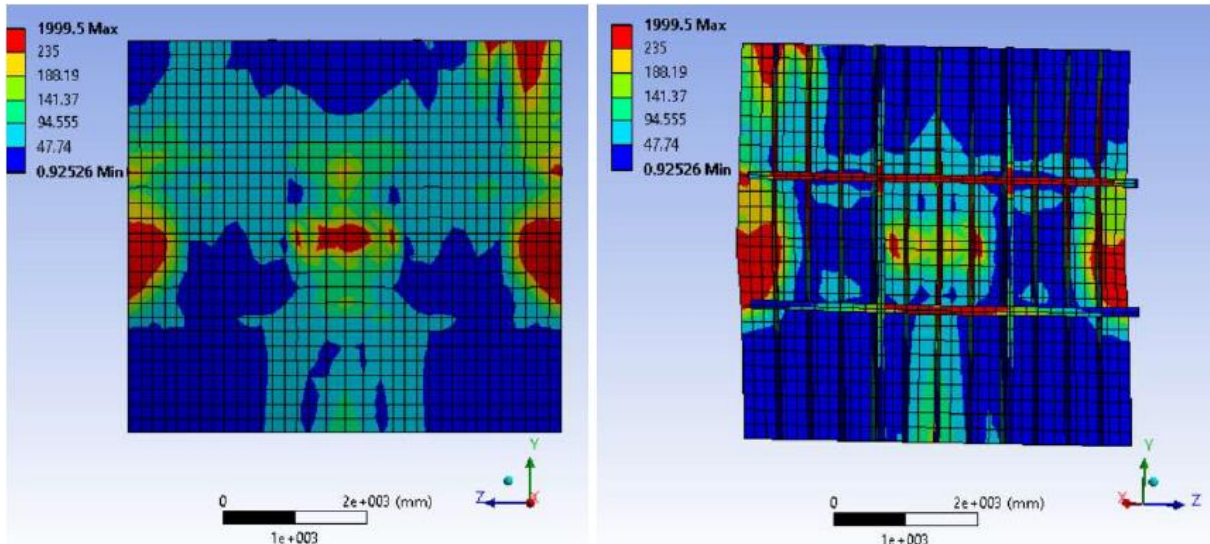
Figure 44 Von Mises stress distribution of the panel

5.3 Reinforcement

Load case 2 is applied and reinforcements are made based on the requirements form FSICR rules. The structural analysis is performed to check if the reinforced plate can meet the requirement.

5.3.1 Increase plate thickness based on FSICR

Based on FSICR, the panel thickness should be 20mm. A simulation is run to see if the structure will survive if the plate thickness is increased. Other controlling aspects are kept constant.
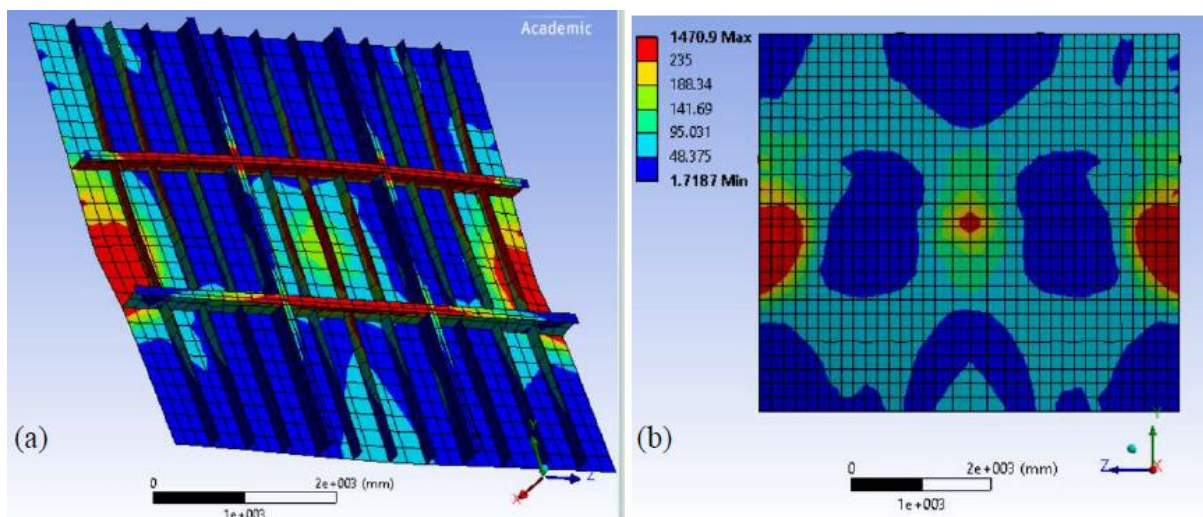
Figure 45 Von Mises stress distribution of the panel

The overall structural performance has been improved, as shown in Figure 45. However, the panel and the webframes still yield in this case.

5.3.2 Further reinforcement based on FSICR requirement

Now, the model is adjusted based on requirements from FSICR, the structural dimension can be seen in *Table 25*. The same failure of the webframe is observed in Figure 46. It is recommended to increase the dimension of webframe furthermore to avoid structural yield phenomenon.

Table 25 Comparison between original structure dimension and one example based on FSICR (unit:mm)

Structural member	Recommendation from FSICR	Original dimension
plate thickness	20	10
Stiffener	I 160x8	I 160x8
Transverse frame	T350x12/120x10	T300x8/100x10
Longitudinal frame	T300x10/100x10	T300x8/100x10
Ice stringer	T350x12/120x10	T300x8/100x10
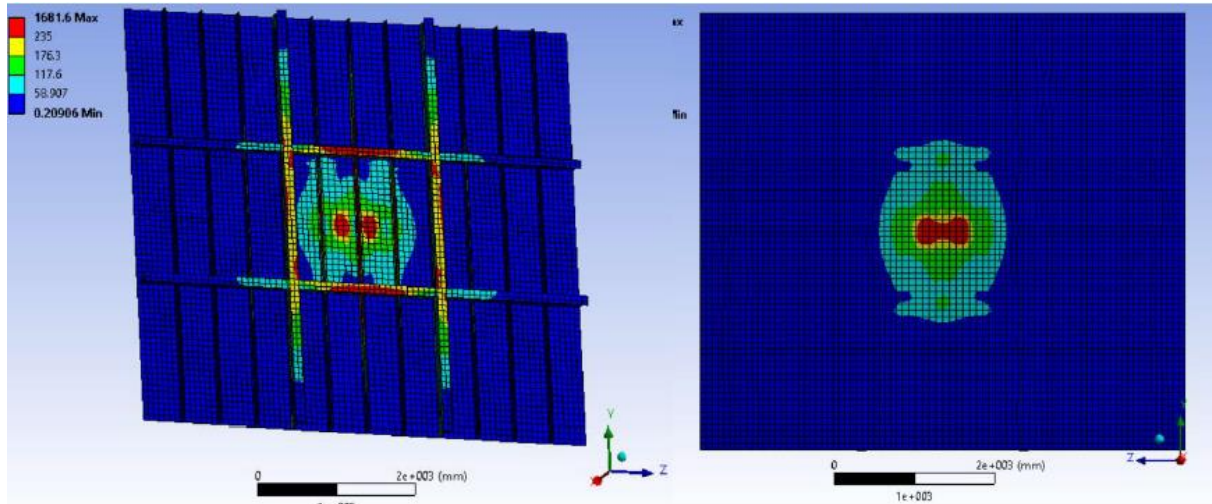
Figure 46 Von Mises stress distribution of the panel using required scantlings based on FSICR IC
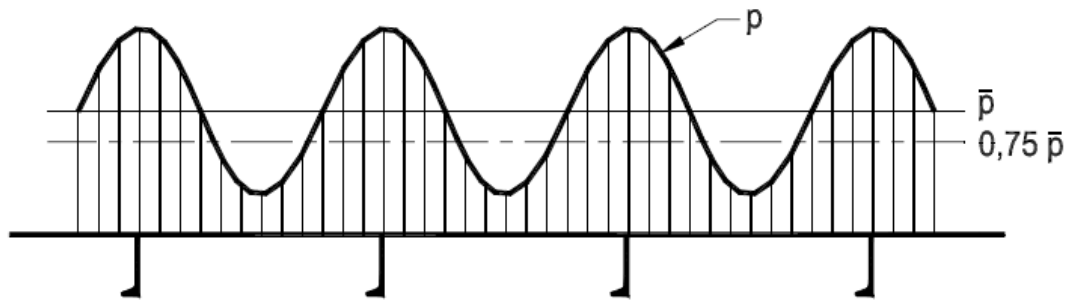
Figure 47 Ice load distribution on a ship's side from FSICR

The simulation shows that if the structure scantlings follow the requirements from FSICR, the bow structure still fails. Two aspects will result in this phenomenon. The first thing is that extreme loads (*Table 19*) are added which are higher than the calculated pressures (*Table 8*) from FSICR. Second reason is the extreme loads applied in the middle of plate (between two adjacent frames). However, from *Figure 47*, it can be seen the highest ice pressure is required to applied on the frame instead based on FSICR.

5.4   Conclusion

Both rule-based calculation and FE simulation show that the bow panel for Amice barge cannot bear the extreme design pressure. The original structural design is too weak under ice loading conditions. The reinforcement measurements should be implemented to make the panel survive. One useful design is adding more webframes, increasing plate thickness and dimensions of stiffeners/frames.

6. Issue III: Potential Propulsion Problems

The performance for ships running on the ice-covered waters is usually described by the speed and the corresponding maximum operational ice thickness, which is known as h-v curve. The concept behind the h-v curve is basically that the traditional ship resistance, e.g. friction, wave resistance etc. plus new ice-induced resistance should be equivalent to the net thrust provided by the propeller. Thus, in order to obtain the h-v curve, ship resistance on icy waterways are computed based on three methods, the Lindqvist [21] method, the Riska [22] method and the Brash channel ice resistance prediction method [23]. The principles of these three methods are described herein. The h-v curves are plotted both for fully loaded and empty loading conditions. Generally, the Riska method is more realistic when the ship comes across the level thin ice. The brash ice-method is more relevant when the ship passes a channel full of ice floes.

6.1 h-v Curves with Different Methods

The ice-induced resistance can be estimated with various methods, three of these methods will be analyzed in this report. Lindqvist [21] developed a formula based on trial tests in the Bay of Bothnia. Different resistance components and impact mechanics were considered within this method. Riska et al. [22] formulated the equations with empirical parameters focusing on the level ice circumstance. Juva and Riska [23] proposed a way to predict the channel (brash ice) resistance which is used in FSICR from the design point of view. This report will consider two loaded cases for each method. The corresponding parameters can be seen in Table 26.

Table 26 Data for two load cases

No	Condition	Design speed(kn)	Economic speed(kn)	draft
1	Fully loaded	11.6	8.3	3.4
2	Empty loading	13.6	10	1.2

Based on FSICR ships that operate on icy water will have a minimum forward draft of at least,

$$(2 + 0.00025 \cdot \Delta) \cdot h_0 = (2 + 0.00025 \times 3938) \times 0.4 = 1.19m \tag{52}$$

The draft for the empty case hereby fulfills the criteria.

6.1.1 Lindqvist method

The Lindqvist method is a rather simple way of estimating the ice resistance. In this model, the resistance is divided into three components with regards to crushing, bending-induced breaking and submergence. The formulae give resistance as a function of main dimensions, hull form, ice thickness, ice friction and strength. The formulae are expressed as,

$$R_{ice} = (R_c + R_b)\left(1 + 1.4\frac{V}{\sqrt{gh_i}}\right) + R_s\left(1 + 9.4\frac{V}{\sqrt{gL}}\right) \tag{53}$$

$$R_c = 0.5\sigma_b h_i^2 \frac{\tan\phi + \mu\cos\phi/\cos\psi}{1 - \mu\sin\phi/\cos\psi} \tag{54}$$

$$R_b = \frac{27}{64}\sigma_b B \frac{h_i^{1.5}}{\sqrt{\frac{E}{12(1-v^2)g\rho_w}}} \frac{\tan\psi + \mu\cos\phi}{\cos\psi\sin\alpha}\left(1 + \frac{1}{\cos\psi}\right) \tag{55}$$

$$R_s = (\rho_w - \rho_i)gh_i B\left(T\frac{B+T}{B+2T} + k\right) \tag{56}$$

$$k = \mu\left(0.7L - \frac{T}{\tan\phi} - \frac{B}{4\tan\alpha} + T\cos\phi\cos\psi\sqrt{\frac{1}{\sin\phi^2} + \frac{1}{\tan\alpha^2}}\right) \tag{57}$$

$$\psi = \arctan\left(\frac{\tan\phi}{\sin\alpha}\right) \tag{58}$$

where R_{ice}, R_c, R_b and R_s represent total ice resistance, crushing resistance, bending resistance and resistance due to submersion; σ_b and *hi* are respectively ice strength in bending and ice thickness; μ, ϕ, α and ψ are respectively the friction coefficient, stem angle, waterline entrance angle and flow angle; g is the gravity acceleration; r_w and r_i are water and ice density.

The computing results based on Lindqvist are presented in Figure 48. Results show that when the ship is operating at empty loading condition, the barge can withstand harsher ice environment and can navigate for longer period per year. Generally, the differences between two loading scenarios are small. But when it comes to the operating time window, the navigable time for different years differs a lot, which will be addressed in Section 7.
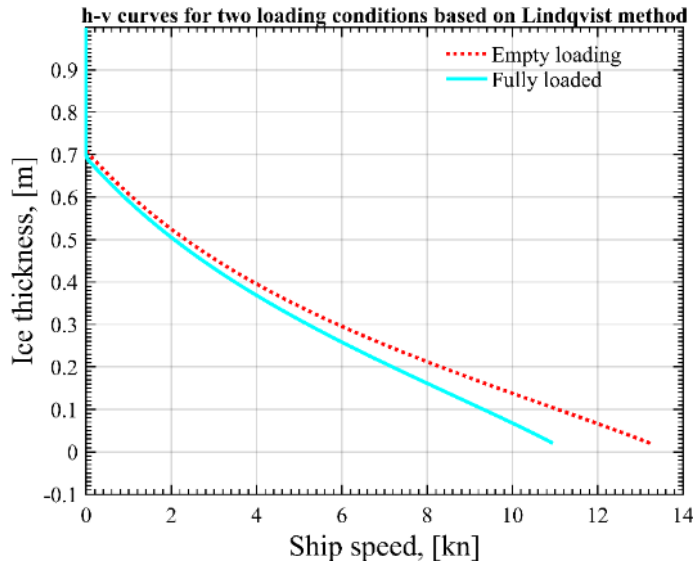
Figure 48 h-v curves based on Lindqvist method

6.1.2   Riska method

Riska et al. (1997) proposed a level ice resistance formula by modifying the formulations of Lindqvist (1989). The formulation is based on a set of empirical coefficients, derived from full-scale tests of a number of ships in ice conditions in the Baltic Sea. The main resistance formula is given below, while constants can be found in Table 27.

$$R_{ice} = C_1 + C_2 V \tag{59}$$

$$C_1 = f_1 \frac{1}{\frac{2T}{B} + 1} BL_{par}h_i + (1 + 0.021\phi) \tag{60}$$

$$(f_2 Bh_i^2 + f_3 L_{bow}h_i^2 + f_4 BL_{bow}h_i)$$

$$C_2 = (1 + 0.063\phi)(g_i h_i^{1.5} + g_2 Bh_i) + g_3 h_i(1 + 1.2T/B)\frac{B^2}{\sqrt{L}} \tag{61}$$

where V, B, T and L are vessel speed, breadth, draught and length, hi is ice thickness, ϕ is the stem angle in degrees, and L_{bow} and L_{par} are the length of bow and parallel sides section, respectively.

Table 27 Constants in Riska formulation for ice resistance in level ice.

Symbol	Value	Unit
f_1	0.23	kN/m^3
f_2	4.58	kN/m^3
f_3	1.47	kN/m^3
f_4	0.29	kN/m^3
g_1	18.9	$kN/(m/sxm^{1.5})$
g_2	0.67	$kN/(m/sxm^2)$
g_3	1.55	$kN/(m/sxm^{2.5})$

The results for Riska method are plotted in Figure 49. It is quite interesting that the two h-v curves intersect around 5.5 knots. For speed lower than 5.5 knots, the fully loaded case can withstand worse ice condition. When the ship goes with a speed larger than 5.5 knot, the empty loading can stand worse ice condition.
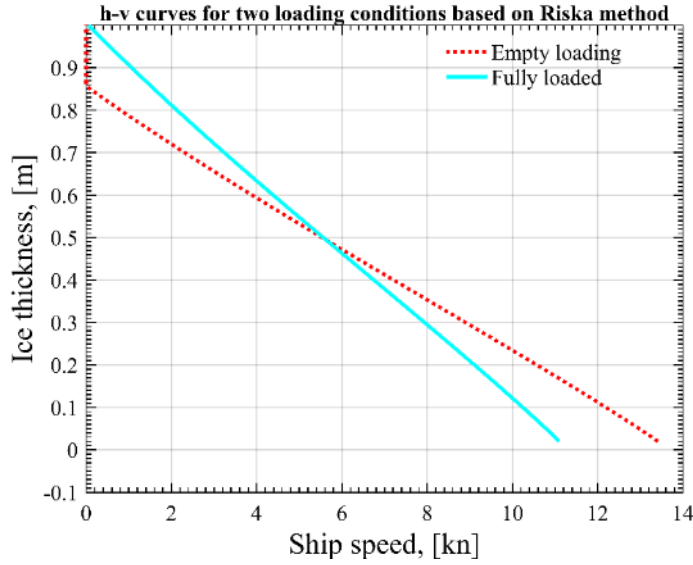
Figure 49 h-v curve based on Riska method

6.1.3 Brash ice

The channel resistance for different ice classes should be taken into account when coms to the design point. According to Juva and Riska (2002), the rule resistance equations are expressed in the following forms,

$$R_{ch} = C_1 + C_2 + C_3[H_F + H_M]^2[B + C_\psi H_F]C_\mu \tag{62}$$

$$+ C_4 L_{par} H_F^2 + C_5 \left[\frac{LT}{B^2}\right]^3 \frac{A_{WF}}{L}$$

$$H_F = 0.26 + (H_M B)^{0.5} \tag{63}$$

$$C_\mu = 0.15 \cos \phi_2 + \sin \psi \sin \alpha, \quad \min 0.45 \tag{64}$$

$$C_\psi = 0.047\psi - 2.115, \quad \min 0.0 \tag{65}$$

$$\psi = \arctan \left[\frac{\tan \phi_2}{\sin \alpha}\right] \tag{66}$$

$$C_1 = f_1 \frac{BL_{par}}{\frac{2T}{B} + 1} + [1 + 0.021\phi_1](f_2 B + f_3 L_{bow} + f_4 B L_{bow}) \tag{67}$$

$$C_2 = [1 + 0.063\phi_1][g_1 + g_2 B] + g_3 \left[1 + 1.2\frac{T}{B}\right]\frac{B^2}{\sqrt{L}} \tag{68}$$

where the term [LT/B²]³ is taken as 20 if it is above 20 and 5 if it is below 5; all other coefficients are shown in Table 28.

48

Table 28 Coefficients for channel resistance formulas.

Symbol	Value	Unit
f_1	23	N/m^2
f_2	4.58	N/m
f_3	14.7	N/m
f_4	29	N/m^2
g_1	1537.3	N
g_2	172.3	N/m
g_3	398.7	$N/m^{1.5}$
C_3	845.576	$kg/(m^2 s^2)$
C_4	41.74	$kg/(m^2 s^2)$
C_5	825.6	kg/s

For brash ice or channel ice, the computing results are given in Figure 50. From Figure 50, it indicates that the ship couldn't run below 2 knots. One explanation could be that speed is one key factor when computing the propeller thrust. This is due to the fact that the thrust component is smaller than the resistance, meaning that the ship cannot move forward. Once exceeding the threshold, the empty loading case shows its advantages.
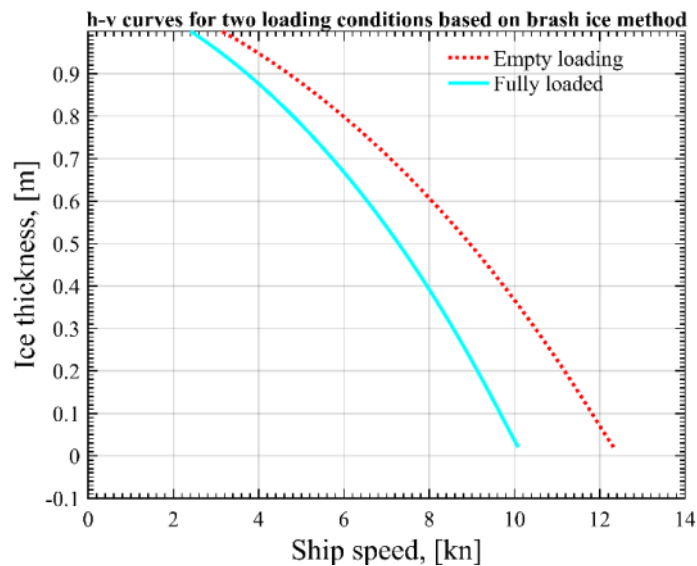
Figure 50 h-v for Brash ice

6.2   Summary

The h-v plots are summarized in *Figure 51*, which gives a clear view of the result discrepancies for each method. It can be seen that the results differ a lot. Moreover, it can be interpreted that Lindqvist predicts the highest ice resistance, while brash ice method gives lowest value and Riska is in between.
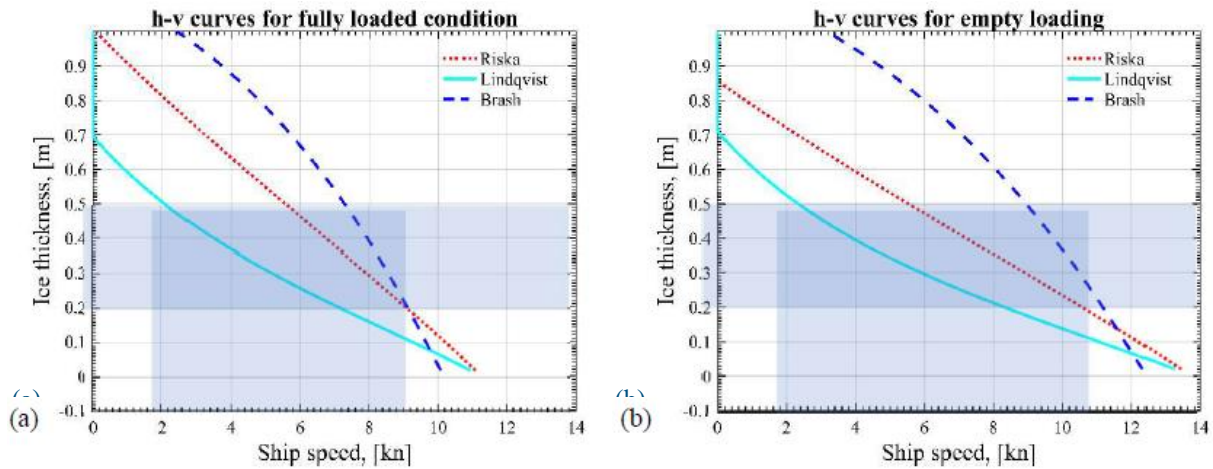
Figure 51 Comparison among different h-v curves

6.3 Discussion

The three methods provide us with different results. Since different parameters are considered within the concepts, attentions should be paid on the real circumstance. The current research shows that for speed lower than 3 knots, the resistance dramatically increases. However, the three prediction methods couldn't coincide with this case and will underestimate the resistance. Thus, for low speed, the accuracy of results in the report is doubtful. However, low speed is not the key concern from the economic point of view. Since the ice thickness varies from 15mm to 50mm, the corresponding speed areas are marked blue in Figure 8. By combining the economic speed (8.3 kn and 10 kn), speed ranges from 2 to 7 knots will be reasonable for loaded condition and 2 to 9 knots for empty loading.

Generally speaking, the Riska method is more realistic when the ship comes across the level thin ice, Figure 52 (a). The brash ice-method can be used when the ship passes the channel full of ice floes, as shown in Figure 52 (b).
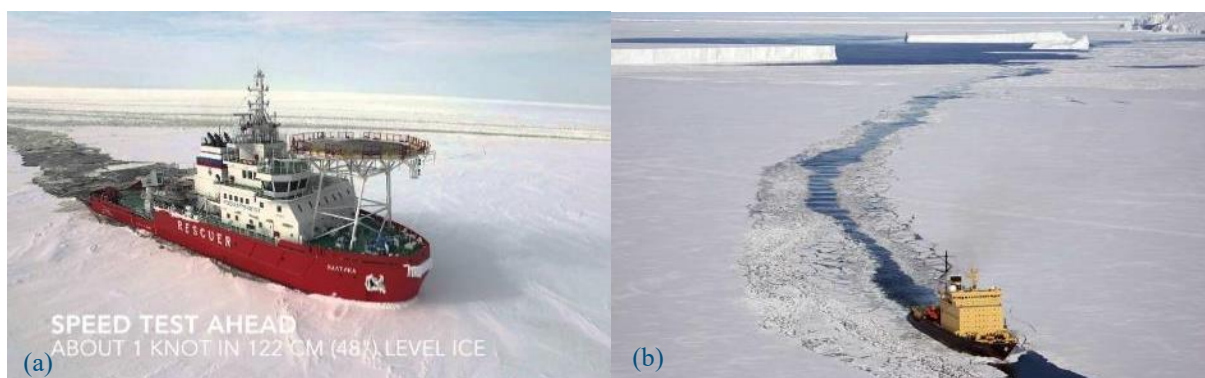
Figure 52 (a)level ice; (b)channel ice

7. Issue IV: Vessel Operating Scenarios

Based on the resistance calculation, the Operating Time Windows (OTWs) are presented here for the user to identify the number of navigable days in relation to speed and ice thickness. The ice thickness probability distribution tables, based on a Weibull distribution, are given as well. This provide understanding of the possibility of a certain operating condition. Two barges, Amice and Veedam, are compared with each other in order to study the influence of different ship-parameters of OTW for same operating water area. It turns out the main engine power is the most important influencing factor. A further study in terms of the different ice conditions is conducted. Lake Vänern and Lake Mälaren are chosen for this comparison. It turns out that Lake Mälaren has more available operating days.

7.1 OTW of Amice Barge

7.1.1 Time Windows

The Operating Time Windows Table 30 - Table 32 give an overview about the operational days of Amice barge in terms of ship speed, ice thickness and probability of the ice for selected years.

In Table 29, h_c shows the ice thickness calculated from h-v curves shown to two decimal figures and only has theoretical meaning; hi means the ice thickness from the records, which is real data and on a multiple of 5. Even though ice thicknesses are regarded as random variables, they are discrete random variables. When saying the probability of one specific value, only real data is applicable. In *Table 29*, the calculated ice thicknesses is rounded to real values. For example, when looking at the first h_c data point, which is 59.01cm, this means when ship runs at a speed of 1 knot, the maximum ice thickness it can go through is 59.01cm. Whenever ice thickness is larger than 59.01cm, the ship will be stuck in ice. However, only 55cm and 60cm will be recorded since 59.01cm doesn't exist in recorded data. According to the cumulative distribution function (CDF), it gives,

$$F(x \leq 59.01) = F(x \leq 55) \tag{69}$$

in this case, thus 55cm will be used instead of 59.01cm.

Table 29 Transform calculated ice thickness into recorded data

	Lindqvist				Riska				Brash ice			
V (kn)	hc	hi	hc	hi	hc	hi	hc	hi	hc	hi	hc	hi
1	59.01	55	\	\	\	\	78.66	75	\	\	\	\
2	50.49	50	52.43	50	81.17	80	72	70	\	\	\	\
3	43.21	40	45.48	45	72.1	70	65.57	65	95.79	95	\	\
4	36.83	35	39.51	35	63.32	60	59.32	55	87.63	85	94.78	90
5	31.09	30	34.25	30	54.73	50	53.21	50	78.01	75	87.82	85
6	25.82	25	29.53	25	46.28	45	47.19	45	66.83	65	79.86	79
7	20.86	20	25.22	25	37.87	35	41.24	40	53.96	50	70.84	70
8	16.12	15	21.20	20	29.44	25	35.32	35	39.22	35	60.71	60
9	11.46	10	17.41	15	20.91	20	29.39	25	22.42	20	49.37	45

10	6.76	5	13.76	10	12.16	10	23.43	20	3.67	0	36.71	35
11	\	\	10.19	10	2.96	0	17.38	15	\	\	22.61	20
12	\	\	6.62	5	\	\	11.2	10	\	\	7.09	5
13	\	\	2.9	0	\	\	4.77	0	\	\	\	\

Table 30 Operating Time window (available days) for yearly round operation based on Lindqvist method

Lindqvist	ice thickness(mm)		2017 mild ice winter		2013normal ice winter		2011 severe ice winter	
Speed (kn)	Full	Empty	Full	Empty	Full	Empty	Full	Empty
1	55	\	365	\	365	\	365	\
2	50	50	365	365	365	365	365	365
3	40	45	365	365	355	365	317	365
4	35	35	365	365	355	355	271	271
5	30	30	365	365	337	337	271	271
6	25	25	365	365	284	284	265	265
7	20	25	365	365	284	284	265	265
8	15	20	350	365	248	284	244	265
9	10	15	328	350	236	248	243	244
10	5	10	298	328	236	236	243	243
11	\	10	\	328	\	236	\	243
12	\	5	\	298	\	236	\	243
13	\	0	\	298	\	236	\	243

Table 31 Operating Time window (available days) for yearly round operation based on Riska method

Riska	ice thickness(mm)		2017 mild ice winter		2013normal ice winter		2011 severe ice winter	
Speed (kn)	Full	Empty	Full	Empty	Full	Empty	Full	Empty
1	\	75	\	365	\	365	\	365
2	80	70	365	365	365	365	365	365
3	70	65	365	365	365	365	365	365
4	60	55	365	365	365	365	365	365
5	50	50	365	365	365	365	365	365
6	45	45	365	365	365	365	365	365
7	35	40	365	365	355	355	271	317
8	25	35	365	365	284	355	265	271
9	20	25	365	365	284	284	265	265
10	10	20	328	365	236	284	243	265
11	0	15	298	350	236	248	243	244

| 12 | \ | 10 | \ | 328 | \ | 236 | \ | 243 |
| 13 | \ | 0 | \ | 298 | \ | 236 | \ | 243 |

Table 32 Operating Time window (available days) for yearly round operation based on Brash ice

Brash ice	ice thickness(mm)		2017 mild ice winter		2013normal ice winter		2011 severe ice winter	
Speed (kn)	Full	Empty	Full	Empty	Full	Empty	Full	Empty
1	\	\	\	\	\	\	\	\
2	\	\	\	\	\	\	\	\
3	95	\	365	\	365	\	365	\
4	85	90	365	365	365	365	365	365
5	75	85	365	365	365	365	365	365
6	65	79	365	365	365	365	365	365
7	50	70	365	365	365	365	365	365
8	35	60	365	365	355	365	271	365
9	20	45	365	365	284	365	265	365
10	0	35	298	365	236	355	243	271
11	\	20	\	365	\	284	\	265
12	\	5	\	298	\	236	\	243
13	\	\	\	\	\	\	\	\

By comparing Table 30 with Table 31, it can be seen that the time window with Riska method is larger than the one obtained from Lindqvist and the time window with brash ice concern is broader than others.

7.1.2 Probability distribution chart

The ice probability distributions of four dataset are elaborated in this section. First, three years are selected to give the ice-covered day and their probability distributions, as shown in *Table 33* and *Table 34*.

Table 33 Ice covered days

Dataset	record period	ice-covered period	probability per year $f1(xi)$	non-ice days
2011	2010.8.1-2011.8.1	135	0,3699	230
2013	2012.8.1-2013.8.1	129	0,3534	236
2017	2016.8.1-2017.8.1	67	0,1836	298

Table 34 Cumulative distribution F(xi) and probability density f(xi) of ice thickness of different datasets for ice-covered days

hi(cm)	2011		2013		2017		20years	
	F(x) (%)	*f(x) (%)*	*F(x) (%)*	*f(x) (%)*	*F(x) (%)*	*f(x) (%)*	*F(x) (%)*	*f(x) (%)*
5	0.12	0.12	5.84	5.84	1.31	1.31	0.11	0.11
10	1.15	3.19	17.65	11.81	17.37	16.06	1.18	1.08
15	4.35	6.53	31.99	14.34	59.71	42.34	4.77	3.58
20	10.88	10.55	46.58	14.59	93.62	33.91	12.46	7.69
25	21.43	14.24	59.93	13.35	99.85	6.23	25.14	12.68
30	35.67	16.38	71.20	11.27	100	0.15	42.10	16.96
35	52.05	16.09	80.12	8.92	100	0	60.74	18.64
40	68.13	13.40	86.80	6.68	100	0	77.43	16.70
45	81.53	9.34	91.55	4.75	100	0	89.40	11.96
50	90.88	5.37	94.78	3.23	100	0	96.08	6.68
55	96.25	2.50	96.89	2.10	100	0	98.91	2.82
60	98.75	1.25	98.20	1.32	100	0	99.78	0.87
65	100	0	100	0	100	0	100	0
>65	100	0	100	0	100	0	100	0

It is more interesting to know the probability for a single event, i.e., the ice with a specific thickness. The chance of this specific ice thickness occurring in a one year period is given as,

$$f_0(x_i) = f(x_i) \cdot f_1(x) \tag{70}$$

where $f(x_i)$ is the probability of the ice with this specific thickness occurring on one of the ice-covered days, and $f_1(x)$ is the probability of ice-covered days occurring in a year. The PDF info can be seen in Table 35.

Table 35 PDF over the whole year

hi(cm)	2011		2013		2017	
	f₀(x) (%)		*f₀(x) (%)*		*f₀(x) (%)*	
	ice-covered period	whole year	ice-covered *period*	whole year	ice-covered period	whole year
5	0.12	0.04	5.84	2.06	1.31	0.24
10	3.19	1.18	11.81	4.17	16.06	2.95
15	6.53	2.42	14.34	5.07	42.34	7.77
20	10.55	3.90	14.59	5.16	33.91	6.23
25	14.24	5.27	13.35	4.72	6.23	1.14
30	16.38	6.06	11.27	3.98	0.15	0.03
35	16.09	5.95	8.92	3.15	0	0

40	13.40	4.96	6.68	2.36	0	0
45	45	9.34	3.46	4.75	1.68	0
50	50	5.37	1.99	3.23	1.14	0
55	55	2.50	0.92	2.10	0.74	0
60	60	1.25	0.46	1.32	0.47	0
65	100	0	100	0	100	0
>65	100	0	100	0	100	0

7.1.3   Interpret Operating Time Window with probability distribution

One example will be introduced here to explain how to use the OTW as a lot of data and information are contained in OTWs, as shown in Figure 53. The data is highlighted by red circles. Starting from the value of 284 and following the arrows, we can see that if the ship speed is 7 knots, the maximum ice thickness it can move forward is 20mm from resistance perspective. From *Table 35*, the PDF for year 2013 with h=20cm is 5.16%, which gives the possibility for this ice thickness to occur.

Lindqvist	ice thickness(mm)		2016 mild ice winter		2013 normal ice winter		2011 severe ice winter	
Speed (kn)	Full	Empty	Full	Empty	Full	Empty	Full	Empty
1	59.01	\	365	\	365	\	365	\
2	50.49	52.43	365	365	365	365	365	365
3	43.21	45.48	365	365	355	365	317	365
4	36.83	39.51	365	365	355	355	271	271
5	31.09	34.25	365	365	337	337	271	271
6	25.82	29.53	365	365	284	284	265	265
7	20.86	25.22	365	365	284	284	265	265
8	16.12	21.20	350	365	248	284	244	265
9	11.46	17.41	328	350	236	248	243	244
10	6.76	13.76	298	328	236	236	243	243
11	\	10.19	\	328	\	236	\	243
12	\	6.62	\	298	\	236	\	243
13	\	2.9	\	298	\	236	\	243

Figure 53 One example to explain TW

7.2   Comparison between Amice and Veedam

Two barges are compared with each other to study the ship-parameters influence of OTW for same operating water area. It can be seen from the green box in Table 37 that Veedam can travel through thicker ice. It also has wider range for the navigable days. The main particulars of two ships are listed in Table 36. It turns out that engine power factor (engine power/ship displacement) is an important parameter to affect OTW.

Table 36 Main particulars for two barges

	Amice	*Veedam*
L	*135.00*	*86.00*
B	*11.45*	*11.45*
D	*4.25*	*4.80*
Vmax	*13.70*	*10.00*
draft	*3.40*	*3.25*
W(kW)	*1588.00*	*1088.00*
Tonnage(tons)	*3938.00*	*1917.00*
W/T	*0.403*	*0.568*

Table 37 Time window for two barges for Lake Mälaren

Riska Speed (kn)	Ice thickness (cm)			2013 normal ice winter. fully loaded			2011 Severe ice winter. fully loaded		
	Veedam	Amice	Difference	Veedam	Amice	Difference	Veedam	Amice	Difference
1	\	\	0	\	\	0	\	\	0
2	\	81	100%	\	365	100%	\	365	100%
3	91	72	-26%	365	365	0	365	365	0
4	79	63	-25%	365	365	0	365	365	0
5	68	55	-24%	365	365	0	365	365	0
6	57	46	-23%	365	365	0	365	365	0
7	47	38	-23%	365	355	-3%	365	271	-35%
8	36	29	-23%	355	284	-25%	271	265	-2%
9	26	21	-23%	284	284	0	265	265	0
10	15	12	-24%	248	236	-5%	244	243	0
11	\	3	100%	\	236	\	\	243	100%

Note: When calculating differences. Amice is used as the reference.

7.3 Comparison between Lake Vänern and Lake Mälaren

A further study in terms of the different ice conditions is conducted. Results from Lake Vänern and Lake Mälaren are compared, with the ice information being downloaded from the SMHI website. The location of the two lakes can be seen in Figure 43 and the ice thickness distribution across the year is plotted in *Figure 55* for Lake Vänern. *Figure 19* gives the maximum ice thickness distribution for Lake Mälaren, which can be used as a comparison.
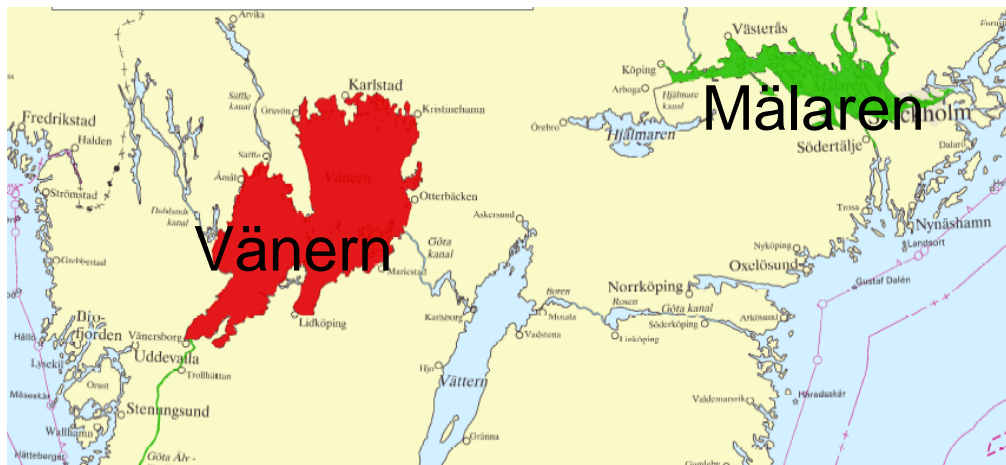
Figure 54 Location of two lakes
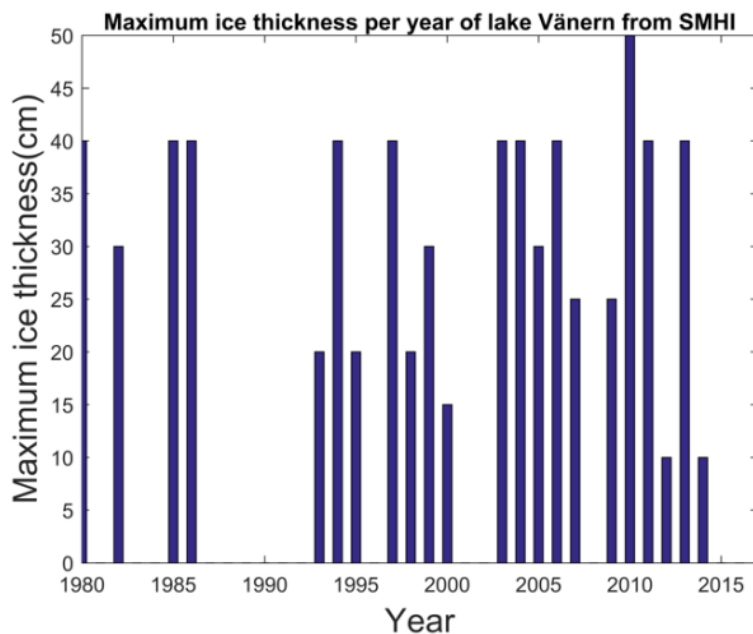
Figure 55 Maximum ice thickness per year recorded from SMHI for Lake Vänern

Veedam barge is studied to evaluate the differences of two lakes. From Table 38, it can be observed that the ice thickness to speed is the same for both ships, which means the relationship between h-v is an inherent property of the ship (main dimensions and engine power control). By looking at the OTW for year 2013, it shows Lake Mälaren has more available operating days. The differences for year 2011 and 2013 show that the colder the winter is, the larger the differences between two ships will be.

Table 38 Time window for two lakes with regards to VEEDAM barge

Lindqvist	ice thickness(cm)	2013 normal ice winter			2011 severe ice winter		
Speed (kn)	Mälaren and Vänern	Vänern	Mälaren	Difference	Vänern	Mälaren	Difference
1	18,18	274	248	-0,105	246	244	-0,008
2	14,44	229	236	0,030	235	243	0,033
3	11,67	229	236	0,030	235	243	0,033
4	9,51	225	236	0,047	231	243	0,049
5	7,74	225	236	0,047	231	243	0,049
6	6,24	225	236	0,047	231	243	0,049
7	4,92	221	236	0,064	226	243	0,070
8	3,73	221	236	0,064	226	243	0,070
9	2,61	221	236	0,064	226	243	0,070
10	\	\	\	0	\	\	0

Note: Fully loaded condition for VEEDAM barge

8. Conclusions

The main conclusions are drawn in this chapter with regards to the four aspects.

- **Ice Load**

This study has used the different methods to evaluate the impact load from ice for Lake Mälaren. The study gives us the design curve as $\alpha = 0.265a^{-0.57}$. In consideration of extreme loading case, the FSICR under predicted the structural scantling compared to the probabilistic method. It was also found that the ice condition in the specific region plays an important role in determining the impact load. For the methods in this work, the ice thickness is of utmost importance.

According to the two different concepts of loading area, the HPZ is more critical. It is recommended to adjust the ice load height instead of using data from FSICR directly. For instance, FSICR IC considers a scenario with 0.4m level ice and a 0.22m of ice load height. However, the study finds 0.32m can be more supportive based on a statistical analysis, and 0.192m is suitable for high-pressure load height.

Figure 37 indicates that the design curve for Amice is slightly higher than N. Bering 83. It is believed that the pressure-area behavior corresponds to ice properties and ice-structure interaction. Since, for fresh water thin ice, the bending failure dominates which is indicated by flexural strength. A higher design expression for this study makes sense. As ram number affects the extreme pressure, manoeuvring should be taken. Furthermore, $x_0 = 0$ gives a conservative prediction and makes the predicted curve for fresh water ice more reliable. Based on reference [24], the interests in design contact area is approximately $0.6m^2$, *Figure 38* also verifies this assumption for the first-year condition.

Generally, the proposed design curve for Amice is applicable for all ships operating on Lake Mälaren. Since in the process of achieving the expression, only the ice situation is considered. The same approach can be used to attain design curve for other inland waterway ice conditions.

FSICR and Probabilistic approach result in different results. The results vary a lot with different design scenarios within the probabilistic approach. The final two load cases can be seen in *Table 19*.

- **Structural strength performance**

Based on the direction calculation from FSICR and FE simulation: the bow structural panel will yield. In order to ensure the structural safety, it is recommended to increase plate thickness, and increase the dimensions and number of frames.

Another reinforcement can be adding ice strengthened bow attachments, shown in *Figure 56*. It can broaden the ice channel and change the pressure distribution along the ship hull.
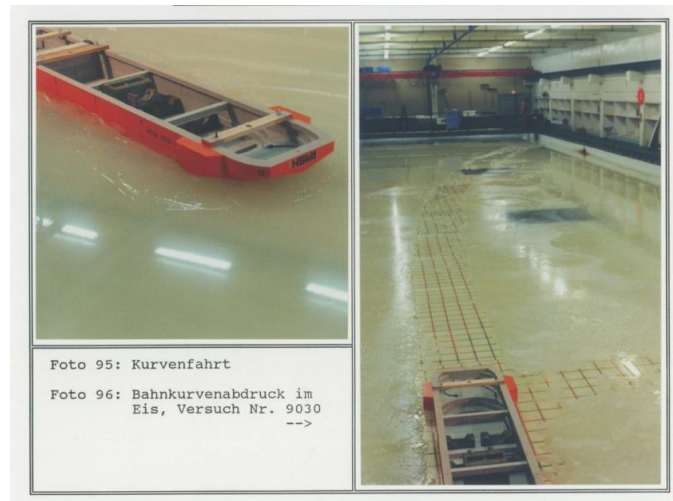
Figure 56 Illustration of bow attachment in the Tank basin

- **Potential Propulsion Problems**

It is recommended to use Riska method to predict resistance when the ship is operating on level ice and to use Brash ice method when ship runs at brash ice channel. In addition, the engine power factor (engine power/ship displacement) has a significant influence on the ship performance in terms of resistance.

Generally speaking, the ice thickness varies from 15cm to 50cm with an expected value of 32cm when assuming Weibull distribution. FSICR IC uses 22cm as ice load height.

By combining the economic speed (8.3 kn and 10 kn), speed ranges from 2 to 7 knots will be reasonable for loaded condition and 2 to 9 knots for empty loading.

- **Vessel Operating scenarios**

Time windows are given in Section 7.1. The probability distribution table can be used to analyze the operating event possibility. In general, the faster the ship goes, the lighter ice condition it can go through, and more navigable days will be. However, the structural problem should be bear in mind for making decisions.

Discussion and limitation

Due to the time limit and work load, there are some aspects not included in the paper. For example, the influencing from the ship itself are not considered is the study as interaction is not the main task. In addition, as the temperature for Lake Mälaren during winter time can go to $-5°$, the structural steel can behave brittle which can make the situation more dangerous. The structural strength simulation is based on static analysis while the ship structure performance can be different when the loading rate is included. What's more, the bow structure should be reinforced until it can meet the requirement from the yield perspective.

References

Wiegmans, B., Witte, P. and Spit, T. (2015). Characteristics of European inland ports: A statistical analysis of inland waterway port development in Dutch municipalities. Transportation Research Part A: Policy and Practice, 78, pp.566-577.

Sihn, W., Pascher, H., Ott, K., Stein, S., Schumacher, A. and Mascolo, G. (2015). A Green and Economic Future of Inland Waterway Shipping. *Procedia CIRP*, 29, pp.317-322.

Kujala, P., and Arughadhoss, S., 2012, "Statistical analysis of ice crushing pressures on a ship's hull during hull–ice interaction", Cold Regions Science and Technology, 70, pp. 1-11.

2018, "Start | SMHI", Smhi.se [Online]. Available: https://www.smhi.se/en. [Accessed: 04- Jan- 2018].

Tõns T., Freeman R., Ehlers S., Jordaan I.J., 2015. Probabilistic design load method for the Northen Sea Route. OMAE, June 5, 2015.

Timco, G.W., O'Brien, S., 1994. Flexural strength equation for sea ice. Cold Regions Science and Technology 22, 285–298.

Timco, G. and Weeks, W. (2010). A review of the engineering properties of sea ice. Cold Regions Science and Technology, 60(2), pp.107-129.

Kujala, P., 1994. On the statistics of ice loads on ship hull in the Baltic. Dissertation. Acta Polytechina Scandinavica, Mechanical Engineering Series No. 116. Helsinki. 98 p.

Riska, K., Wilhelmson, M., Englund, K. and Leiviskä, T., 1997. Performance of merchant vessels in the baltic. Research report no 52. Espoo: Helsinki university of technology, ship laboratory, Winter Navigation Research Board.

Taylor, R., Jordaan, I., Li, C., and Sudom, D., 2010. Local Design Pressures for Structures in Ice: Analysis of Full-Scale Data. Journal of Offshore Mechanics and Arctic Engineering, 132(3), p. 031502.

Rahman, M., Taylor, R., Kennedy, A., Simões Ré, A., and Veitch, B., 2015. Probabilistic Analysis of Local Ice Loads on a Lifeboat Measured in Full-Scale Field Trials. Journal of Offshore Mechanics and Arctic Engineering, 137(4), p. 041501.

Trafi, 2010. Ice Class Regulations 2010: Finnish-Swedish Ice Class Rules 2010. Finnish Transport Safety Agency, 23.11.2010 TRAFI/31298/03.04.01/2010, 48 p.

Lubbad, R., and Løset, S., 2011. A numerical model for real-time simulation of ship–ice interaction. Cold Regions Science and Technology, 65(2), pp. 111-127.

Jordaan, I., Maes, M., Brown, P., and Hermans, I., 1993. Probabilistic Analysis of Local Ice Pressures. Journal of Offshore Mechanics and Arctic Engineering, 115(1), p. 83.

Ralph. F., Jordaan I.J., 2013. Probabilistic Methodology for Design of Arctic Ships. OMAE, June 2013.

Masterson, D., and Frederking, R., 1993, "Local contact pressures in ship/ice and structure/ice interactions", Cold Regions Science and Technology, 21(2), pp. 169-185.

Keinonen, A., Browne, R.P., 1991. Icebreaker performance prediction. SNAME Transactions, Vol. 99, 1991, pp. 221-248.

Ralph. F., Jordaan I.J., 2013. Probabilistic Methodology for Design of Arctic Ships. OMAE, June 2013.

Kujala, P., Suominen, M., Riska, K., 2009. Statistics of Ice Loads Measured on MT Uikku in the Baltic. Proceedings of POAC 2009.

Erceg, B., Taylor, R., Ehlers, S., Leira, B.J., 2015. A response comparison of a stiffened panel subjected to rule-based and measured ice loads. Submitted to the 34th International Conference on Ocean, Offshore and Arctic Engineering. OMAE 2015.

Lindqvist, G., 1989. A straightforward method for calculation of ice resistance of ships. In: Proceedings of 10th International Conference on Port and Ocean Engineering under Arctic Conditions (POAC), Lulea, Sweden, 12-16 June 1989, pp. 722-735.

Riska, K., Wilhelmson, M., Englund, K., Leiviskä, T., 1997. Performance of Merchant Vessels in the Baltic. Research report no 52. Helsinki university of technology, ship laboratory, Winter Navigation Research Board, Espoo.

Juva, M., Riska, K., 2002. On the Power Requirement in the Finnish-swedish Ice Class Rules. Research report no 53. Helsinki university of technology, ship laboratory, Winter Navigation Research Board, Espoo.

Frederking, R., 2000, "Local Ice Pressures from the Louis S. St Laurent 1994 North Pole Transit," Canadian Hydraulics Centre, National Research Council, Report No. HYD-CR-054.

Appendix - Veedam barge

This part summaries the calculation results for Veedam barge. The same procedures are conduced according to the evaluating processes for Amice barge. The main particulars can be read in *Table 36*.
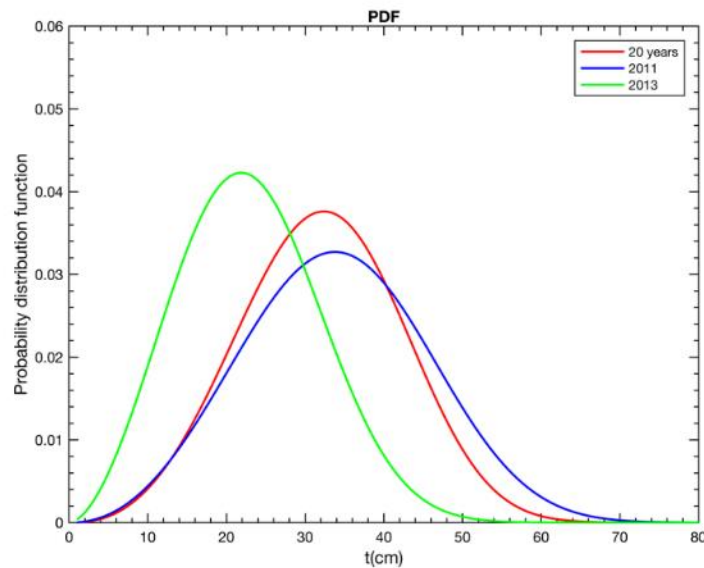
A.1 Ice conditions in Lake Vänern

Figure 57 Weibull distribution PDF of ice thickness

Table 39 Estimated parameters for Weibull distribution fit

dataset	k	λ
20 years	**35.7**	**3.5**
year 2010-11	38.0	3.2
year 2012-13	25.8	2.7

Note, parameters for 20years data are same compared with Lake Mälaren. This information means that for long period, the ice thickness distribution for Lake Vanern and Mälaren is same. Thus, 0.32m can be used for Veedam as well.

Table 40 Ice Properties (Same as Mälaren)

Factor	value
H	$0.32m$
σ_t	$167KPa$
σ_f	$1.76Pa$
σ_c	$738KPa$
σ_{pc}	$196KPa$

The nominal contact area and contact height can be obtained

$$\text{when } h_i = 0.32m \text{ , } h_c = 0.173m, \ A_c = 0.086m^2$$
$$\text{when } h_i = 0.22m \text{ , } h_c = 0.129m, \ A_c = 0.065m^2 \tag{37}$$

A.2 Design load and scantling based on FSICR

Table 41 Design pressure for Veedam

Design ice pressure (MPa)	Forward	Midship	Aft
Transverse shell member	1.5306	0.6315	0.3158
Longitudinal shell member	1.4611	0.6028	0.3014

Table 42 Plate thickness requirement based on FSICR IC

Plate thickness in the ice belt(mm)	Forward	Midship	Aft
Shell member	18	12	9.2

Table 43 Supporting members and dimensions

Structural member	Dimensions	Structural member
Plate thickness	10 (mm)	
Stiffener	HP 160 x 8 (mm)	W=34 (cm^3) A=13 (cm^2)
Longitudinal Web frames	I 250 x20	W=16.67 (cm^3) A=5 (cm^2)
Transverse Web frames	T 300x10/120x10	W=221.9 (cm^3) A=42 (cm^2)

Table 44 Requirements from FSICR and example structural scantlings

Structural member	Requirement	Recommendation: one example	
Transverse frame	W=192 (cm^3)	keep same	
Longitudinal frame	W=126 (cm^3) A=16 (cm^2)	T300x8/100x10	W=128 (cm^3) A=30 (cm^2)
Ice stringer	W=208 (cm^3) A=16 (cm^2)	transverse web is taken same as the original one	

A.3 Extreme Design load for Veedam in Lake Vänern

The route for Veedam barge is from Port of Karlstad to Port of Goteborg (Gothenburg) which gives a distance 215 nautical miles. One trip include charge and discharge will take 22hours. One trip one day. Assume 4 months with ice condition and $Pe = 0.01$, the extreme pressure for Veedam barge can be seen in Table 45 - Table 47.

Table 45 Results summary Based on Taylor

C_i	$P(MPa)$	Load ($F = P \cdot A_c$ [KN]) with different h	
		$0.32\ m$	$0.22m$
C_L	5.228	449.61	339.82
C_M	4.205	361.63	273.33
C_H	7.115	611.89	462.48

Table 46 Results summary Based on Rahman

C_i	$P(MPa)$	Load ($F = P \cdot A_c$ [KN]) with different h	
		$0.32\ m$	$0.22m$
C_L	0.964	82.90	62.66
C_M	1.159	99.67	75.34
C_H	1.354	116.44	88.01

Table 47 Load cases for Veedam Barge

Load case 1	$P_1 = 1.354 MPa, F_1 = 130 KN;$
Load case 2	$P_2 = 7.115 MPa, F_2 = 612 KN$

A.4 FE static structural analysis

The structural analysis shows that the bow will fail under the ice loading conditions. Even the recommended scantlings are used based on FSICR, the bow still fails. Further reinforcements should be added in order to make the panel survive.
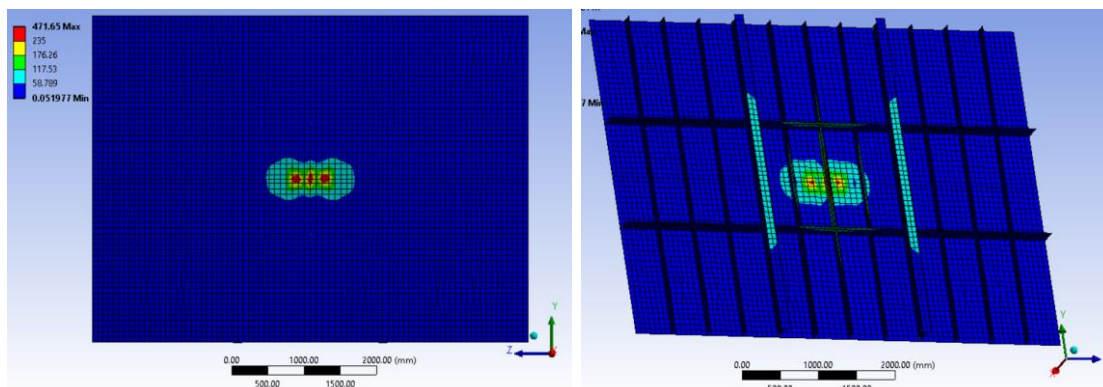
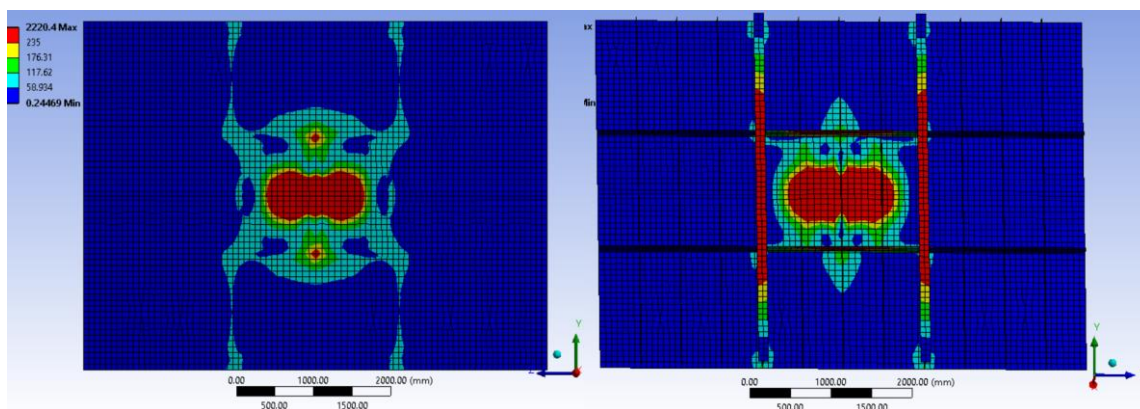*Figure 58 Von Mises stress distribution of the panel for load case 1*

Figure 59 Von Mises stress distribution of the panel for load case 2
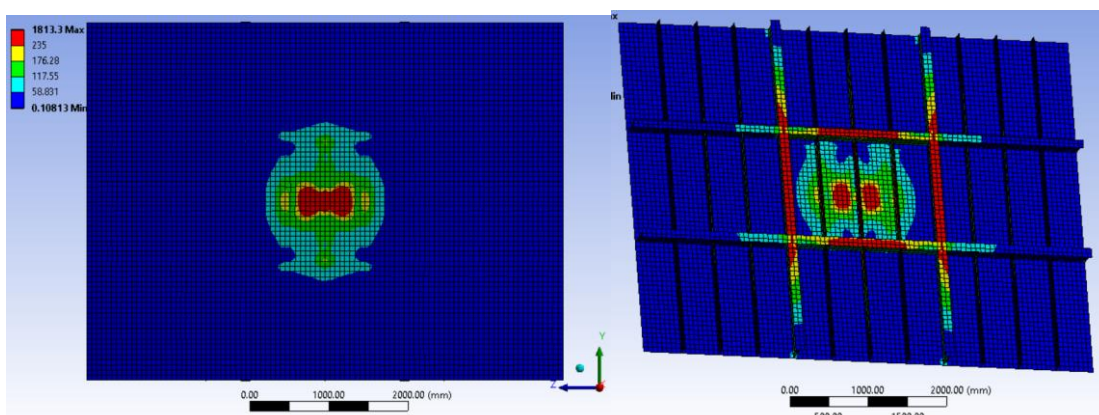

Figure 60 Von Mises stress distribution of the panel using required scantlings based on FSICR IC
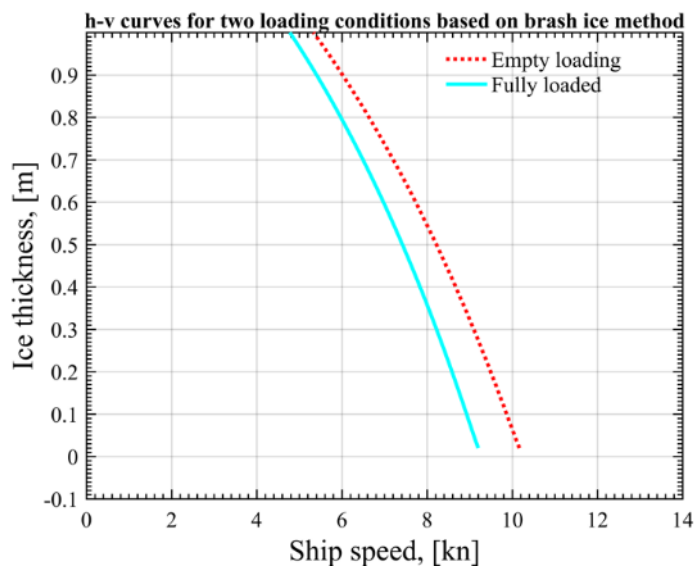
A.5 h-v curve

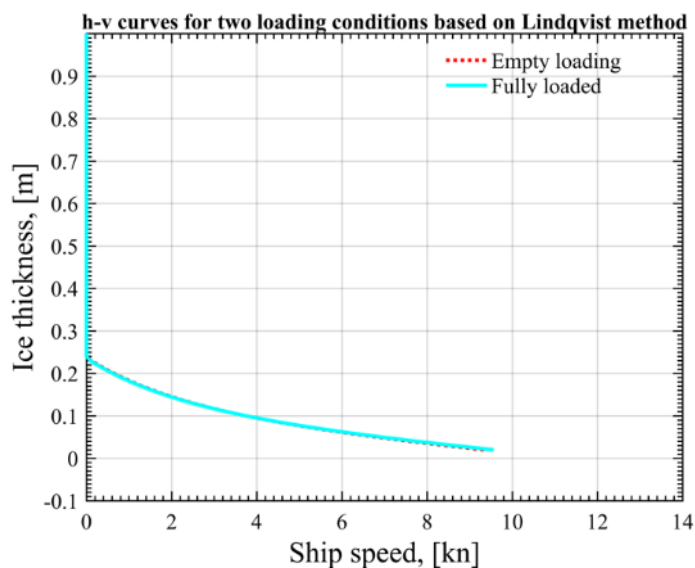*Figure 61 h-v curves based on Lindqvist method*

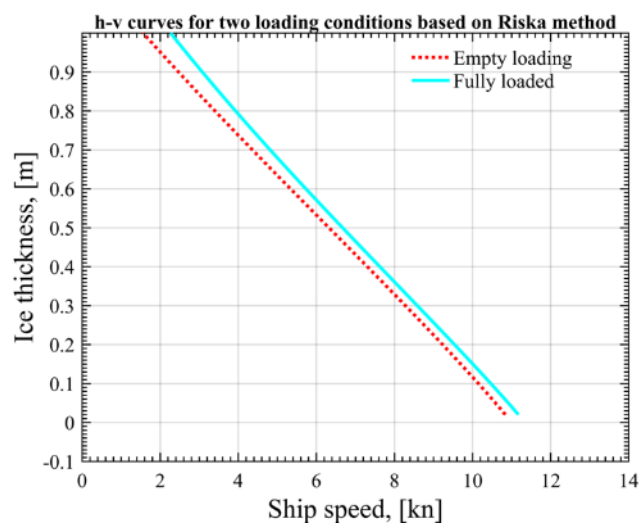*Figure 62 h-v curves based on Brash ice method*
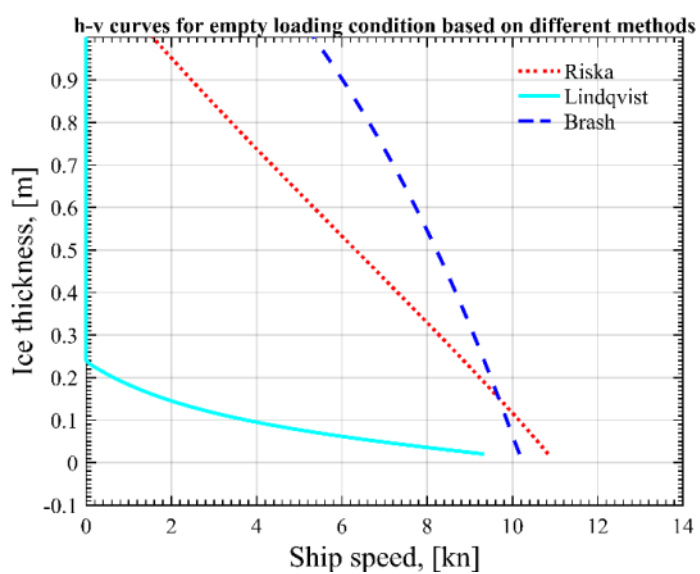
Figure 63 h-v curves based on Riska method

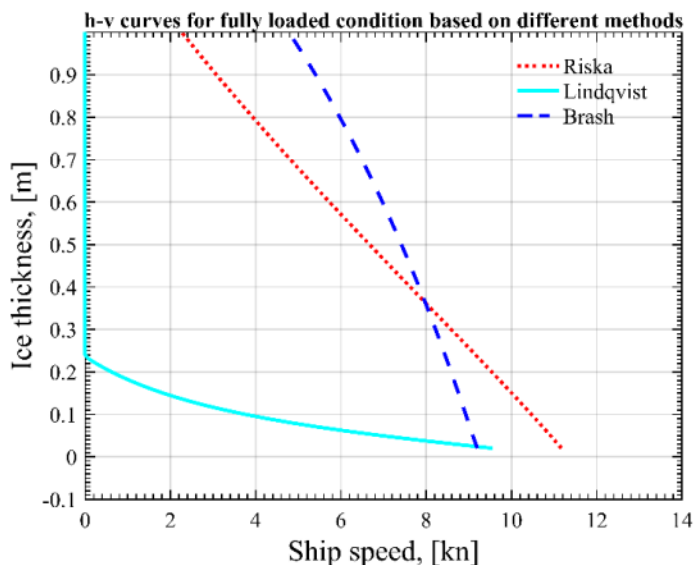*Figure 64 Comparison among different h-v curves for empty loading*

Figure 65 Comparison among different h-v curves for fullyi loaded condition

A.6 Time window

Table 48 Time window (available days) for yearly round operation based on Riska method

Riska	ice thickness(mm)		2013normal ice winter		2011 severe ice winter	
Speed (kn)	Full	Empty	Full	Empty	Full	Empty
1						
2		95,12		365		365
3	90,94	84,27	365,00	365	365,00	365
4	79,19	73,75	365,00	365	365,00	365
5	67,96	63,44	365,00	365	365,00	365
6	57,12	53,26	365,00	365	365,00	365
7	46,54	43,11	350,00	337	350,00	337
8	36,10	32,89	279,00	277	279,00	277
9	25,66	22,47	262,00	260	262,00	260
10	15,08	11,67	246,00	235	246,00	235

Table 49 Time window (available days) for yearly round operation based on Lindqvist method

Lindqvist	ice thickness(mm)		2013normal ice winter		2011 severe ice winter	
Speed (kn)	Full	Empty	Full	Empty	Full	Empty
1	18,18	18,29	274	274	246	246
2	14,44	14,50	229	229	235	235
3	11,67	11,69	229	229	235	235
4	9,51	9,49	225	225	231	231
5	7,74	7,69	225	225	231	231

69

6	6,24	6,15	225	225	231	231
7	4,92	4,79	221	221	226	226
8	3,73	3,56	221	221	226	226
9	2,61	2,38	221	221	226	226
10	\	\	\	\	\	\

Table 50 Time window (available days) for yearly round operation based on Brash ice method

Brash ice	**ice thickness(mm)**		**2013normal ice winter**		**2011 severe ice winter**	
Speed (kn)	Full	Empty	Full	Empty	Full	Empty
1	\	\	\	\	\	\
2	\	\	\	\	\	\
3	\	\	\	\	\	\
4	\	\	\	\	\	\
5	96,56	\	365	\	365	\
6	79,50	90,23	365	365	365	365
7	59,44	73,70	365	365	365	365
8	35,80	54,56	355	365	355	365
9	7,83	32,31	225	353	225	277
10	\	6,43	\	225		231

Reference

 [1]http://ports.com/sea-route/#/?a=15191&b=2780&c=Port%20of%20Karlstad,%20Sweden&d=Port%20of%20Goteborg%20(Gothenburg),%20Sweden.

CHEMICAL TANKER

CONCEPT PROJECT
OF RE-EQUIPMENT

EXPLANATORY NOTE

144-PT-001

KLAIPĖDOS MOKSLO IR
TECHNOLOGIJŲ PARKAS

WESTERN BALTIC
ENGINEERING
BLRT GRUPP

Table of Contents

1 INTRODUCTION

This explanatory note describes the concept of re-equipping an existing inland waterway vessel with a diesel power plant into a vessel with zero harmful emissions in the exhaust. As an initial vessel for the conversion, a hypothetical chemical tanker for inland waterways, similar to "Veendam", was chosen.

The illustration to this Explanatory Note is presented in General Arrangement drawing No. 144-PT-002 and other documents of the conceptual design.

2 INITIAL DATA ABOUT HYPOTHETIC SHIP BEFORE RE-EQUIPMENT

Type of ship - steel, single-propeller with diesel main power plant, with the location of engine room and superstructure in the stern, with the bow thruster.

Main dimensions

- Length over all   86.00 m
- Width   11.45 m
- Height   4.70 m
- Summer draft from base   3.25 m
- Volume of cargo tanks   2,158 m^3

Main engine

- Engine type   Caterpillar 3,512 (B) DI-TA$
- Power   1,088 kW (1,480 hp)
- Rotation speed   1,600 min-1

3 CONCEPT OF REDUCING EMISSIONS OF HARMFUL SUBSTANCES

To reduce sulfur, nitrogen and carbon oxides, as well as solid particles in the ship's emissions, as required by Annex VI of MARPOL MC, it is proposed to use liquefied biological gas (LBG) as a fuel.

When using LBG as fuel, the reduction in emissions will be reduced to 90%.

To optimize the operation of the power plant in fractional modes at a speed of 7 knots or less, or in case of a failure of the main engine (ME), it is proposed to use an electric drive.

In this case the main engine is disconnected from the reduction gear by a coupling.

As a propeller in this mode, it is proposed to use a shaft generator - an electric motor running in the electric motor mode.

Power to the electric motor is supplied from the ship power station, or from the batteries through an inverter that converts the DC voltage of the batteries into an alternating voltage.

If it is necessary to increase speed to 11.4 knots, main engine is connected to the reduction gear and the shaft generator-electric motor operates in the electric motor mode.

Charging of batteries is carried out from the ship's or from the shore network.

4 POWER PLANT

The arrangement of equipment in the engine room (ER) is shown at dwg. No.144-PT-003 Engine Room Arrangement.

4.1 Main engine

As the main engine, it is proposed to use gas piston engines with a power of at least 1000 kW. This condition is satisfied by the engines of the following manufacturers:

- ANGLO BELGIAN CORPORATION - 8DZD with a power of 1200 kW at a frequency of 900 min-1;
- ROLLS – ROYCE – Bergen Marine Engines C26:33 L – series-gas with a power of 1400 kW at a frequency of 900 min-1;
- ROLLS – ROYCE – MTU engine series 4000 MO5-N with a power 1000 kW at a frequency of 1800 min-1;

As an example, the characteristics of a gas piston engine manufactured by Anglo Belgian Corporation are given below.

- Engine model   8 DZD
- Power   1200 kW
- Rotation frequency   900 min-1
- Number of cylinders   8
- The diameter of the cylinder   256 mm
- Piston stroke   310 mm
- Used gas   bio, waste, natural, landfill

In addition to these, other types of gas piston engines, which satisfy the stated requirements, can be used.

4.2 Auxiliary biogas generators

As sources of electrical energy, it is proposed to install two Biogas Generator Sets (BGS) manufactured by CUMMINS type EG250B with a generator power of 250 kW.

- Engine model   Cummins NT855
- Volume of cylinders   14 liters
- Rotation frequency   1500/1800 min-1
- Number of cylinders   6

ENHANCING INLAND NAVIGATION
EMMA

EU STRATEGY FOR THE BALTIC SEA REGION
FLAGSHIP

Interreg
Baltic Sea Region

EUROPEAN
REGIONAL
DEVELOPMENT
FUND
EUROPEAN UNION

- • The diameter of the cylinder   140 mm
- • Piston stroke   152 mm
- • Type of used gases   waste
- • Generator model   Engga EG280L-250N
- • Generator power   250 kW
- • Voltage   400 V

Other types of gas-piston biogas generators, which satisfy the stated requirements, can be used.

4.3 Reduction gear

To transfer energy from the main engine to the shaft line and to the shaft generator, and also to transfer energy from the electric motor to the shaft line, a reduction gear is installed.

- • Power on input shaft from ME   1400 kW
- • Power on power take-off/receive shaft   500 kW
- • Power on output shaft to shaft line   1400 kW

5 FUEL SYSTEM

5.1 General

This Explanatory Note describes a schematic diagram of the use of gas for a power plant, as it will be presented in more detail at a later stage after the final choice of the equipment supplier and will in many respects be determined by the requirements for the gaseous fuel supply system dictated by the engine supplier and supervisors.

The location of the equipment and the basic principles underlying it will be determined by the technical solutions offered by the equipment suppliers. At this stage it is supposed that the engine room is considered as non-hazardous.

The hazardous area scheme was developed in accordance with IMO Resolution MSC 391 (95).

The vessel will have a system for LBG receiving, storing, preparing and feeding to the main engine and auxiliary Biogas Generator Sets according to scheme 144-PT-007 "Fuel system of Biogas".

The system will include:

- • Two tanks for gas storage with double casing. The space between casings is vacuum insulated;
- • Gas pipelines for the supply of liquefied gas and gaseous fuels;
- • Gas preparation container, including gas evaporator;
- • A gas supply system, including a valves block, for each engine;
- • Emergency gas emission system;
- • Ventilation systems;
- • Safety systems;
- • Auxiliary systems necessary for safe maintenance.

Interreg-baltic.eu   Page **4** of 11

EUROPEAN
REGIONAL
DEVELOPMENT
FUND
EUROPEAN UNION

The system will also include a scheme for LBG receiving, pumping and delivery. The gas delivery and degassing system for the tanks will be carried out according to the supplier's documentation.

LBG storage tanks will be placed on the Upper deck, as shown at General Arrangement drawing. The gas preparation containers will be located nearby.

LBG tanks will be designed taking into account the minimum pressure in them, as well as the calculated loads from the flow of liquid gas and inertial forces during rolling in accordance with the Rules for their actual position on the vessel.

The equipment of the LBG system, including the pipelines, will be designed for perceiving of forces when colliding with an obstacle at the ship's course at a speed of up to 10 knots, and also for perceiving of inertial forces of ship board collision with an acceleration of 2g.

The LBG storage system and gas supply to the valves unit will be designed, manufactured, assembled, tested and commissioned by a supplier with experience in similar operations. According to the Rules, the supplier is obliged to provide instructions for the maintenance of the entire system and a risk analysis for the installation of LBG.

An instruction will be developed for the reception of LBG on board the vessel.

Unless otherwise specified, cold-resistant austenitic stainless steel materials will be used to install the LBG.

The control and management of the entire LBG unit will be included in the ship's emergency alarm system (EAS). Data of the consumption will be presented on a mnemonic diagram. The vessel's EAS will include indications of the degree of filling of the tanks with gas and a signal of the detection of a gas leak.

5.2   LBG pumping lines - hoses

LBG will be taken aboard the vessel from shore terminals, from tanker vessels, or will be delivered by road trains consisting of a truck tractor and a LBG transport tank.

For gas reception the station of fuel reception will be provided.

There will be provided hoses permanently connected to LBG storage tanks:

- LBG transfer hoses – double, vacuum insulated;
- Hoses for return of evaporating gas from storage tanks to a transport tank;

All hoses will be equipped with quick-release couplings.

Pipes coming from LBG storage tanks to the connection points of gas preparation containers and to the ventilation system of gas removal will be laid in stationary pallets.

Stainless steel pallets will be installed under all equipment where gas leaks are possible. The leaks will be drained from the pallets by a stainless steel pipe to the waterline area.

The hoses will be controlled from a safe post on the bridge using a video camera or from another convenient location.

The pressure in the gas storage tanks and the level of liquid gas will be controlled in the gas preparation containers. These data will be transmitted into the ship's EAS system.

5.3   Pipes of gas ventilation system

To withdraw gas into the atmosphere as a result of the operation of the safety valve of the LBG system, ventilation pipes will be installed on the vessel - see the General Arrangement drawing. The gas will be emitted at a safe distance from the entrances, sources of ignition, etc. in accordance with the requirements of the Rules.

The construction of the pipelines will ensure the thermal movement of the pipelines relative to the ventilation pipe when cooling the pipelines with LBG jets.

The ventilation pipes will be made of AISI 316L stainless steel and painted.

5.4   Ventilation of gas preparation containers, double pipes and cofferdams

Ventilation of gas preparation containers and double pipes of gas pipelines will provide a 30-fold air exchange per hour.

For gas-hazardous premises, the intake openings of the ventilation ducts will be located at a safe distance from the equipment, doors, etc., situated in danger zone. The ventilation ducts will ensure a balanced flow of air into the ventilated rooms.

The extraction will be provided with an explosion-proof fan installed in a safe place. The fan will be low-noise and variable speed. An auxiliary fan will be provided.

Remote-controlled dampers will be provided for supply and exhaust ventilation pipes.

Instead of forced ventilation, double pipes can be filled with an inert gas.

5.5   Gas storage tanks

The vessel will be equipped with two double-hull LBG storage tanks with a capacity of about 25 m^3 each.

The design pressure of the gas inside the tank is 7.5 ÷ 9.0 bar.

The design of tanks will comply with the Rules, taking into account their location on board and variable filling from 0 to 95%, as well as taking into account the operating conditions of the vessel with different heeling and trim angles under adverse weather conditions.

The construction of LBG tanks will consist of an inner vessel made of cold-resistant stainless steel and designed to perceived internal pressure, and an outer jacket acting as a secondary barrier. The outer jacket can be made of stainless or carbon steel with a nickel content of 9%.

The space between the two hulls will be evacuated and filled with perlite.

The places of connection of pipelines and hoses to the tank will be reliably protected by a steel fence.

5.6 Gas preparation containers

The gas preparation containers with heat exchangers will be installed on the Upper deck.

Containers will be a safety barrier, in which, as a rule, maintenance personnel will not be located. Access to the containers through the doors will be provided from the open deck. The doors leading to the containers will be equipped with portholes, clips and hinges.

For access during maintenance or dismantling of evaporators, a hatch will be provided at the top of the containers.

Valves, cryogenic equipment and a gas flow meter will be placed in the container rooms.

The premises will be monitored for the absence or presence of leaks, which can accumulate in it.

The premises will be gas-tight, relative to the surrounding space in accordance with the requirements of the Rules and are provided with excessive ventilation with a 30-fold air exchange per hour.

Containers refer to a hazardous area. Insulation - class A-60.

5.7 Valve blocks

Valve blocks will be installed in the engine room in the immediate vicinity of the engines. The valve blocks will include gas flow control valves for main engine, BGS, gas valves and gas filters.

The valve blocks will be gas-tight, relative to the surrounding space according to the requirements of the Rules and will be filled with an inert gas.

Valve blocks refers to a hazardous area. Insulation - class A-60.

5.8 Gas evaporation system

To convert a liquid gas into a gaseous state, an evaporation system will be provided. Gas evaporation will occur in the evaporators.

The evaporation system will consist of an pressure circuit to create the required operating pressure in the storage tanks and an additional evaporative circuit for supplying gas to the engines.

Each evaporation system will provide 100% of the ship's need for gas fuel at its maximum consumption.

The design of heat exchangers will ensure their operation with a water-glycol mixture with a ratio of 50:50 at an internal temperature of 30 ° C.

5.9 Gas supply system

The gas supply system from the evaporators of the preparation containers to valve blocks will be carried out according to the requirements of the equipment supplier.

All components of the equipment, including valve blocks, will be part of the delivery of the ME and BGS. The design pressure of the gas supplied to the valve blocks will correspond to the required value of pressure for the engines.

The arrangement of equipment in engine room, as well as in the premises outside the valve blocks installation, will meet the principle of "safe machinery space in terms of gas absence".

Pipelines going from valve blocks to ME and BGS will be double, made of AISI 304 or AISI 316 L stainless steel. The outer pipes can be galvanized steel.

The space between the double walls of the pipelines will be filled with nitrogen at a pressure higher than the gas pressure in the inner tube. When the nitrogen pressure in the tube space decreases, the gas valves will automatically close with the signal output to the emergency alarm system.

Pipelines with double walls will be laid in separate ducts, in which there will be 15-fold ventilation in the usual mode and 30-fold in case of gas leakage.

Gas detection sensors will be installed in accordance with the requirements of the Rules.

5.10 Nitrogen purging system

For nitrogen purging of pipes from the main gas valves to the ME and BGS after the shutdown and for purging the hoses after bunkering, four cylinders with nitrogen will be located on the Upper deck.

The capacity of one cylinder is 50 liters.

The nitrogen pressure is 200 bar.

5.11 Sea endurance by fuel reserves

The total volume of gas in two tanks of 45 m^3 ensures continuous operation of the power plant at 100% load for about 3 days.

When the speed decreases, the power consumption decreases in proportion to the cube of the decrease in speed.

If we assume that, at a load of 100%, the ship's speed was 10 knots, then with a decrease in speed, the sea endurance by gas reserves will increase as follows.

Speed, knots	10	9	8	7	6	5
Power, kW	1000	805	580	440	280	190
Endurance, h	76	94	131	173	271	400

6 ELECTRIC POWER PLANT

6.1 Electric power sources

As the main current source, alternating current of 400 V, frequency of 50 Hz is adopted.

As the main sources of electric power two Biogas Generator Sets (BGS) with generators Engga EG280L-250N with a generator power of 250 kW to be arranged.

As additional sources of electrical energy ten batteries Powerpacks model IP35 / NEMA 3R manufactured by Tesla to be arranged.

- Rated capacity: 210 kWh (AC) per Powerpack unit;
- Communication lines: Modbus, TCP / IP, DNP3;
- Operating temperature range: -22 ° F to 122 ° F / -30 ° C to 50 ° C
- Rated output power: 50 kW (AC) per Powerpack unit;
- Climatic design: IP67

To convert the direct current of the batteries to alternating current and to supply the propulsion motor and ship consumers to be installed:

Inverter IP66 / NEMA 4 manufactured by Tesla.

- Maximum inverter capacity: from 50 kVA to 625 kVA (at 480 V);
- System efficiency (AC): 88% in both directions (2 hours of reservation) / 89% in both directions (4 hours of reservation);
- Depth of Discharge (DoD): 100%.

The inverter will also be used to convert AC to DC when charging batteries from the ship or from the shore network.

6.2 Electromotive system

For navigation with share loads and for navigation in areas with a regulated mode of silence, an electromotive system is provided.

As a propeller motor in the electromotion system, there is a shaft generator - an electric motor with an alternating current of 500 kW.

The electric motor can operate with the ME switched off and in conjunction with the ME to increase the ship's speed to 11.4 knots.

The total energy reserve in batteries of 2100 kWh ensures continuous operation of the electric motor at a power of 500 kW and feeding of ship equipment for approx. 4 hours.

At the same time, the ship's speed will be 7.5 knots, the cruising distance will be 30 miles.

With a decrease in speed, the endurance by the reserves of electrical energy will vary according to the table:

Speed, knots	7,5	6	5
Endurance, h	4	7	10
Distance, miles	30	42	50

The structural diagram of the electric power plant is shown in drawing 144-PT-004.

7 MAIN EQUIPMENT PRICING

Equipment		TD	Manufacturer	Price
MAIN ENGINE				
1	Rolls-Royce Bergen Marine Engines C26:33 L	1460 kW at 900 rpm, operated on Gas	Rolls-Royce Marine Bergen	855.000 €
2	ABC type 8DZD-900-125-A	1200 kW, 900 rpm operated on Gas	Anglo Belgian Corporation nv	513.607 €
REDUCTION GEARBOX				
	Single input Gear Wartsila SCV42	power range 140 kW	Wärtsilä	200.000 €
BIO GAS STORAGE TANKS				
	Biogas tanks + tank room	2x25 m³	Furuise Europe	355.000 € (for 2 units)
GAS GENSET				
1	PowerLink GE250NG	250 kW, 400 V	POWERLINK - UK	69.000 €
2	AKSA ADG365C	250 kW, 400 V	AKSA - Turkey	140.000 €
ENERGY STORAGE SYSTEM				
	Corvus ESS (including Battery Power Packs)	2.240 kWh	Corvus Energy	2.000.000 €